

Triple oxygen isotope variations in natural and anthropogenic carbon dioxide

Dissertation
zur Erlangung des Doktorgrades
der Mathematisch-Naturwissenschaftlichen Fakultäten
der Georg-August-Universität zu Göttingen

vorgelegt von

Magdalena Else Gabriele Hofmann
aus Roßdorf (bei Darmstadt)



Göttingen 2012

Referent:	Prof. Dr. Andreas Pack
Korreferent:	Prof. Dr. Jochen Hoefs
Tag der mündlichen Prüfung:	21.09.2012

Abstract

The oxygen and carbon isotope composition ($^{18}\text{O}/^{16}\text{O}$ and $^{13}\text{C}/^{12}\text{C}$) of atmospheric carbon dioxide is an excellent tool to investigate the atmospheric CO_2 cycle. In recent years, it has been suggested that the triple oxygen isotope composition ($^{17}\text{O}/^{16}\text{O}$ and $^{18}\text{O}/^{16}\text{O}$) of tropospheric CO_2 might be a potential new tracer for the terrestrial gross primary production. This study investigates whether and to which extent this new tracer might complement conventional stable isotope investigations of tropospheric CO_2 .

This thesis presents (i) a new high-precision technique for triple oxygen isotope analysis in carbon dioxide; (ii) an experimental study on triple oxygen isotope exchange between CO_2 and water, the most important process controlling the triple oxygen isotope composition of tropospheric CO_2 ; (iii) experimental data on the triple oxygen isotope composition of combustion CO_2 , in particular anthropogenic CO_2 emissions; (iv) observational data of tropospheric CO_2 and a global mass balance model.

In chapter 2, we describe the new high-precision analytical technique that allows detecting small variations in near-surface tropospheric CO_2 and in the various CO_2 sources to the troposphere. The method is based on CO_2 - CeO_2 equilibration at elevated temperature ($T = 685\text{ }^\circ\text{C}$) and subsequent laser fluorination of the equilibrated CeO_2 . The released molecular oxygen is then analyzed for its triple oxygen isotope composition on a mass spectrometer. The oxygen isotope composition of the sample CO_2 can be inferred from the triple oxygen isotope composition of the equilibrated CeO_2 . The analytical uncertainty of triple oxygen isotope analysis of CO_2 has been improved by about an order of magnitude compared to former techniques.

The triple oxygen isotope composition of tropospheric CO_2 is largely controlled by CO_2 -water exchange in plant leaves, soils and in ocean surface water. Thus, chapter 3 presents a laboratory study on the equilibrium fractionation exponent for oxygen isotope exchange between CO_2 and water at three different temperatures ($2\text{ }^\circ\text{C}$, $23\text{ }^\circ\text{C}$ and $37\text{ }^\circ\text{C}$). Our experimental results agree well with theoretical calculations. Knowledge of this equilibrium fractionation process is a prerequisite for estimating the triple oxygen isotope composition of natural CO_2 gross fluxes from the bio- and hydrosphere.

In chapter 4, we investigate the triple oxygen isotope composition of CO_2 from propane-butane and wood combustion, car exhaust and human breath. The experimental studies show that high-temperature combustion CO_2 largely inherits its distinct triple oxygen

isotope signature from ambient air O₂. For low-temperature combustion, such as wood combustion, the triple oxygen isotope signature of the released CO₂ is also affected by CO₂-water equilibration or other oxygen sources, such as wood inherent oxygen. The oxygen isotope composition of human breath is solely controlled by isotope exchange with body water. The experimental data demonstrate that the triple oxygen isotope composition of anthropogenic CO₂ emissions can be clearly distinguished from natural CO₂ sources.

In chapter 5, we present the first high-precision triple oxygen isotope data of tropospheric CO₂. The data set of ambient air CO₂ sampled in Göttingen shows a significant temporal variation, which only in part follows the seasonal cycle of the ¹⁸O/¹⁶O ratio of tropospheric CO₂. The triple oxygen isotope composition of tropospheric CO₂ sampled on top of the Brocken Mountain (1140 m, Harz Mountains, Germany) falls within the range observed in Göttingen. The mass balance prediction for the triple oxygen isotope composition of global tropospheric CO₂ only in part agrees with the observational data. The modeling results suggest that the observed temporal variation in $\Delta^{17}\text{O}$ cannot be attributed to seasonal variations in plant activity, but it may be that the influx of stratospheric CO₂ significantly affects the temporal $\Delta^{17}\text{O}$ variations of tropospheric CO₂.

This study presents the basis for triple oxygen isotope analysis in tropospheric CO₂ and its meaningful interpretation. Yet, not all characteristics of the triple oxygen isotope signature of tropospheric CO₂ can be explained calling for future studies.

Kurzfassung

Die stabilen Isotopenverhältnisse von Sauerstoff und Kohlenstoff ($^{18}\text{O}/^{16}\text{O}$ und $^{13}\text{C}/^{12}\text{C}$) in atmosphärischem Kohlendioxid sind besonders geeignet, um den CO_2 Kreislauf zu untersuchen. Vor einigen Jahren wurde die Hypothese aufgestellt, dass die 3-Sauerstoffisotopen-Verhältnisse ($^{17}\text{O}/^{16}\text{O}$ und $^{18}\text{O}/^{16}\text{O}$) von troposphärischem Kohlendioxid ein neuer Isotopenindikator für die terrestrische Bruttoprimärproduktion ist. In dieser Arbeit wird untersucht, ob und inwieweit dieser neuartige Isotopenindikator konventionelle stabile Isotopenuntersuchungen von troposphärischem Kohlendioxid ergänzen kann.

Die vorliegende Arbeit gliedert sich in vier Teile: (i) Die Entwicklung einer analytischen Methode, mit der die Sauerstoffisotopie ($^{17}\text{O}/^{16}\text{O}$, $^{18}\text{O}/^{16}\text{O}$) von Kohlendioxid mit höchster Präzision gemessen werden kann. (ii) Eine experimentelle Untersuchung zum 3-Sauerstoffisotopen-Austausch zwischen CO_2 und Wasser. Dieser Austauschprozess ist von grundlegender Bedeutung für die Isotopen-Signatur von troposphärischem CO_2 . (iii) Eine Studie zur 3-Sauerstoffisotopen-Zusammensetzung von Kohlendioxid aus Verbrennung mit einem besonderen Fokus auf anthropogene CO_2 Emissionen. (iv) Abschließend werden troposphärische CO_2 Daten vorgestellt und mit einem globalen Massenbilanzmodell verglichen.

In Kapitel 2 wird die neuartige Methode zur 3-Sauerstoffisotopen-Analyse von CO_2 beschrieben. Diese Methode ermöglicht es, kleinste Variationen in troposphärischem Kohlendioxid und den unterschiedlichen CO_2 Quellen zur Troposphäre zu untersuchen. Die Methode beruht auf Isotopenäquilibration zwischen CO_2 und CeO_2 bei erhöhter Temperatur ($T = 685\text{ °C}$) und anschließender Laser-Fluorinierung des äquilibrierten Cerdioxids. Der freigesetzte Sauerstoff wird anschließend massenspektrometrisch auf seine 3-Sauerstoffisotopen-Zusammensetzung untersucht. Die Sauerstoffisotopie ($^{17}\text{O}/^{16}\text{O}$, $^{18}\text{O}/^{16}\text{O}$) der Kohlendioxid Probe kann aus der Isotopie des CeO_2 berechnet werden. Die Messgenauigkeit konnte im Vergleich zu früheren Methoden um etwa eine Größenordnung verbessert werden.

Die Sauerstoffisotopie ($^{17}\text{O}/^{16}\text{O}$, $^{18}\text{O}/^{16}\text{O}$) von troposphärischem Kohlendioxid wird hauptsächlich durch den Isotopenaustausch zwischen CO_2 und Wasser in Pflanzenblättern, Böden und in der obersten Meeresschicht bestimmt. Daher widmet sich Kapitel 3 der experimentellen Bestimmung der Gleichgewichtsfractionierung ($^{17}\text{O}/^{16}\text{O}$, $^{18}\text{O}/^{16}\text{O}$) zwischen CO_2 und Wasser bei drei unterschiedlichen Temperaturen (2 °C , 23 °C und

37 °C). Die experimentellen Ergebnisse stimmen mit theoretischen Berechnungen überein. Die Kenntnis dieses Gleichgewichtsfraktionierungsprozesses ist eine Grundvoraussetzung, um die 3-Sauerstoffisotopen-Zusammensetzung der natürlichen CO₂ Quellen aus der Bio- und Hydrosphäre abzuschätzen.

In Kapitel 4 werden die experimentellen Ergebnisse zur 3-Sauerstoffisotopen-Zusammensetzung von Kohlendioxid aus Verbrennung dargestellt (Propan-Butan-Verbrennung, Holzverbrennung, Autoabgase und CO₂ aus Atemluft). Die Ergebnisse zeigen, dass bei Hochtemperatur-Verbrennungsprozessen die Sauerstoffisotopie von Luft-O₂ (¹⁷O/¹⁶O, ¹⁸O/¹⁶O) größtenteils auf das Kohlendioxid übertragen wird. Bei niedrigen Verbrennungstemperaturen, wie der Holzverbrennung, wird die Sauerstoffisotopen-Zusammensetzung des freigesetzten Kohlendioxids auch durch CO₂-Wasser Äquilibration und andere Sauerstoffquellen, wie z.B. im Holz gebundener Sauerstoff, beeinflusst. Die Sauerstoffisotopen-Zusammensetzung von Kohlendioxid aus Atemluft wird hingegen nur durch den Isotopenaustausch mit Körperwasser bestimmt. Die experimentellen Daten zeigen, dass man anthropogenes Kohlendioxid anhand seiner Sauerstoffisotopie (¹⁷O/¹⁶O, ¹⁸O/¹⁶O) eindeutig von Kohlendioxid aus natürlichen Quellen unterscheiden kann.

In Kapitel 5 werden die ersten hoch-präzisen 3-Sauerstoffisotopen-Analysen von troposphärischem Kohlendioxid vorgestellt. Der Datensatz von CO₂ Proben aus Göttingen zeigt eine deutliche zeitliche Variation in der 3-Sauerstoffisotopen-Zusammensetzung. Diese zeitliche Schwankung stimmt nur teilweise mit der saisonalen Variation des ¹⁸O/¹⁶O Verhältnisses von troposphärischem CO₂ überein. Messungen von CO₂ Proben vom Brocken (1140 m, Harz, Deutschland) stimmen mit den gemessenen Daten in Göttingen überein. Die Massenbilanz Vorhersage für die 3-Sauerstoffisotopen-Zusammensetzung von troposphärischem CO₂ stimmt nur teilweise mit den gemessenen Daten überein. Die Modellierung legt nahe, dass die zeitlichen Variationen in der 3-Sauerstoffisotopen-Zusammensetzung nicht durch saisonale Schwankungen der biologischen Aktivität erklärt werden können, stattdessen könnte der Zustrom von stratosphärischem CO₂ die zeitlichen Schwankungen verursachen.

Diese Untersuchung bereitet die Grundlage für 3-Sauerstoffisotopen Analysen von troposphärischem Kohlendioxid und deren aussagekräftige Interpretation. Allerdings können nicht alle Merkmale der gemessenen Isotopendaten erklärt werden, es werden künftig weitere Untersuchungen notwendig sein.

Acknowledgments

Above all, I thank my supervisor Prof. Dr. Andreas Pack for providing me with this topic and his continuous support during my time as a PhD student. I enjoyed the various discussions, which were always characterized by his scientific curiosity. I also thank Prof. Dr. Jochen Hoefs for being my co-supervisor.

I thank Balázs Horváth for being a very helpful colleague at all times. Working on the same project with him and sharing the same office was crucial for the day-to-day motivation!

I thank my two PhD fellows, Alexander Gehler and Verena Bendel, for sharing the ups and downs of a dissertation project. I wish you all the best for finishing your dissertations!

I thank Reinhold Przybilla, Ingrid Reuber and Axel Dierschke for their technical support in the laboratory.

I also thank our student assistants, especially Maximilian Troche and Andres Höweling, for helping me in the lab.

I am thankful to the INTRAMIF organizers, in particular Thomas Röckmann, Jan Kaiser and Amaelle Landais, who initiate two great summer schools on stable isotopes and beyond. It was always a pleasure for me meeting all the INTRAMIF PhD students!

Moreover, I thank Hauke Vollstaedt for an ongoing friendship from the first introductory lectures in geology to the highly specialized world of geochemistry. The conversations on academia in general and specific scientific problems were always a welcome change!

In particular, I enjoyed the rehearsals and concerts with the AOV Göttingen during my time as a PhD student, which were always a valuable balance to daily work. Especially, I thank Liane Lühmann for many cheerful moments!

I also thank my mother Heide Lore Hofmann for always listening and giving a fresh perspective on life!

Finally, I am grateful to my beloved Christian for his scientific advice and for being a wonderful companion!

Table of contents

Abstract	iii
Kurzfassung	v
Acknowledgments	vii
Table of contents	viii
1 Introduction.....	1
1.1 Background.....	1
1.2 Triple oxygen isotope notation	2
1.2.1 Basic definitions.....	2
1.2.2 The $\Delta^{17}\text{O}$ value and the reference line	4
1.2.3 Triple oxygen isotope exponents: λ and θ values	6
1.3 ^{17}O -excess in atmospheric gases.....	9
1.4 The global carbon cycle.....	11
1.5 Focus of study.....	14
1.6 References.....	16
2 Technique for high-precision analysis of triple oxygen isotope ratios in carbon dioxide	20
2.1 Abstract.....	20
2.2 Introduction.....	20
2.3 Methods	22
2.3.1 Definitions.....	22
2.3.2 Oxygen and carbon isotope analyses	22
2.3.3 Exchange experiments between CO_2 and CeO_2	23
2.3.4 Determination of $\Delta^{17}\text{O}$ of CO_2	25
2.4 Results.....	26
2.4.1 Terrestrial fractionation line.....	26
2.4.2 Isotopic composition of the starting materials	27
2.4.3 Equilibration experiments	28
2.4.4 Uncertainty in $\Delta^{17}\text{O}$ determination on CO_2	31
2.5 Discussion.....	31
2.6 Acknowledgment.....	32
2.7 References.....	33

3	Triple oxygen isotope equilibrium fractionation between carbon dioxide and water	35
3.1	Abstract.....	35
3.2	Introduction.....	35
3.3	Methods	37
3.3.1	Definitions.....	37
3.3.2	Isotope exchange experiments between CO ₂ and water	37
3.3.3	Triple oxygen isotope analyses of CO ₂ and water	39
3.4	Results.....	40
3.5	Discussion.....	45
3.5.1	The triple oxygen isotope equilibrium fractionation exponent $\theta_{\text{CO}_2\text{-water}}$ in the context of experimental and theoretical literature data	45
3.5.2	Relevance of the $\theta_{\text{CO}_2\text{-water}}$ value for the identification of major CO ₂ sources to the troposphere.....	49
3.6	Acknowledgment.....	50
3.7	References.....	51
4	On the triple oxygen isotope composition of carbon dioxide from some combustion processes.....	54
4.1	Abstract.....	54
4.2	Introduction.....	54
4.3	Materials and methods	56
4.3.1	Definitions.....	56
4.3.2	Sampling	56
4.3.3	Experimental procedures.....	57
4.3.4	Analytical procedures	58
4.4	Results.....	60
4.5	Discussion.....	64
4.5.1	Carbon isotope ratios	64
4.5.2	Oxygen isotope ratios.....	64
4.5.3	Can the $\Delta^{17}\text{O}$ value of CO ₂ be used as a tracer to distinguish between different CO ₂ sources?	71
4.6	Conclusions.....	72
4.7	Acknowledgments	72
4.8	References.....	73
5	Triple oxygen isotope composition of tropospheric CO₂: Observational data and model simulation	78
5.1	Abstract.....	78
5.2	Introduction.....	79

5.3	Method.....	80
5.3.1	Triple oxygen isotope notation	80
5.3.2	Model description	81
5.3.3	Sampling of tropospheric CO ₂ and isotope analyses	97
5.4	Results and discussion	99
5.4.1	Modeled triple oxygen isotope composition of tropospheric CO ₂	99
5.4.2	Impact of the major CO ₂ sources and sinks on the global mean $\Delta^{17}\text{O}$ value of tropospheric CO ₂	99
5.4.3	Is $\Delta^{17}\text{O}$ of tropospheric CO ₂ a potential tracer for the terrestrial gross primary production?	102
5.4.4	Observational triple oxygen isotope data of tropospheric CO ₂	103
5.5	Conclusions.....	106
5.6	Acknowledgments	106
5.7	References.....	107
6	Conclusions and outlook	111
7	List of publications	114
8	Curriculum vitae.....	117

1 Introduction

1.1 Background

Today, the increase in atmospheric CO₂ concentration and the concomitant climate change is one of the most pressing environmental challenges that society is facing (IPCC, 2007). Stable isotope geochemistry has traditionally played an important role in unraveling the magnitude of anthropogenic and natural CO₂ sources and sinks to the atmosphere. Assessing and understanding the mechanisms of the disturbed current global carbon cycle is a prerequisite for meaningful future climate change predictions.

During the late 1950s and the 1960s, Charles Keeling was the first to investigate simultaneously variations in the atmospheric CO₂ concentration and in the ¹³C/¹²C isotope ratio of atmospheric CO₂, and thus, he was able to ascribe seasonal variations in CO₂ concentration to seasonal variations in plant activity (Keeling, 1958; Keeling, 1960; Keeling, 1961). Since then, various studies on the stable carbon isotope ratio of atmospheric CO₂ followed, and ultimately, allowed to partition the global net CO₂ uptake between the terrestrial biosphere and the ocean (e.g. Ciais et al., 1995). The underlying principle is that plants preferentially take up the light ¹²C isotope compared to the heavy ¹³C isotope, whereas dilution of CO₂ in the ocean hardly affects the ¹³C/¹²C ratio of the residual atmospheric CO₂.

Since the late 1970s, stable oxygen isotope analysis of atmospheric CO₂ gained in importance. At that time, the main focus was on analyzing the ¹⁸O/¹⁶O ratio¹. In contrast to the stable carbon isotope composition of atmospheric CO₂, the stable oxygen isotope composition of tropospheric CO₂ is largely controlled by CO₂-water exchange in leaves, soils and ocean surface water (Farquhar et al., 1993; Francey and Tans, 1987). Thus, investigating the ¹⁸O/¹⁶O ratio of atmospheric CO₂ allows inferring the CO₂ gross fluxes from the terrestrial biosphere and soil respiration (Ciais et al., 1997; Cuntz et al., 2003a; Cuntz et al., 2003b; Peylin et al., 1999). Recently, it has been suggested that interannual variations in the ¹⁸O/¹⁶O ratio of atmospheric CO₂ could also trace changes in the

¹ Oxygen has three stable isotopes: ¹⁶O, ¹⁷O and ¹⁸O. Oxygen with mass 16 u is the far most abundant isotope accounting for about 99.76%. The rare isotopes ¹⁷O and ¹⁸O have an abundance of only 0.039% and 0.201%, respectively.

terrestrial gross primary production (Welp et al., 2011).

During the 1980s, Thiemens and Heidenreich (Thiemens and Heidenreich, 1983; Heidenreich and Thiemens, 1986) were the first to identify large enrichments in ^{17}O in an atmospheric tracer gas, namely ozone. The reason for this large enrichment in ^{17}O were so-called mass-independent fractionation effects during the formation process of ozone. Subsequent, this large enrichment in the rare ^{17}O isotope was discovered in stratospheric CO_2 (Thiemens et al., 1995a; Thiemens and Jackson, 1991; Thiemens et al., 1995b), and it was found that this excess in ^{17}O was also passed on to almost all other oxygen-bearing trace gases in the atmosphere. Thus, exploring the triple oxygen isotope composition of atmospheric gases became a powerful tool to investigate atmospheric chemistry or atmosphere-biosphere interactions (e.g. Luz et al., 1999).

Nowadays, high-precision measurement of triple oxygen isotope ratios in tropospheric carbon dioxide is a promising tracer to complement the traditional stable oxygen and carbon isotope analyses. In 2005, Hoag et al. pointed out that the triple oxygen isotope composition of tropospheric CO_2 might contain information on the current-day terrestrial gross primary production. It is the ultimate goal of this study to test the potential of this new tracer for the global carbon cycle.

1.2 Triple oxygen isotope notation

1.2.1 Basic definitions

In general, variations of stable isotope ratios in natural terrestrial materials are small. Thus, the isotopic ratio of a sample is not given as an absolute value, but as a deviation from an international reference material. The small isotopic variations are given as δ -values describing the relative isotopic enrichment of a sample to a reference material:

$$\delta = \left[\frac{R_{\text{sample}}}{R_{\text{reference}}} - 1 \right] \quad \text{Eq. 1-1}^2$$

The variable R describes the ratio of the heavy to light stable isotope in the sample and the reference material.

² Note that the δ -notation in Eq.1-1 often contains a numerical factor of 1000. However, recently Coplen (2011) recommended to omit this factor for consistent stable isotope notation.

For the case of oxygen, there are three stable isotopes (^{16}O , ^{17}O , ^{18}O) so that one can define $\delta^{18}\text{O}$ - and $\delta^{17}\text{O}$ -values:

$$\delta^{17}\text{O} = \left[\frac{\left(^{17}\text{O} / ^{16}\text{O} \right)_{\text{sample}}}{\left(^{17}\text{O} / ^{16}\text{O} \right)_{\text{VSMOW}}} - 1 \right] \quad \text{Eq. 1-2}$$

and

$$\delta^{18}\text{O} = \left[\frac{\left(^{18}\text{O} / ^{16}\text{O} \right)_{\text{sample}}}{\left(^{18}\text{O} / ^{16}\text{O} \right)_{\text{VSMOW}}} - 1 \right] \quad \text{Eq. 1-3}$$

For oxygen isotope notation, the primary reference material is Vienna Standard Mean Ocean Water (VSMOW). Alternatively, oxygen isotope ratios are given relative to Vienna Pee Dee Belemnite (VPDB), which is also the most common reference material for carbon isotope ratios. Note, that conversion from one oxygen isotope reference scale to the other can be easily done applying the relationship given in Coplen et al. (1983).

For mass-dependent fractionation processes, i.e. equilibrium and kinetic isotope exchange reactions, the ratios of multi isotope species are related via a power law function. For the triple oxygen isotope ratios, the mass-dependent fractionation law can be given by the following relationship (Young et al., 2002):

$$\frac{\left(^{17}\text{O} / ^{16}\text{O} \right)_{\text{sample}}}{\left(^{17}\text{O} / ^{16}\text{O} \right)_{\text{VSMOW}}} = \left[\frac{\left(^{18}\text{O} / ^{16}\text{O} \right)_{\text{sample}}}{\left(^{18}\text{O} / ^{16}\text{O} \right)_{\text{VSMOW}}} \right]^{\lambda} \quad \text{Eq. 1-4}$$

The exponent λ differs for equilibrium and kinetic fractionation processes. In theory, the exponent λ for oxygen isotope fractionation can vary between 0.509 and 0.530 for kinetic and equilibrium fractionation processes (Young et al., 2002). Note that the exponent is generally denoted with λ if one is reporting isotope variations of a certain reservoir (e.g. meteoric water or terrestrial rocks and minerals) representing a statistical triple oxygen isotope distribution in this reservoir. However, the exponent for pure equilibrium fractionation between two phases A and B, e.g. oxygen isotope exchange between CO_2 and water, is denoted with the greek symbol θ in this study:

$$\frac{\delta^{17}\text{O}^A+1}{\delta^{17}\text{O}^B+1} = \left[\frac{\delta^{18}\text{O}^A+1}{\delta^{18}\text{O}^B+1} \right]^\theta \quad \text{Eq. 1-5}$$

where $\delta^{17}\text{O}^A$ and $\delta^{18}\text{O}^A$ are the isotopic values of a phase A and $\delta^{17}\text{O}^B$ and $\delta^{18}\text{O}^B$ are the isotopic values of phase B. Nowadays, it is possible to detect slight variations in the exponent θ for equilibrium fractionation between compounds due to a steady increase in analytical precision. A short literature review on different theoretical and experimental λ and θ values will be given below (see section 1.2.3).

In order to obtain a linear relationship between $\delta^{18}\text{O}$ and $\delta^{17}\text{O}$ values, the equations Eq. 1-2 and Eq. 1-3 can be rearranged to give

$$\delta^{17,18}\text{O} = \ln(\delta^{17,18}\text{O}+1) \quad \text{Eq. 1-6}$$

From Eq. 1-4 it follows that the two new variables $\delta^{18}\text{O}$ and $\delta^{17}\text{O}$ describe a linear relationship with the variable λ as coefficient:

$$\delta^{17}\text{O} = \lambda \times \delta^{18}\text{O} \quad \text{Eq. 1-7}$$

Thus, the variable λ corresponds to a slope in a $\delta^{18}\text{O}$ vs. $\delta^{17}\text{O}$ plot and the θ value represents a line connecting two points: the $\delta^{18}\text{O}$ and $\delta^{17}\text{O}$ value of a phase A (e.g. CO_2) and the $\delta^{18}\text{O}$ and $\delta^{17}\text{O}$ value of a phase B (e.g. water).

1.2.2 The $\Delta^{17}\text{O}$ value and the reference line

In general, triple oxygen isotope ratios are given relative to a reference line in a triple oxygen isotope plot (Fig. 1-1). Deviations from a mass-dependent reference line (RL) are defined as $\Delta^{17}\text{O}$ values according to Eq. 1-7:

$$\Delta^{17}\text{O} = \delta^{17}\text{O} - \lambda_{\text{RL}} \times \delta^{18}\text{O} + \gamma_{\text{RL}} \quad \text{Eq. 1-8}$$

The variables λ_{RL} and γ_{RL} describe the slope and the intercept of the reference line in a triple oxygen isotope plot. Deviations from a mass-dependent reference line, expressed as $\Delta^{17}\text{O}$ value, are most often called oxygen isotope anomaly or ^{17}O -excess.

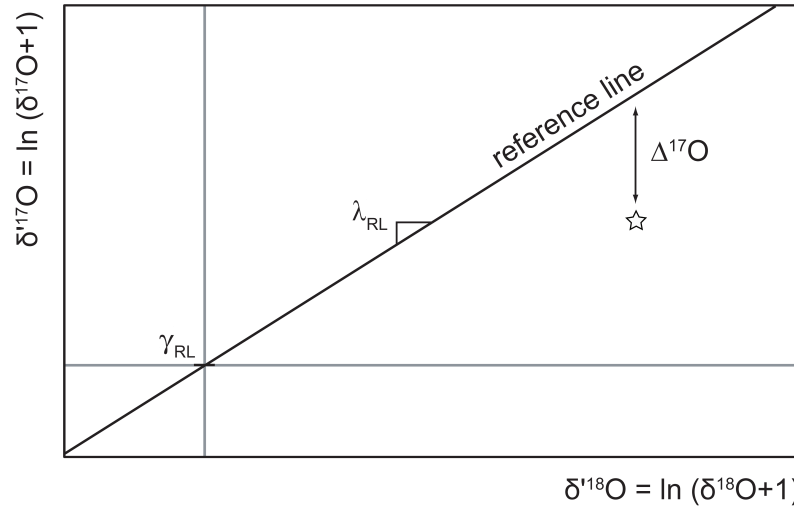


Fig. 1-1: Notation of triple oxygen isotope data. Small variations of triple oxygen isotope data are generally reported as a deviation from a reference line ($\Delta^{17}\text{O}$ values) with a slope λ_{RL} and an intercept γ_{RL} .

Different reference lines were used within this dissertation (Table 1-1). At the beginning of this PhD project, a terrestrial fractionation line (TFL) was chosen as reference line because the main focus of the stable isotope laboratory in Göttingen lies on the analysis of rocks and minerals. During the course of this PhD project, the equilibrium exponent for CO_2 -water exchange was determined (Chapter 3). Subsequently, triple oxygen isotope data of tropospheric CO_2 are given relative to a CO_2 -water equilibrium line with a slope of 0.522 and zero intercept (Chapter 4 and 5). The CO_2 -water equilibrium line was chosen as the new reference line because equilibrium exchange between CO_2 and water in the bio- and hydrosphere is the dominant process controlling the triple oxygen isotope composition of tropospheric CO_2 . The zero intercept was chosen for simplicity.

Table 1-1: Overview of the different reference lines used within this dissertation.

	type	slope	intercept [‰]
Chapter 2	TFL	0.5252	-0.015
Chapter 3	TFL	0.5251	0.00
Chapter 4	CO_2 -water line	0.522	0.00
Chapter 5	CO_2 -water line	0.522	0.00

1.2.3 Triple oxygen isotope exponents: λ and θ values

Understanding slight variations in triple oxygen isotope ratios in terrestrial compounds requires knowledge of the exponent λ or θ for the involved exchange mechanisms. The exponent differs for kinetic and equilibrium fractionation because kinetic fractionation results from differences in the effective molecular mass of the involved gases (or liquids) whereas equilibrium fractionation depends on the atomic masses of the involved isotopes.

Equilibrium fractionation

The exponent θ for equilibrium fractionation depends on the partition function ratio of the oxygen-bearing isotopologues. The overall partition function ratio describes the translational, rotational and vibrational energy of a molecule, and thus, the equilibrium exponent θ can be derived from quantum mechanical calculations. The exponent for high-temperature exchange (temperatures exceeding about 500 °C) can be approximated for any exchange reaction between two oxygen-bearing compounds from the mass ratios of the stable oxygen isotopes (Young et al., 2002):

$$\theta = \frac{\frac{1}{m_{^{16}\text{O}}} - \frac{1}{m_{^{17}\text{O}}}}{\frac{1}{m_{^{16}\text{O}}} - \frac{1}{m_{^{18}\text{O}}}} \quad \text{Eq. 1-9}$$

From this it follows that equilibrium fractionation at high-temperatures proceeds with $\theta = 0.53$. For low temperature equilibration processes, the approximation in Eq. 1-8 is not valid anymore, and thus, the exponent θ can be significantly lower than the high temperature limit of 0.53 (see Cao and Liu, 2011).

Experimental results on θ values for equilibrium fractionation processes are still scarce (Fig. 1-2). Barkan and Luz (2005) determined an exponent θ for water–water vapor exchange of 0.529 ± 0.001 in the temperature range from 11 to 42 °C, which was also confirmed by theory (Cao and Liu, 2011). Simultaneous to this dissertation, several other θ values for equilibrium exchange reactions were determined experimentally within the stable isotope group in Göttingen: $\theta_{\text{apatite-water}} = 0.526 \pm 0.002$ at about 37 °C, $\theta_{\text{quartz-fayalite-magnetite}} = 0.530 \pm 0.002$ at $T \geq 700$ °C and $\theta_{\text{SiO}_2(\text{opal})\text{-water}} = 0.521 \pm 0.001$ for temperatures between 2 and 10 °C (Pack et al., 2012).

Recently, Cao and Liu (2011) presented theoretical estimates for different equilibrium exponents (Fig. 1-2). The authors confirm that the equilibrium exponent for water-water vapor exchange at low temperatures is identical to the high-temperature limit of 0.53. Additionally, they also give estimates for various other equilibrium exponents including $\theta_{\text{quartz-water}} = 0.525$ and $\theta_{\text{calcite-water}} = 0.524$ at room temperature.

It is an integral part of this study to determine experimentally the exponent θ for CO_2 -water exchange which is the dominant process controlling the triple oxygen isotope composition of tropospheric CO_2 (see chapter 3).

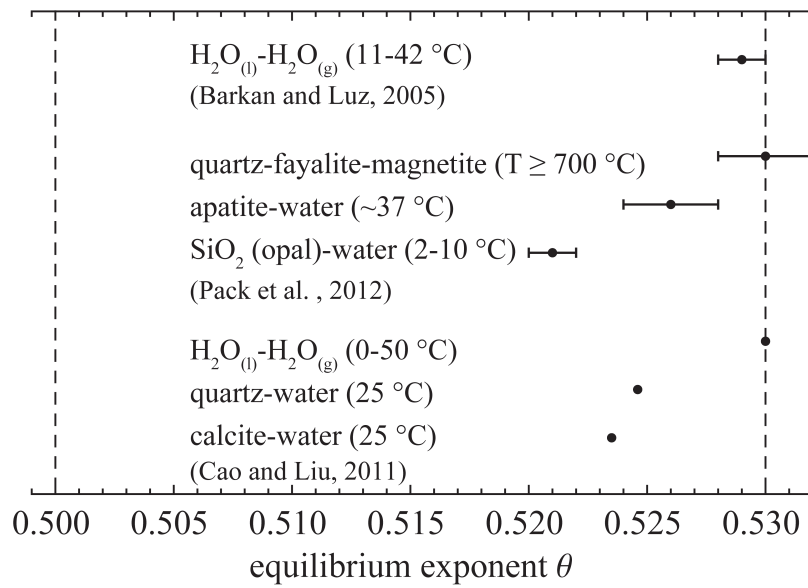


Fig. 1-2: Overview of equilibrium exponents. Data points with error bars are based on experimental studies; data points without error bars are based on theoretical studies. All equilibrium exponents must fall between the high temperature limit of 0.53 and the lower limit of 0.509 typical for kinetic fractionation (Young et al., 2002).

Kinetic fractionation

In theory, the exponent λ for kinetic fractionation processes (e.g. diffusion of a water vapor molecule in vacuo) depends on the kinetic energy of the involved molecules, and thus, it depends solely on the masses m of the oxygen isotopologues (Young et al., 2002):

$$\lambda = \frac{\ln\left(\frac{m_1}{m_2}\right)}{\ln\left(\frac{m_1}{m_3}\right)} = \frac{\ln \alpha_{2/1}}{\ln \alpha_{3/1}} \quad \text{Eq. 1-10}$$

where m_1 , m_2 and m_3 denote the masses of the isotopologues in ascending order. This relationship can be simplified replacing the mass ratios with the fractionation factors $\alpha_{2/1}$ and $\alpha_{3/1}$. For example, for water vapor diffusion $m_1 = 18$, $m_2 = 19$ and $m_3 = 20$ resulting in a λ value of 0.513 and for diffusion of O_2 , the exponent λ is equal to 0.509.

For gas mixtures, e.g. water vapor diffusion in air, the mass m of the isotopologue is replaced by the reduced mass μ :

$$\mu_1 = \frac{m^B m_1^A}{m^B + m_1^A} \quad \text{Eq. 1-11}$$

where the superscript denotes the two gases A and B and the subscript denotes the involved isotopologue. Inserting the reduced masses for all isotopologues in Eq. 1-10 gives:

$$\lambda = \frac{\ln\left(\frac{\mu_1}{\mu_2}\right)}{\ln\left(\frac{\mu_1}{\mu_3}\right)} = \frac{\ln\left(\frac{m^B m_1^A}{m^B + m_1^A} \frac{m^B m_2^A}{m^B + m_2^A}\right)}{\ln\left(\frac{m^B m_1^A}{m^B + m_1^A} \frac{m^B m_3^A}{m^B + m_3^A}\right)} \quad \text{Eq. 1-12}$$

For water vapor diffusion in air, for example, where $m_{\text{air}} = 29$ g/mol, the theoretical λ value is 0.518.

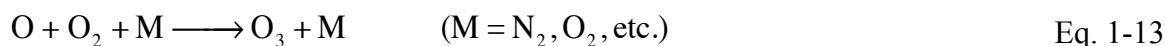
Oxygen isotope reservoirs: TFL and GMWL

The most extensive studies on triple oxygen isotope reservoirs on Earth have been carried out on terrestrial rocks and minerals and on meteoric water. Various studies showed that for terrestrial rocks and minerals the slope λ_{TFL} for a terrestrial fractionation line (TFL) falls between 0.524 to 0.526 (Miller et al., 1999b; Pack et al., 2007; Rumble et al., 2007). The exact slope seems to depend on the choice of rocks and minerals reflecting the formation process. Luz and Barkan (2010) analyzed a great number of meteoric waters from all over the world and found that these water fall on a line with a slope $\lambda_{\text{GMWL}} = 0.528 \pm 0.001$ and an intercept of $\gamma_{\text{GMWL}} = +0.033 \pm 0.003\text{‰}$ in a $\delta^{18}\text{O}$ vs. $\delta^{17}\text{O}$ plot. This line is known as the global meteoric water line (GMWL). Recently, Tanaka and Nakamura (2012) simultaneously analyzed terrestrial rocks and minerals and meteoric waters and found that their TFL and GMWL differ both in their slope and in their intercept: $\lambda_{\text{TFL}} = 0.5270 \pm 0.0005$ and $\gamma_{\text{TFL}} = -0.070 \pm 0.005\text{‰}$ vs. $\lambda_{\text{GMWL}} = 0.5281 \pm 0.0004$ and $\gamma_{\text{GMWL}} = -0.011 \pm 0.015\text{‰}$.

1.3 ^{17}O -excess in atmospheric gases

All oxygen bearing trace gases from the strato- and mesosphere (except water) show a large oxygen isotope anomaly (Fig. 1-3). This anomaly has its origin in the formation of ozone in the upper atmosphere, and subsequently, is passed on to other trace gases by a variety of reaction mechanisms.

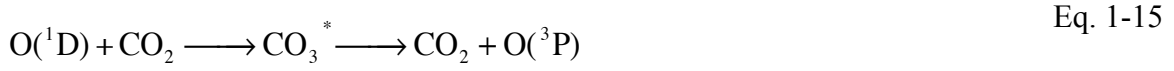
Ozone is formed in the upper atmosphere due to a recombination reaction between atomic oxygen and molecular oxygen:



The third collision partner M is required to carry away the excess energy. Ultimately, this reaction, which is part of the so-called Chapman cycle, produces ozone that has a large positive oxygen isotope anomaly ($\delta^{18}\text{O} \approx 80 - 150\text{‰}$, $\Delta^{17}\text{O} \approx 40\text{‰}$) (Krakowsky et al., 2000; Lämmerzahl et al., 2002; Mauersberger, 1981), see Fig. 1-3.

Thiemens and Heidenreich (1983) were the first to reproduce these stratospheric observations in a simple experiment where ozone was produced by electrical discharge. They postulated that the formation of $^{17}\text{O}^{16}\text{O}^{16}\text{O}$ was equally fast as the formation of $^{18}\text{O}^{16}\text{O}^{16}\text{O}$, and thus, giving rise to an exponent $\lambda = 1$.

Subsequent to ozone formation, the ozone molecule is decomposed due to photolysis and the oxygen isotope anomaly is transferred to stratospheric CO₂ via the electronically excited singlet oxygen O(¹D) (Yung et al., 1991):



As a result, carbon dioxide from the strato- and mesosphere shows a large positive oxygen isotope anomaly (Boering et al., 2004; Kawagucci et al., 2008; Lämmerzahl et al., 2002; Thieme et al., 1995b) (see Fig. 1-4). Tropospheric O₂, however, is depleted in its ¹⁷O composition with Δ¹⁷O = -0.365 (relative to λ_{RL}=0.522) (Barkan and Luz, 2011; Luz and Barkan, 2005).

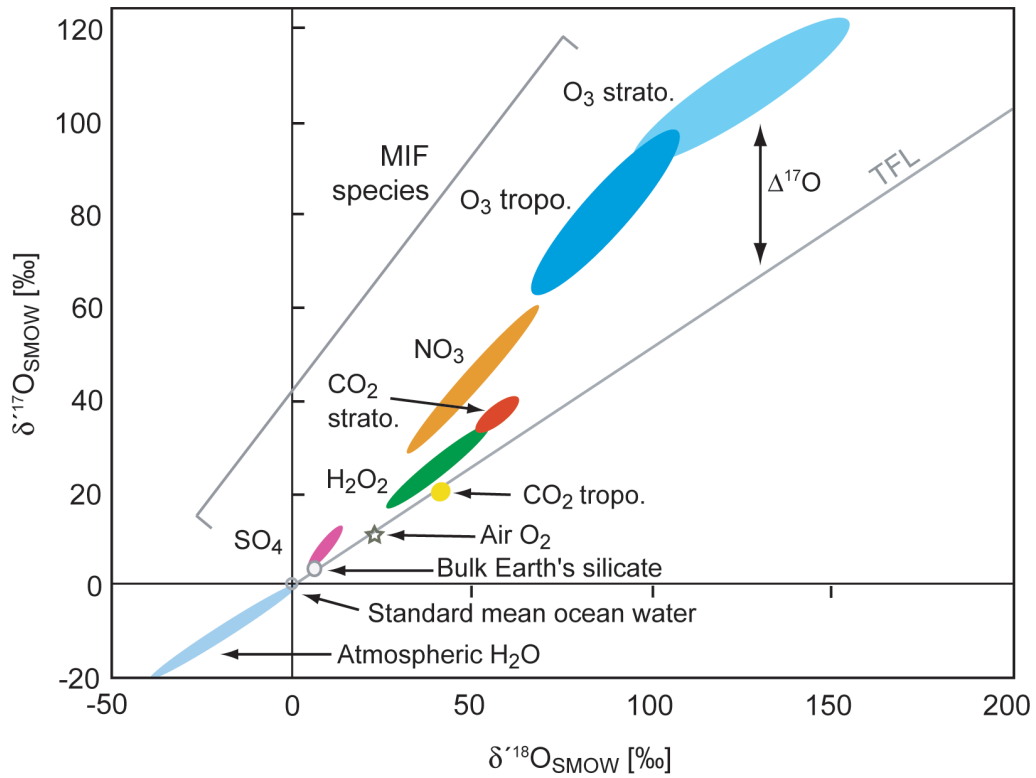


Fig. 1-3: Triple oxygen isotope ratios of atmospheric species (adapted from Thieme et al., 2006). Stratospheric gases show distinct deviations from the terrestrial fractionation line, whereas tropospheric gases, namely O₂ and CO₂ show only a small or no deviation from a mass-dependent reference line, such as the terrestrial fractionation line.

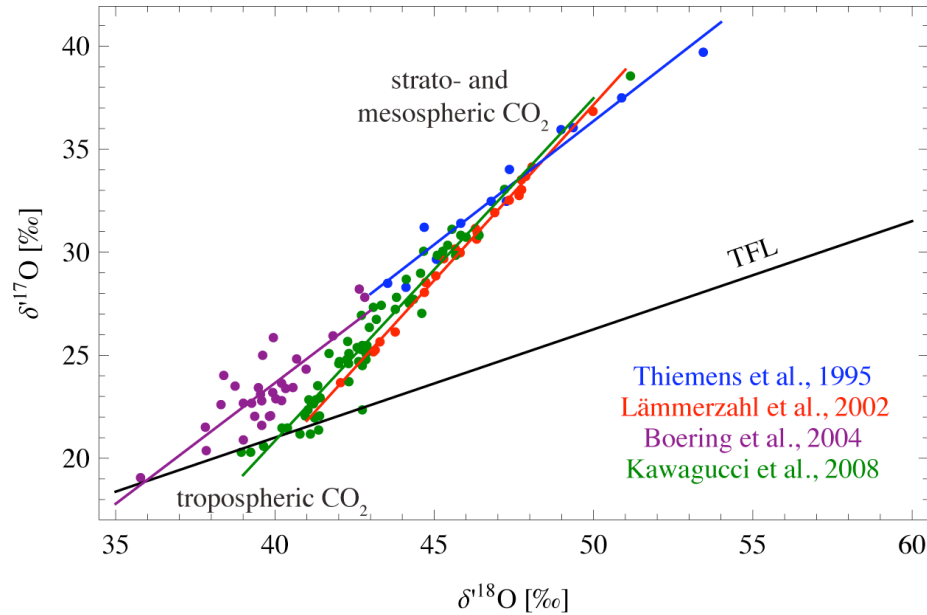


Fig. 1-4: Triple oxygen isotope composition of atmospheric CO_2 . Strato- and mesospheric carbon dioxide shows a large oxygen isotope anomaly with $\Delta^{17}\text{O}$ values of up to 10‰. The distinct anomaly is a result of atmospheric reaction mechanisms. Note that the Boering et al. (2004) dataset slightly deviates from the other datasets (Kawagucci et al., 2008; Lämmerzahl et al., 2002; Thiemens et al., 1995b). Most likely, these CO_2 samples were affected by exchange with water during storage (see Boering et al., 2004). Tropospheric CO_2 shows $\delta^{18}\text{O}$ values of approximately 39 to 42‰ (corresponding to $\delta^{18}\text{O}$ values of about 40 to 43‰) and $\Delta^{17}\text{O}$ values close to zero. It is the aim of this project to determine the exact magnitude and variability of the $\Delta^{17}\text{O}$ signature of a tropospheric end-member.

1.4 The global carbon cycle

Almost all carbon in the atmosphere is present as carbon dioxide. The tropospheric CO_2 concentration and its isotopic composition are controlled by various gross fluxes between the atmosphere and the bio- and hydrosphere: photosynthesis, respiration, soil invasion, oceanic carbon uptake and release, stratosphere–troposphere exchange and anthropogenic CO_2 emissions (Fig. 1-5). In the pre-industrial era, the carbon cycle was in steady state, i.e. the CO_2 sources were balanced by equivalent CO_2 sinks and the carbon dioxide concentration remained constant at about 270 ppm. Since about 1850, the atmospheric carbon cycle is not in a steady state anymore but the CO_2 concentration increases at about 1.9 ppm per year, corresponding to a carbon flux of about 4.1 PgC/yr (Canadell et al., 2007; Le Quéré et al., 2009). At present, the atmospheric CO_2 concentration is approximately at 390 ppm, corresponding to an atmospheric reservoir size of about 830 PgC (Canadell et al., 2007; Le Quéré et al., 2009).

The largest gross fluxes are carbon uptake and release by the biosphere. Terrestrial plants take up carbon dioxide and water to produce organic matter, and as a by-product, release molecular oxygen:



This process is well known as photosynthesis. The overall rate of photosynthetic carbon fixation is referred to as gross primary production. Today, about 120 PgC/yr are fixed by the terrestrial ecosystem (Beer et al., 2010). A fraction of the organic matter is decomposed by respiration.

Besides terrestrial respiration, there is also an abiotic flux coming from soils named soil invasion (Miller et al., 1999a; Tans, 1998). This term describes the process where CO₂ diffuses into the uppermost soil column, and after a certain residence time diffuses back to the atmosphere. Overall, the soil invasion flux has no effect on the atmospheric CO₂ concentration but due to isotope exchange between the carbon dioxide and soil water it might have a significant effect on the oxygen isotope composition of atmospheric CO₂ (Wingate et al., 2009). In the first place, it was thought that only about 20 PgC/yr diffuse from the troposphere into the upper soil layer and vice versa, but recent estimates from Wingate et al. (2009) suggest this exchange flux might be as large as 450 PgC/yr.

Carbon dioxide exchange between the ocean and the atmosphere amounts to about 90 PgC/yr (Heimann and Maier-Reimer, 1996). Overall, there is a small oceanic net sink of about 2 PgC/yr (Canadell et al., 2007; Le Quéré et al., 2009).

Due to atmospheric mixing processes, about 100 PgC/yr are exchanged between the tropo- and stratosphere (Appenzeller et al., 1996). Overall, the mixing process does not affect the CO₂ concentration, but it might be of importance to the triple oxygen isotope composition of tropospheric CO₂ (Hoag et al., 2005).

Anthropogenic CO₂ emissions are small (~9 PgC/yr, see Canadell et al., 2007; Le Quéré et al., 2009) compared to the large gross fluxes from the bio- and hydrosphere. However, as they constantly accumulate in the atmosphere these emissions lead to an alarming increase in CO₂ concentration in the global atmosphere.

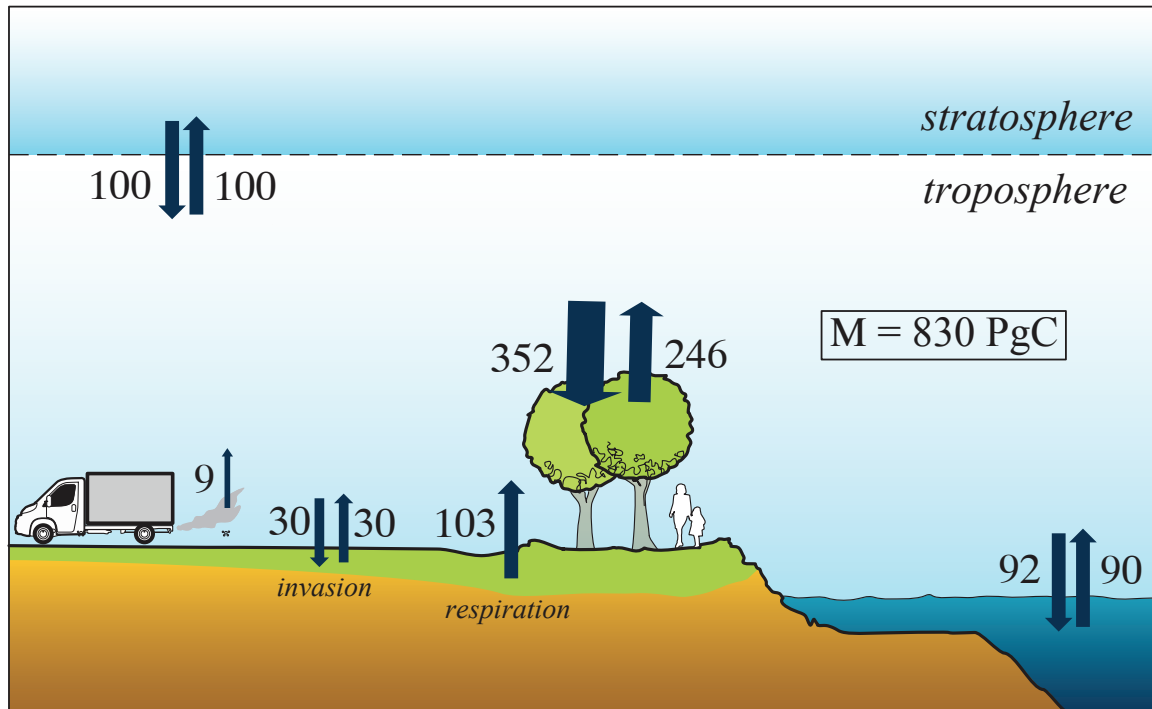


Fig. 1-5: The current day global carbon cycle. Various biogeochemical processes in the bio- and hydrosphere control the atmospheric CO_2 concentration and its carbon and oxygen isotopic composition. The sketch illustrates the major gross fluxes (for a detailed description also see chapter 5). The terrestrial respiration and assimilation fluxes are based on a gross primary production (GPP) of 120 PgC/yr (Beer et al., 2010) and a chloroplast to atmosphere CO_2 concentration ratio of 0.70 (see chapter 5). Since the industrial era, anthropogenic CO_2 emissions have a major effect on atmospheric CO_2 concentrations.

1.5 Focus of study

The aim of this study is to test the potential of ^{17}O -excess as a new tracer in the global and regional carbon cycle. In order to do so, the project was divided into four sub-topics:

- **Chapter 2:** Technique for high-precision analysis of triple oxygen isotope ratios in carbon dioxide

Originally, the triple oxygen isotope analysis of carbon dioxide aimed at detecting large variations in ^{17}O -excess in stratospheric CO_2 samples. As a consequence, state-of-the-art techniques had an analytical uncertainty that was appropriate for the object of study. However, in order to detect small variations in ^{17}O -excess in tropospheric CO_2 , a new technique for high-precision triple oxygen isotope analysis was developed.

- **Chapter 3:** Triple oxygen isotope equilibrium fractionation between carbon dioxide and water

The triple oxygen isotope composition of tropospheric CO_2 is largely controlled by mass-dependent equilibrium fractionation between CO_2 and water in the hydro- and biosphere. Thus, in order to understand small-scale variations in ^{17}O -excess of tropospheric CO_2 it is crucial to know the exact triple oxygen isotope equilibrium fractionation factor described by the exponent θ in the power law function for mass-dependent fractionation.

- **Chapter 4:** On the triple oxygen isotope composition of carbon dioxide from some combustion processes

Anthropogenic CO_2 emissions lead to a steady increase in atmospheric CO_2 concentration on a global scale. In particular, they have a significant influence on the CO_2 concentration and carbon isotope composition of urban air CO_2 . Chapter 4 investigates if and to which extent anthropogenic CO_2 inherits the oxygen isotope anomaly of ambient air O_2 . Carbon dioxide from natural gas and propane-butane combustion, wood chips burning, car exhaust and human breath were investigated. The aim of this project was to test if the triple oxygen isotope composition of CO_2 (denoted with $\Delta^{17}\text{O}$) could act as a tracer for anthropogenic CO_2 emissions in urban air studies.

- **Chapter 5:** Triple oxygen isotope composition of tropospheric CO₂: Observational data and model simulation

Chapter 5 presents triple oxygen isotope data of ambient air CO₂ sampled in Göttingen over the course of 2 years and on top of the Brocken Mountain. The experimental data are compared to a global mass balance model for the triple oxygen isotope composition of tropospheric CO₂. In particular, the mass balance model investigates the sensitivity of $\Delta^{17}\text{O}$ of tropospheric CO₂ to changes in the terrestrial gross primary production.

1.6 References

- Appenzeller, C., Holton, J. R., Rosenlof, K. H., 1996. Seasonal variation of mass transport across the tropopause. *J. Geophys. Res.-Atmos.* 101, 15071-15078.
- Barkan, A., Luz, B., 2011. The relationship among the three stable isotopes of oxygen in air, seawater and marine photosynthesis. *Rapid Commun. Mass Spec.* 25, 2367–2369.
- Barkan, E., Luz, B., 2005. High precision measurements of $^{17}\text{O}/^{16}\text{O}$ and $^{18}\text{O}/^{16}\text{O}$ ratios in H_2O . *Rapid Commun. Mass Spec.* 19, 3737-3742.
- Beer, C., Reichstein, M., Tomelleri, E., Ciais, P., Jung, M., Carvalhais, N., Rödenbeck, C., Arain, M. A., Baldocchi, D., Bonan, G. B., Bondeau, A., Cescatti, A., Lasslop, G., Lindroth, A., Lomas, M., Luyssaert, S., Margolis, H., Oleson, K. W., Rouspard, O., Veenendaal, E., Viovy, N., Williams, C., Woodward, F. I., Papale, D., 2010. Terrestrial gross carbon dioxide uptake: global distribution and covariation with climate. *Science* 329, 834-838.
- Boering, K. A., Jackson, T., Hoag, K. J., Cole, A. S., Perri, M. J., Thiemens, M., Atlas, E., 2004. Observations of the anomalous oxygen isotopic composition of carbon dioxide in the lower stratosphere and the flux of the anomaly to the troposphere. *Geophys. Res. Lett.* 31.
- Canadell, J. G., Le Quéré, C., Raupach, M. R., Field, C. B., Buitenhuis, E. T., Ciais, P., Conway, T. J., Gillett, N. P., Houghton, R. A., Marland, G., 2007. Contributions to accelerating atmospheric CO_2 growth from economic activity, carbon intensity, and efficiency of natural sinks. *Proc. Natl. Acad. Sci.* 104, 18866-18870.
- Cao, X., Liu, Y., 2011. Equilibrium mass-dependent fractionation relationships for triple oxygen isotopes. *Geochim. Cosmochim. Acta* 75, 7435-7445.
- Ciais, P., Denning, A. S., Tans, P. P., Berry, J. A., Randall, D., Collatz, J. G., Sellers, P. J., White, J. W., Troler, M., Meijer, H. A. J., Francey, R. J., Monfray, P., Heimann, M., 1997. A three-dimensional synthesis study of $\delta^{18}\text{O}$ in atmospheric CO_2 : Part 1 Surface fluxes. *J. Geophys. Res.* 102, 5857-5872.
- Ciais, P., Tans, P. P., Troler, M., White, J. W. C., Francey, R. J., 1995. A large northern hemisphere terrestrial CO_2 sink indicated by the $^{13}\text{C}/^{12}\text{C}$ ratio of atmospheric CO_2 . *Science* 269, 1098-1102.
- Coplen, T. B., 2011. Guidelines and recommended terms for expression of stable-isotope-ratio and gas-ratio measurement results. *Rapid Commun. Mass Spec.* 25, 2538-2560.
- Coplen, T. B., Kendall, C., Hopple, J., 1983. Comparison of stable isotope reference samples. *Nature* 302, 236-238.

- Cuntz, M., Ciais, P., Hoffmann, G., Allison, C. E., Francey, R. J., Knorr, W., Tans, P. P., White, J. W. C., Levin, I., 2003a. A comprehensive global three-dimensional model of $\delta^{18}\text{O}$ in atmospheric CO_2 : 2. Mapping the atmospheric signal. *J. Geophys. Res.* 108, ACH2.1-ACH2.19.
- Cuntz, M., Ciais, P., Hoffmann, G., Knorr, W., 2003b. A comprehensive global three-dimensional model of $\delta^{18}\text{O}$ in atmospheric CO_2 : 1. Validation of surface processes. *J. Geophys. Res.* 108, ACH1-ACH23.
- Farquhar, G. D., Lloyd, J., Taylor, J. A., Flanagan, L. B., Syvertsen, J. P., Hubick, K. T., Wong, S. C., Ehleringer, J. R., 1993. Vegetation effects on the isotope composition of oxygen in atmospheric CO_2 . *Nature* 363, 439-443.
- Francey, R. J., Tans, P. P., 1987. Latitudinal variation in oxygen-18 of atmospheric CO_2 . *Nature* 327, 495-497.
- Heimann, M., Maier-Reimer, E., 1996. On the relations between the oceanic uptake of CO_2 and its carbon isotopes. *Global Biogeochem. Cy.* 10, 89-110.
- Hoag, K. J., Still, C. J., Fung, I. Y., Boering, K. A., 2005. Triple oxygen isotope composition of tropospheric carbon dioxide as a tracer of terrestrial gross carbon fluxes. *Geophys. Res. Lett.* 32, 1-5.
- IPCC, 2007. Climate change 2007: The physical science basis: Contribution of Working Group I to the Fourth Assessment Report of the Intergovernmental Panel on Climate Change. Cambridge University Press, New York, p. 996.
- Kawagucci, S., Tsunogai, U., Kudo, S., Nakagawa, F., Honda, H., Aoki, S., Nakazawa, T., Tsutsumi, M., Gamo, T., 2008. Long-term observation of mass-independent oxygen isotope anomaly in stratospheric CO_2 . *Atmos. Chem. Phys.* 8, 6189-6197.
- Keeling, C. D., 1958. The concentration and isotopic abundances of atmospheric carbon dioxide in rural areas. *Geochim. Cosmochim. Acta* 13, 322-334.
- Keeling, C. D., 1960. The concentration and isotopic abundances of carbon dioxide in the atmosphere. *Tellus* 12, 200-203.
- Keeling, C. D., 1961. The concentration and isotopic abundances of carbon dioxide in rural and marine air. *Geochim. Cosmochim. Acta* 24, 277-298.
- Krankowsky, D., Lämmerzahl, P., Mauersberger, K., 2000. Isotopic measurements of stratospheric ozone. *Geophys. Res. Lett.* 27, 2593-2595.
- Lämmerzahl, P., Röckmann, T., Brenninkmeijer, C. A. M., Krankowsky, D., Mauersberger, K., 2002. Oxygen isotope composition of stratospheric carbon dioxide. *Geophys. Res. Lett.* 29, 1582.

- Le Quéré, C., Raupach, M. R., Canadell, J. G., Marland, G., et al., 2009. Trends in the sources and sinks of carbon dioxide. *Nature Geosci.* 2, 831-836.
- Luz, B., Barkan, E., 2005. The isotopic ratios $^{17}\text{O}/^{16}\text{O}$ and $^{18}\text{O}/^{16}\text{O}$ in molecular oxygen and their significance in biogeochemistry. *Geochim. Cosmochim. Acta* 69, 1099-1110.
- Luz, B., Barkan, E., 2010. Variations of $^{17}\text{O}/^{16}\text{O}$ and $^{18}\text{O}/^{16}\text{O}$ in meteoric waters. *Geochim. Cosmochim. Acta* 74, 6276-6286.
- Luz, B., Barkan, E., Bender, M. L., Thiemens, M. H., Boering, K. A., 1999. Triple-isotope composition of atmospheric oxygen as a tracer of biosphere productivity. *Nature* 400, 547-550.
- Mauersberger, K., 1981. Measurement of heavy ozone in the stratosphere. *Geophys. Res. Lett.* 8, 935-937.
- Miller, J. B., Yakir, D., White, J. W. C., Tans, P. P., 1999a. Measurement of $^{18}\text{O}/^{16}\text{O}$ in the soil-atmosphere CO_2 flux. *Global Biogeochem. Cy.* 13, 761-774.
- Miller, M. F., Franchi, I. A., Sexton, A. S., Pillinger, C. T., 1999b. High precision $\delta^{17}\text{O}$ isotope measurements of oxygen from silicates and other oxides: method and applications. *Rapid Commun. Mass Spec.* 13, 1211-1217.
- Pack, A., Albrecht, N., Hofmann, M. E. G., Horváth, B., Gehler, A., 2012. Experimental data on variations in triple oxygen isotope equilibrium fractionation exponents. ISI, Washington DC.
- Pack, A., Toulouse, C., Przybilla, R., 2007. Determination of oxygen triple isotope ratios of silicates without cryogenic separation of NF_3 - technique with application to analyses of technical O_2 gas and meteorite classification. *Rapid Commun. Mass Spec.* 21, 3721-3728.
- Peylin, P., Ciais, P., Denning, A. S., Tans, P. P., Berry, J. A., White, J. W. C., 1999. A 3-dimensional study of $\delta^{18}\text{O}$ in atmospheric CO_2 : contribution of different land ecosystems. *Tellus B* 51, 642-667.
- Rumble, D., Miller, M. F., Franchi, I. A., Greenwood, R. C., 2007. Oxygen three-isotope fractionation lines in terrestrial silicate minerals: An inter-laboratory comparison of hydrothermal quartz and eclogitic garnet. *Geochim. Cosmochim. Acta* 71, 3592-3600.
- Tanaka, R., Nakamura, E., 2012. Kinetic isotope fractionation effect observed in oxygen triple isotope ratios in terrestrial silicate minerals. Sixth International Symposium on Isotopomers, Washington DC.
- Tans, P. P., 1998. Oxygen isotopic equilibrium between carbon dioxide and water in soils. *Tellus B* 50, 163-178.

- Thiemens, M., Jackson, T., Brenninkmeijer, C. A. M., 1995a. Observation of a mass independent oxygen isotopic composition in terrestrial stratospheric CO₂, the link to ozone chemistry, and the possible occurrence in the Martian atmosphere. *Geophys. Res. Lett.* 22, 255-257.
- Thiemens, M. H., 2006. History and applications of mass-independent isotope effects. *Annu. Rev. Earth Planet. Sci.* 34, 217-262.
- Thiemens, M. H., Heidenreich, J. E. I., 1983. The mass-independent fractionation of oxygen: A novel isotope effect and its possible cosmochemical implications. *Science* 219, 1073-1075.
- Thiemens, M. H., Jackson, T., 1991. Oxygen isotope fractionation in stratospheric CO₂. *Geophys. Res. Lett.* 18, 669-672.
- Thiemens, M. H., Jackson, T., Zipf, E. C., Erdman, P. W., van Egmond, C., 1995b. Carbon dioxide and oxygen isotope anomalies in the mesosphere and stratosphere. *Science* 270, 969-972.
- Welp, L. R., Keeling, R. F., Meijer, H. A. J., Bollenbacher, A. F., Piper, S. C., Yoshimura, K., Francey, R. J., Allison, C. E., Wahlen, M., 2011. Interannual variability in the oxygen isotopes of atmospheric CO₂ driven by El Nino. *Nature* 477, 579-582.
- Wingate, L., Ogée, J., Cuntz, M., Genty, B., Reiter, I., Seibt, U., Yakir, D., Maseyk, K., Pendall, E. G., Barbour, M. M., Mortazavi, B., Burlett, R. g., Peylin, P., Miller, J., Mencuccini, M., Shim, J. H., Hunt, J., Grace, J., 2009. The impact of soil microorganisms on the global budget of $\delta^{18}\text{O}$ in atmospheric CO₂. *Proc. Natl. Acad. Sci.* 106, 22411-22415.
- Young, E. D., Galy, A., Nagahara, H., 2002. Kinetic and equilibrium mass-dependent isotope fractionation laws in nature and their geochemical and cosmochemical significance. *Geochim. Cosmochim. Acta* 66, 1095-1104.
- Yung, Y. L., Demore, W. B., Pinto, J. P., 1991. Isotopic exchange between carbon dioxide and ozone via O(¹D) in the stratosphere. *Geophys. Res. Lett.* 18, 13-16.

2 Technique for high-precision analysis of triple oxygen isotope ratios in carbon dioxide

Hofmann, M.E.G. and Pack, A., 2010. Technique for high-precision analysis of triple oxygen isotope ratios in carbon dioxide. *Anal. Chem.* 82, 4357-4361

2.1 Abstract

Since the discovery of mass-independent isotope effects in stratospheric and tropospheric gases, the analysis of triple oxygen isotope abundance in carbon dioxide gained in importance. However, precise triple oxygen isotope determination in carbon dioxide is a challenging task due to mass-interference of ^{17}O and ^{13}C variations. Here, we present a novel analytical technique that allows us to determine slight deviations of CO_2 from the terrestrial fractionation line (TFL). Our approach is based on isotopic equilibration between CO_2 gas and CeO_2 powder at 685 °C and subsequent mass spectrometric analysis of ceria powder by infrared-laser fluorination. We found that $\beta_{\text{CO}_2\text{-CeO}_2}$, the exponent in the relation $\alpha^{17/16} = (\alpha^{18/16})^\beta$, amounts to 0.5240 ± 0.0011 at 685 °C.¹ The oxygen isotope anomaly of CO_2 ($\Delta^{17}\text{O}$) can be determined for a single analysis of CeO_2 with a precision of $\pm 0.05\text{‰}$ (1σ). Our CO_2 - CeO_2 equilibration procedure is performed with an excess of CO_2 so that one analysis of $\Delta^{17}\text{O}$ on CO_2 requires at least 3.5 mmol of CO_2 gas. Our new technique allows accurate and precise determination of $\Delta^{17}\text{O}$ in CO_2 and opens up a new field for investigating triple oxygen isotope abundance in various types of natural CO_2 .

2.2 Introduction

Oxygen isotope anomalies of atmospheric trace gases (O_3 , NO_3 , CO_2 , H_2O_2 , SO_4 , CO , N_2O) (Thiemens, 2006) originate from UV-induced photoreactions (Thiemens and

¹ Note that in this chapter the exponent for CO_2 - CeO_2 isotope exchange and the slope of the terrestrial fractionation line are both denoted with β . Apart from this chapter, triple oxygen isotope exponents are defined as λ and θ values as introduced in section 1.2.2 and 1.2.3.

Heidenreich, 1983), namely, in association with the formation of O₃. Stratospheric CO₂ inherits its oxygen isotope anomaly of $\Delta^{17}\text{O} \approx +10 \text{ ‰}$ from isotopic exchange of electronically excited oxygen, O(¹D) and CO₂ (Perri et al., 2003; Yung et al., 1991). The distinct anomaly of stratospheric CO₂ is diluted with isotopically normal CO₂ when it enters the troposphere so that ground level CO₂ shows little if any anomaly (Thiemens and Jackson, 1991; Thiemens et al., 1995b). Hoag et al. (2005), however, predicted an oxygen isotope anomaly of tropospheric CO₂ of $\Delta^{17}\text{O} = +0.15 \text{ ‰}$ (relative to the TFL with a slope of $\beta = 0.516$). They suggest that high-precision data on $\Delta^{17}\text{O}$ of tropospheric CO₂ will improve geochemical modeling of terrestrial gross carbon fluxes.

Published data on the triple oxygen isotope composition of tropospheric CO₂ are too imprecise to verify the presence of such a small anomaly as predicted by Hoag et al (2005). Precise determination of oxygen isotope anomalies in CO₂ is a challenging task, namely, due to mass-interference of ¹²C¹⁷O¹⁶O on ¹³C¹⁶O₂.

To date, four techniques have been developed to determine $\Delta^{17}\text{O}$ in CO₂. Thiemens and Jackson (1991) fluorinated CO₂ at 800 °C for 48 h using BrF₅ as the reactant. The oxygen isotope ratios are measured on the resulting molecular oxygen. The measurement error of $\Delta^{17}\text{O}$ amounts to about 0.1 ‰. Brenninkmeijer and Röckmann (1998) described a procedure where CO₂ reacts with H₂ to methane and water. The latter is fluorinated, and the oxygen isotope anomaly is analyzed on the resulting O₂. The precision and accuracy of $\Delta^{17}\text{O}$ analysis is specified as $\pm 0.2 \text{ ‰}$. Assonov and Brenninkmeijer (2001) described an alternative approach that is based on oxygen isotope exchange of CO₂ with solid CeO₂. The $\Delta^{17}\text{O}$ of CO₂ can be deduced by comparing the mass ratios 45/44 and 46/44 of the CO₂ before and after equilibrating the gas sample with CeO₂. The procedure goes along with a relatively large error of $\Delta^{17}\text{O}$ of $\pm 0.33 \text{ ‰}$. Kawagucci et al. (2005) developed a simple analytical system where one CO₂ aliquot is measured directly in the mass spectrometer, the other aliquot exchanges its oxygen isotopes with CuO at 900 °C prior to mass spectrometric analysis. As in the case of the technique described by Assonov and Brenninkmeijer (2001), the $\Delta^{17}\text{O}$ of CO₂ is determined by comparison of the mass ratios 45/44 and 46/44 of the two subsamples. This procedure requires only nanomole quantities of sample CO₂, but the standard deviation of $\Delta^{17}\text{O}$ is $\pm 0.35 \text{ ‰}$.

Despite these recent advancements in $\Delta^{17}\text{O}$ analysis, the uncertainties remain too large to reveal the predicted oxygen isotope anomaly of tropospheric CO₂. This study aims at establishing a new analytical technique that allows accurate and precise determination of $\Delta^{17}\text{O}$ in CO₂ with an uncertainty better than $\pm 0.1 \text{ ‰}$.

2.3 Methods

2.3.1 Definitions

In this study, $\delta^{17}\text{O}$ and $\delta^{18}\text{O}$ values are given relative to SMOW. $\Delta^{17}\text{O}$ values are reported relative to the rocks- and minerals-defined TFL with a slope of 0.52520 and an intercept of -0.015 ± 0.019 ‰. The $\Delta^{17}\text{O}$ -value is defined by the vertical deviation of a sample from the TFL in a $\delta^{17}\text{O}$ vs. $\delta^{18}\text{O}$ diagram (Miller, 2002; Miller et al., 2002; Pack et al., 2007), where $\delta^{17}\text{O} = 10^3 \ln (\delta^{17}\text{O}/10^3 + 1)$ and $\delta^{18}\text{O} = 10^3 \ln (\delta^{18}\text{O}/10^3 + 1)$ (Miller et al., 2002; Young et al., 2002). All data on $\Delta^{17}\text{O}_{\text{TFL}}$ (Table 2-1 and 2-2) can be converted to any other reference line (RL), e.g. the meteoric water line (Barkan and Luz, 2005; Meijer and Li, 1998), according to the relation: $\Delta^{17}\text{O}_{\text{RL}} = \delta^{17}\text{O} - \delta^{18}\text{O} \times \beta_{\text{RL}}$, given that the reference line passes through the origin. The TFL was defined by a large number of analyses of rocks and minerals (MORB glass, Bushveld complex chromite, UWG-2 garnet, NBS-28 quartz, Dörentrup quartz and sapphire) in Göttingen during the period of June 2008 to January 2009 (data shown in section 2.4).

2.3.2 Oxygen and carbon isotope analyses

All triple oxygen isotope data on CeO_2 were measured by laser fluorination (Sharp, 1990) in combination with continuous flow isotope ratio monitoring mass spectrometry (CF-irmMS). Our in-house reference O_2 gas was calibrated relative to SMOW by E. Barkan (Institute of Earth Sciences, Hebrew University of Jerusalem) and has a $\delta^{18}\text{O}_{\text{SMOW}} = +13.472$ ‰ and a $\delta^{17}\text{O}_{\text{SMOW}} = +6.702$ ‰. Positively charged O_2 ions were analyzed on three Faraday cups in a Thermo MAT 253 gas mass spectrometer. We used ~ 20 mbar purified F_2 gas (Asprey, 1976) as the oxidation agent. Excess F_2 was reacted with NaCl to Cl_2 , which was trapped at -196 °C in a cold trap. Interference of NF ($m/z = 33$) on $^{17}\text{O}^{16}\text{O}$ was eliminated by means of a 5 Å gas chromatography column (Pack et al., 2007).

In the continuous flow mode, the reference gas was injected via an open split valve using a Thermo Gasbench II. The reference gas peaks were ~ 10 V high and ~ 40 s wide. The peak shape was rectangular. The sample peaks were injected by releasing O_2 from a 5 Å molecular sieve trap that was placed in the helium gas stream. The resultant smooth peaks were slightly asymmetric with an amplitude of ~ 20 - 30 V and full width at half-maximum of ~ 15 s. Accuracy and precision of the continuous flow method has been tested by repeated analyses of reference O_2 . The reference gas was expanded into the extraction line and treated as if it had been released from fluorination. The $\delta^{18}\text{O}$ of the analyzed gas was

within ± 0.2 ‰ identical to the reference gas value. The $\delta^{17}\text{O}$ showed a small systematic offset of $+0.080$ ‰, which is due to limitations in linearity of the ion source. All data have been corrected in $\delta^{17}\text{O}$ by 0.080 ‰. Tests with dual inlet did not show any systematic deviation from the expected values.

The error of $\Delta^{17}\text{O}$ was ± 0.05 ‰ (1σ) for a single analysis, and the error in $\delta^{18}\text{O}$ was typically ± 0.25 ‰ (1σ). One run generally contained eight CeO_2 samples (~ 2.5 - 3.1 mg per sample) and four terrestrial reference silicates (~ 1.0 - 1.2 mg per sample). All samples were placed on a nickel sample holder and were baked out overnight in a fluorine atmosphere at 70°C . The terrestrial rocks with $-1\text{ ‰} < \delta^{18}\text{O} < +24\text{ ‰}$ were used to determine the TFL.

Bottle O_2 that was used for O_2 to CO_2 conversion was analyzed by means of dual inlet mass spectrometry using the Thermo MAT 253 relative to the in-house reference O_2 gas ($\delta^{18}\text{O}_{\text{SMOW}} = 13.472$ ‰, $\delta^{17}\text{O}_{\text{SMOW}} = 6.702$ ‰). The $\Delta^{17}\text{O}$ of the in-house reference O_2 was determined by comparison with rock and mineral data that define the TFL. The uncertainty in $\Delta^{17}\text{O}$ is ± 0.02 ‰.

Analyses of $\delta^{18}\text{O}$ and $\delta^{13}\text{C}$ (relative to PDB) of CO_2 gas were performed on a Finnigan Delta plus mass spectrometer. The CO_2 samples were analyzed in a dual inlet mode. Values of $\delta^{13}\text{C}$ and $\delta^{18}\text{O}$ were standardized by comparison with CO_2 generated by phosphoric acid decomposition of NBS-19 ($\delta^{18}\text{O}_{\text{SMOW}} = +28.65$ ‰; $\delta^{13}\text{C}_{\text{PDB}} = +1.95$ ‰). The uncertainty in $\delta^{18}\text{O}$ and $\delta^{13}\text{C}$ is in the range of ± 0.1 ‰.

2.3.3 Exchange experiments between CO_2 and CeO_2

It has been demonstrated by Assonov and Brenninkmeijer (2001) that CeO_2 exchanges oxygen with CO_2 gas at temperatures in the range of 650°C in less than 30 min. In our approach, we analyze small amounts of CeO_2 after equilibration with large excesses of gaseous CO_2 .

The equilibration system consists of a quartz glass tube ($V \approx 650\text{ cm}^3$) that is inserted in a horizontal tube furnace (Fig. 2-1). The glass tube can be evacuated by a rotary vane pump (Pfeiffer DUO 005M). The reaction tube can be opened on both endings in order to place the sample shuttle with the CeO_2 powder inside the furnace. Ceria powder was placed on a small platinum plate in order to avoid any exchange with the ceramic shuttle. After insertion of the sample, the line was evacuated and heated to the experimental temperature. Subsequent to evacuation, the reaction tube was filled with sample CO_2 . We admitted ~ 1000 mbar to the reactor. After equilibration, CO_2 was pumped to waste and the furnace

was switched off to cool down CeO_2 to room temperature. This procedure avoided equilibration with ambient air oxygen.

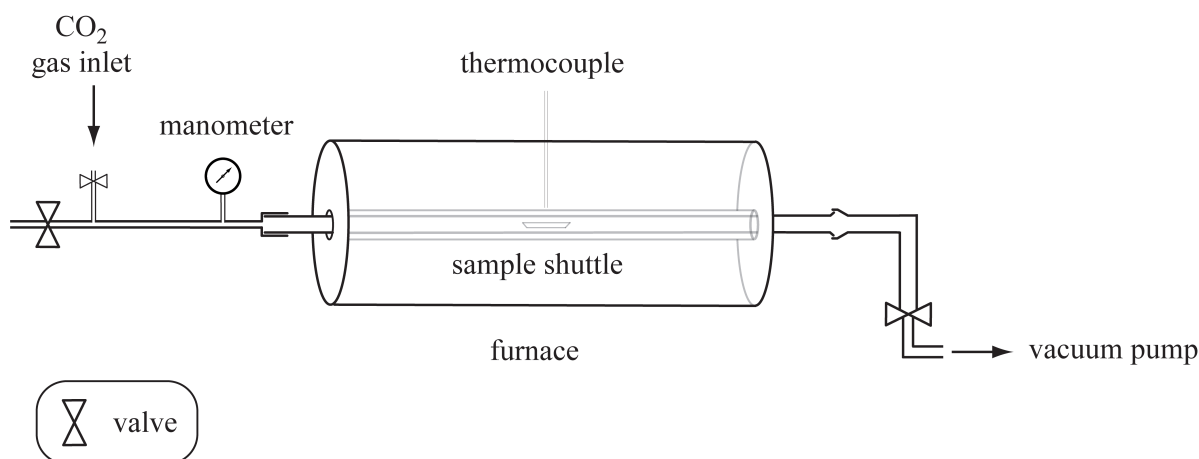


Fig. 2-1: Schematic illustration showing the equilibration apparatus. The apparatus consists of a quartz glass reaction tube that can be opened on both endings to load the sample shuttle, a tube furnace and a furnace thermocouple, a metal gas inlet, a manometer, and a vacuum pump. The isotopic equilibration system ($\approx 650 \text{ cm}^3$) is used to equilibrate ceria and CO_2 at 685°C .

We ran time-dependent CO_2 - CeO_2 equilibration experiments at 635 , 685 , 735 , and 935°C to test if equilibrium is reached within 30 min (Assonov and Brenninkmeijer, 2001). The $\delta^{18}\text{O}$ and $\Delta^{17}\text{O}$ values of CeO_2 of these experiments showed that equilibrium was reached within <10 min for all temperatures investigated. Subsequently, CO_2 - CeO_2 exchange experiments were carried out at 685°C for 30 min to 1 h. The experimental temperature was chosen with respect to earlier research showing that exchange experiments are best carried out at temperatures above 550°C (Assonov and Brenninkmeijer, 2001; Holmgren et al., 1999). Temperatures exceeding 900°C were avoided due to possible oxygen isotope exchange between the quartz glass reaction tube and the gaseous sample (Barkan and Luz, 1996).

Granulated CeO_2 (Merck no. 2263) was ground to a powder in order to facilitate diffusive isotopic exchange. Equilibration experiments were carried out with untreated ceria (as supplied by Merck) and with the same ceria but after heating it in air for 7 h at 1035°C . For each equilibration experiment, 12-24 mg of CeO_2 (~ 70 - $140 \mu\text{mol}$) exchanged with ~ 18 mmol of gas. The molar CO_2/CeO_2 ratios always exceeded ~ 130 . The $\delta^{18}\text{O}$ analyses of CO_2 before and after equilibration showed that the influence of CeO_2 oxygen on the isotopic composition of the bulk system was negligible. Mass balance calculations confirm that the initial isotopic signature of CeO_2 did not affect the isotopic signature of CO_2 , that

is the theoretical shifts in $\delta^{18}\text{O}$ and $\Delta^{17}\text{O}$ values of CO_2 are $<0.1\text{‰}$ and $<0.0005\text{‰}$, respectively. The amount of ceria was chosen to be as low as possible, but it should allow several measurements on the mass spectrometer, each measurement requiring $\sim 2.5\text{--}3.1\text{ mg}$ of ceria.

In order to determine the triple oxygen isotope fractionation, we equilibrated CeO_2 with CO_2 with known $\delta^{18}\text{O}$ and $\Delta^{17}\text{O}$ at 685 °C . The CO_2 with known $\Delta^{17}\text{O}$ was produced by combustion of electrically heated graphite in pure O_2 with known $\delta^{18}\text{O}$ and $\Delta^{17}\text{O}$. Complete conversion was checked by pressure monitoring (CO_2 was cryotrapped during the conversion). The $\delta^{18}\text{O}$ values of the produced CO_2 were also compared with the $\delta^{18}\text{O}$ value of the starting O_2 .

2.3.4 Determination of $\Delta^{17}\text{O}$ of CO_2

In order to use CeO_2 as proxy for the $\Delta^{17}\text{O}$ value of CO_2 , we must know the exponent $\beta_{\text{CO}_2\text{-CeO}_2}$ for the equilibration reaction. $\beta_{\text{CO}_2\text{-CeO}_2}$ is calculated according to

$$\beta_{\text{CO}_2\text{-CeO}_2} = \frac{\Delta^{17}\text{O}_{\text{CO}_2} - \Delta^{17}\text{O}_{\text{CeO}_2}}{\delta^{18}\text{O}_{\text{CO}_2} - \delta^{18}\text{O}_{\text{CeO}_2}} + \beta_{\text{TFL}} \quad \text{Eq. 2-1}$$

The β_{TFL} value denotes the slope of the TFL, and the $\Delta^{17}\text{O}$ values describe deviations from the TFL (Fig. 2-2). The $\Delta^{17}\text{O}$ and $\delta^{18}\text{O}$ values of CO_2 and CeO_2 denote the isotopic composition of CO_2 and CeO_2 after equilibration. The exponent $\beta_{\text{CO}_2\text{-CeO}_2}$ was determined in equilibrium exchange experiments between CeO_2 and CO_2 with known $\Delta^{17}\text{O}$.

The oxygen isotope anomaly of CO_2 gas is determined from the isotope composition of CeO_2 :

$$\Delta^{17}\text{O}_{\text{CO}_2} = \Delta^{17}\text{O}_{\text{CeO}_2} + (\beta_{\text{CO}_2\text{-CeO}_2} - \beta_{\text{TFL}}) (\delta^{18}\text{O}_{\text{CO}_2} - \delta^{18}\text{O}_{\text{CeO}_2}) \quad \text{Eq. 2-2}$$

Again, β_{TFL} denotes the slope of the TFL and $\Delta^{17}\text{O}$ the deviations from the TFL (Fig. 2-2). The $\delta^{18}\text{O}$ values denote the isotopic signature of CO_2 and CeO_2 brought to equilibrium, whereby $\delta^{18}\text{O}$ does not change during the equilibration process as equilibration is conducted under excess CO_2 conditions.

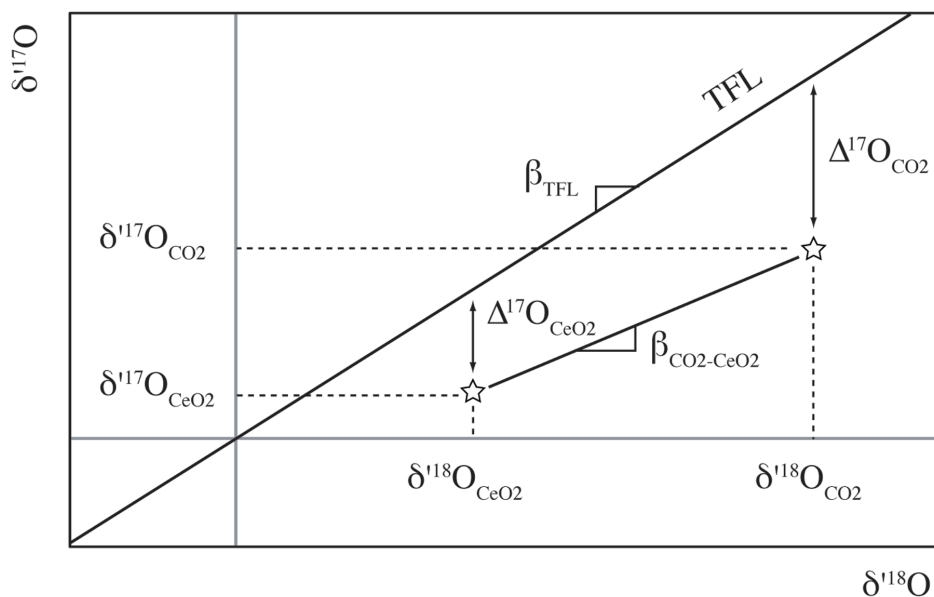


Fig. 2-2: Sketch showing a $\delta^{17}\text{O}$ vs. $\delta^{18}\text{O}$ diagram with all parameters that are involved in $\Delta^{17}\text{O}$ determination of CO_2 .

2.4 Results

2.4.1 Terrestrial fractionation line

The TFL was defined by 161 analyses of rocks and minerals (Fig. 2-3). A Williamson-York regression yielded a TFL with a slope of 0.52520 ± 0.00085 and an intercept of -0.015 ± 0.019 ‰. The regression parameters were calculated using an Excel spreadsheet set up by Cantrell (2008).

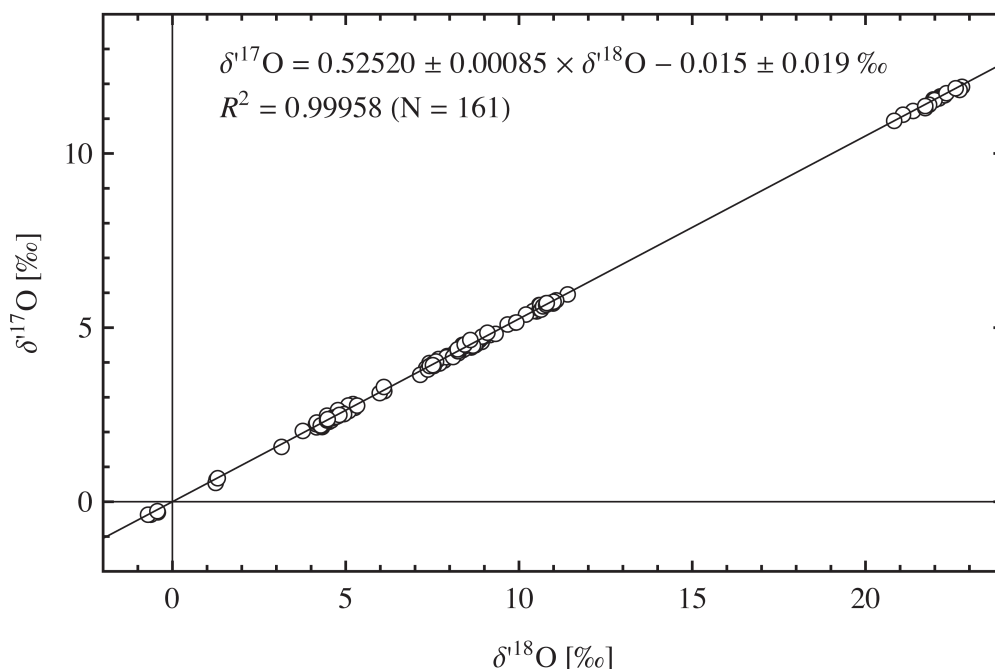


Fig. 2-3: Terrestrial fractionation line. A total of 161 analyses of terrestrial rocks and minerals define the TFL. The bivariate regression line is based on a Williamson-York approach (Cantrell, 2008).

2.4.2 Isotopic composition of the starting materials

Two types of CeO_2 were used as starting material (Table 2-1). Untreated CeO_2 from Merck had a $\delta^{18}\text{O}$ value of $+3.78 \pm 0.27 \text{ ‰}$ and a $\Delta^{17}\text{O}$ value of $-0.23 \pm 0.01 \text{ ‰}$. A fraction of the Merck CeO_2 was preheated in air resulting in a $\delta^{18}\text{O}$ value of $+19.64 \pm 0.08 \text{ ‰}$ and a $\Delta^{17}\text{O}$ value of $-0.37 \pm 0.02 \text{ ‰}$. For determination of $\beta_{\text{CO}_2\text{-CeO}_2}$, bottle O_2 with $\delta^{18}\text{O} = 11.45 \pm 0.03 \text{ ‰}$, $\delta^{17}\text{O} = 5.62 \pm 0.02 \text{ ‰}$, and $\Delta^{17}\text{O}_{\text{TFL}} = -0.38 \pm 0.01 \text{ ‰}$ was used for O_2 to CO_2 conversion and subsequent $\text{CO}_2\text{-CeO}_2$ equilibration.

Table 2-1: Isotopic composition of the two types of CeO₂ starting materials. The $\Delta^{17}\text{O}_{\text{TFL}}$ values are reported relative to the terrestrial fractionation line with a slope of 0.52520 and an intercept of -0.015‰.

sample material	$\delta^{18}\text{O}_{\text{SMOW}} [\text{‰}]$	$\delta^{17}\text{O}_{\text{SMOW}} [\text{‰}]$	$\Delta^{17}\text{O}_{\text{TFL}} [\text{‰}]$
CeO ₂ untreated	3.340	1.494	-0.246
	3.560	1.611	-0.243
	3.666	1.718	-0.192
	4.555	2.143	-0.234
average \pm std error	3.780 \pm 0.267	1.742 \pm 0.142	-0.229 \pm 0.013
CeO ₂ preheated in air (1035 °C, 7 h)	19.690	10.002	-0.324
	19.774	10.012	-0.358
	19.704	9.919	-0.414
	19.410	9.810	-0.369
average \pm std error	19.644 \pm 0.080	9.936 \pm 0.047	-0.367 \pm 0.019

2.4.3 Equilibration experiments

Four CO₂-CeO₂ equilibration experiments were carried out in order to determine $\beta_{\text{CO}_2\text{-CeO}_2}$ at 685 °C (Table 2-2). For each experiment, the equilibrated CeO₂ was analyzed three or four times. The equilibration experiments are based on quantitative conversion of O₂ ($\delta^{18}\text{O} = 11.45 \text{ ‰}$; $\delta^{17}\text{O} = 5.62 \text{ ‰}$; $\Delta^{17}\text{O} = -0.38 \text{ ‰}$) to CO₂ and subsequent exchange of oxygen-atoms between CeO₂ and CO₂ with known $\Delta^{17}\text{O}$. Conversion of O₂ ($\delta^{18}\text{O} = 11.45 \pm 0.03 \text{ ‰}$) to CO₂ ($\delta^{18}\text{O} = 11.42 \pm 0.08 \text{ ‰}$) did not result in fractionation in $\delta^{18}\text{O}$, and thus, the $\Delta^{17}\text{O}$ value of the produced CO₂ must equal the $\Delta^{17}\text{O}$ of the initial O₂ gas. The slope $\beta_{\text{CO}_2\text{-CeO}_2}$ for the CO₂-CeO₂ equilibrium was determined to 0.5240 ± 0.0011 at 685 °C (Fig. 2-4). The fractionation factor $1000 \ln \alpha$ between CO₂ and CeO₂ was determined as $10.89 \pm 0.44 \text{ ‰}$.

Table 2-2: Data obtained from four CeO₂-CO₂ equilibration experiments. The $\Delta^{17}\text{O}_{\text{TFL}}$ values are reported relative to the terrestrial fractionation line with a slope of 0.52520 and an intercept of -0.015‰.

no.	T	equili- bration time	sample material	$\delta^{18}\text{O}_{\text{SMOW}}$ [‰]	$\delta^{17}\text{O}_{\text{SMOW}}$ [‰]	$\Delta^{17}\text{O}_{\text{TFL}}$ [‰]	$\beta_{\text{CO}_2\text{-CeO}_2}$ \pm std error
1	685 °C	1 h	CeO ₂ (preheated) + CO ₂ ($\delta^{18}\text{O}$ = 11.6‰)	0.720	0.731	0.338	
				0.593	0.597	0.270	
				0.722	0.765	0.371	
				0.538	0.614	0.316	
				0.720	0.731	0.338	
			average \pm std error	-0.643 \pm 0.046	-0.677 \pm 0.042	-0.324 \pm 0.021	0.5209 \pm 0.0021
2	685 °C	30 min	CeO ₂ (untreated) + CO ₂ ($\delta^{18}\text{O}$ = 11.6‰)	0.516	0.196	0.452	
				0.511	0.102	0.355	
				0.482	0.017	0.255	
				0.591	0.128	0.423	
			average \pm std error	0.525 \pm 0.023	-0.111 \pm 0.037	-0.371 \pm 0.044	0.5248 \pm 0.0021
3	685 °C	30 min	CeO ₂ (untreated) + CO ₂ ($\delta^{18}\text{O}$ = 11.6‰)	1.007	0.208	-0.307	
				0.914	0.050	-0.415	
				0.889	0.079	-0.372	
				0.854	0.021	-0.412	
			average \pm std error	0.916 \pm 0.033	0.089 \pm 0.041	-0.377 \pm 0.025	0.5252 \pm 0.0021
4	685 °C	30 min	CeO ₂ (untreated) + CO ₂ ($\delta^{18}\text{O}$ = 11.6‰)	1.449	0.400	-0.345	
				1.609	0.405	-0.425	
				1.571	0.445	-0.365	
			average \pm std error	1.543 \pm 0.042	0.417 \pm 0.012	-0.378 \pm 0.021	0.5254 \pm 0.0021

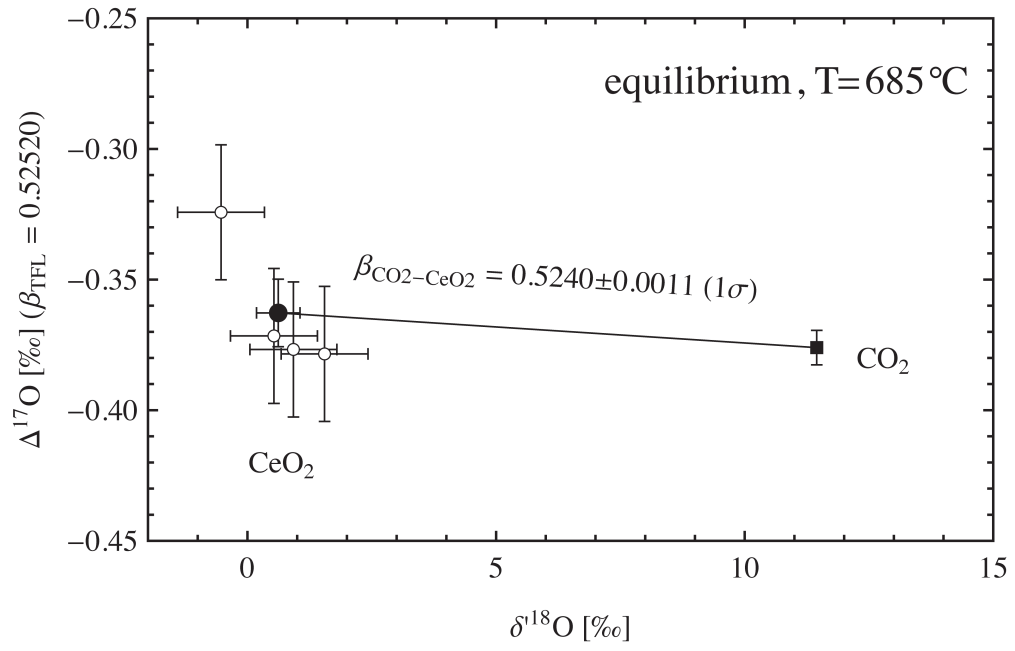


Fig. 2-4: Plot of $\Delta^{17}\text{O}$ vs. $\delta^{18}\text{O}$ showing the composition of CeO_2 and CO_2 at equilibrium ($T = 685^{\circ}\text{C}$, four experiments, \circ). Determination of $\beta_{\text{CO}_2-\text{CeO}_2}$ is based on mean $\delta^{18}\text{O}$ and $\Delta^{17}\text{O}$ values of the four equilibration experiments (\bullet) and the data point for CO_2 (\blacksquare , $N = 7$)

2.4.4 Uncertainty in $\Delta^{17}\text{O}$ determination on CO_2

The uncertainty of $\Delta^{17}\text{O}_{\text{CO}_2}$ was determined for a single analysis to $\pm 0.05\%$ (1σ). The uncertainty is based on error propagation for Eq. 2-2. The uncertainty in $\Delta^{17}\text{O}$ of CeO_2 is $\pm 0.05\%$ and dominates the overall uncertainty in $\Delta^{17}\text{O}$ analysis of CO_2 since the influence of the uncertainties of β_{TFL} , $\beta_{\text{CO}_2\text{-CeO}_2}$, $\delta'^{18}\text{O}_{\text{CO}_2}$, and $\delta'^{18}\text{O}_{\text{CeO}_2}$ on the overall uncertainty $\Delta^{17}\text{O}_{\text{CO}_2}$ is an order of magnitude smaller than the uncertainty of $\Delta^{17}\text{O}_{\text{CeO}_2}$.

2.5 Discussion

Our data show that full equilibrium is reached within 30 min at 685 °C. The equilibration experiments confirm earlier findings of Assonov and Brenninkmeijer (2001) that ceria is an excellent oxygen exchange medium in CO_2 exchange experiments.

We determined $\beta_{\text{CO}_2\text{-CeO}_2}$ to 0.5240 ± 0.0011 at 685 °C. Our β value for equilibrium fractionation between $\text{CO}_2\text{-CeO}_2$ is lower than the high-temperature limit of β given as 0.529 (Young et al., 2002). This demonstrates that $\beta = 0.529$ is not a universal value even for equilibration at 685 °C. For $\text{CO}_2\text{-H}_2\text{O}$ equilibrium, Matsuhisa et al. (1978) predicted also a β value < 0.529 . The authors also demonstrate that the exponent β for $\text{CO}_2\text{-H}_2\text{O}$ equilibrium is temperature dependent. For water-steam fractionation, however, β is identical to the high-temperature approximation of 0.529 (Barkan and Luz, 2005).

We show that measurement of ceria that has been in equilibrium with CO_2 is a suitable proxy for $\Delta^{17}\text{O}$ of CO_2 . On the basis of the $\beta_{\text{CO}_2\text{-CeO}_2}$ value determined in this study, $\Delta^{17}\text{O}$ of CO_2 can be deduced from $\text{CO}_2\text{-CeO}_2$ equilibration at 685 °C according to:

$$\Delta^{17}\text{O}_{\text{CO}_2} = \Delta^{17}\text{O}_{\text{CeO}_2} + (0.5240 - 0.5252) \times 10.90\% \quad \text{Eq. 2-3}$$

Since the relative errors of β_{TFL} , $\beta_{\text{CO}_2\text{-CeO}_2}$, and $\delta'^{18}\text{O}$ on both CO_2 and CeO_2 are comparatively small, the uncertainty largely depends on the uncertainty in $\Delta^{17}\text{O}$ analysis of CeO_2 . As $\Delta^{17}\text{O}$ of CeO_2 can be analyzed with a precision of $\pm 0.05\%$ (1σ), $\Delta^{17}\text{O}$ of CO_2 can be determined with a precision of $\pm 0.05\%$ (1σ) for a single analysis.

The analytical error of our approach is by a factor of 3-5 smaller than the analytical uncertainty indicated by Kawagucci et al. (2005), Assonov and Brenninkmeijer (2001), and Brenninkmeijer and Röckmann (1998). It is by a factor of ~ 2 better than the analytical error indicated by Thiemens and Jackson (1991).

A clear disadvantage of our procedure is that it requires a large amount of CO₂ because we need a high molar CO₂/CeO₂ ratio (>200). For CO₂ samples whose $\delta^{18}\text{O}$ composition falls between ~ 10 and ~ 50 ‰ and whose $\Delta^{17}\text{O}$ value is $-1 \text{ ‰} \leq \Delta^{17}\text{O} \leq +1 \text{ ‰}$, at least 3.5 mmol of CO₂ (~ 80 mL STP) are required for equilibration with ~ 3 mg of CeO₂.

Sampling of millimole quantities of natural CO₂ might be difficult and time-consuming because CO₂ is a trace gas in the atmosphere. However, Brenninkmeijer and Röckmann (Brenninkmeijer, 1991; Brenninkmeijer and Röckmann, 1996) present a cryogenic trap that is suitable for extracting millimole quantities of CO₂ from natural gas mixtures.

Our analytical technique opens up a new field for investigating the triple oxygen isotope abundance of various types of natural and anthropogenic CO₂ in the lowermost troposphere and biosphere. The most promising application is high-precision analysis of tropospheric CO₂, which will be useful to investigate carbon circulation between the atmosphere and the biosphere (Hoag et al., 2005). $\Delta^{17}\text{O}$ analysis of ambient air CO₂ allows us to verify the prediction of Hoag et al (2005) that tropospheric CO₂ should have an oxygen isotope anomaly of -0.22 ‰ (relative to TFL with $\beta_{\text{TFL}} = 0.525$). The precision of our new technique is by a factor of 4 smaller than the predicted oxygen isotope anomaly of tropospheric CO₂, and thus, we will be able to resolve such small deviations from the TFL. Future data are likely to elucidate the potential of $\Delta^{17}\text{O}$ as a tracer of biosphere-atmosphere interaction.

2.6 Acknowledgment

We thank E. Barkan for calibration of our in-house reference O₂ gas relative to SMOW. We also thank the anonymous reviewers for their helpful comments. This project was partly funded by the German Science Foundation (AP, Project PA909/4-1).

2.7 References

- Asprey, L. B., 1976. Preparation of very pure fluorine gas. *J. Fluor. Chem.* 7, 359-361.
- Assonov, S. S., Brenninkmeijer, C. A. M., 2001. A new method to determine the ^{17}O isotopic abundance in CO_2 using oxygen isotope exchange with a solid oxide. *Rapid Commun. Mass Spec.* 15, 2426-2437.
- Barkan, E., Luz, B., 1996. Conversion of O_2 into CO_2 for high-precision oxygen isotope measurements. *Anal. Chem.* 68, 3507-3510.
- Barkan, E., Luz, B., 2005. High precision measurements of $^{17}\text{O}/^{16}\text{O}$ and $^{18}\text{O}/^{16}\text{O}$ ratios in H_2O . *Rapid Commun. Mass Spec.* 19, 3737-3742.
- Brenninkmeijer, C. A. M., 1991. Robust, high-efficiency, high-capacity cryogenic trap. *Anal. Chem.* 63, 1182-1184.
- Brenninkmeijer, C. A. M., Röckmann, T., 1996. Russian doll type cryogenic traps: improved design and isotope separation effects. *Anal. Chem.* 68, 3050-3053.
- Brenninkmeijer, C. A. M., Röckmann, T., 1998. A rapid method for the preparation of O_2 from CO_2 for mass spectrometric measurement of $^{17}\text{O}/^{16}\text{O}$ ratios. *Rapid Commun. Mass Spec.* 12, 479-483.
- Cantrell, C. A., 2008. Technical Note: Review of methods for linear least-squares fitting of data and application to atmospheric chemistry problems. *Atmos. Chem. Phys.* 8, 5477-5487.
- Hoag, K. J., Still, C. J., Fung, I. Y., Boering, K. A., 2005. Triple oxygen isotope composition of tropospheric carbon dioxide as a tracer of terrestrial gross carbon fluxes. *Geophys. Res. Lett.* 32, 1-5.
- Holmgren, A., Duprez, D., Andersson, B., 1999. A model of oxygen transport in Pt/ceria catalysts from isotope exchange. *J. Cat.* 182, 441-448.
- Kawagucci, S., Tsunogai, U., Kudo, S., Nakagawa, F., Honda, H., Aoki, S., Nakazawa, T., Gamo, T., 2005. An analytical system for determining $\delta^{17}\text{O}$ in CO_2 using continuous flow-isotope ratio MS. *Anal. Chem.* 77, 4509-4514.
- Matsuhisa, Y., Goldsmith, J. R., Clayton, R. N., 1978. Mechanisms of hydrothermal crystallization of quartz at 250°C and 15kbar. *Geochim. Cosmochim. Acta* 42, 173-182.
- Meijer, H. A. J., Li, W. J., 1998. The use of electrolysis for accurate $\delta^{17}\text{O}$ and $\delta^{18}\text{O}$ isotope measurements in water. *Isot. Environ. Healt. S.* 34, 349 - 369.

- Miller, M. F., 2002. Isotopic fractionation and the quantification of ^{17}O anomalies in the oxygen three-isotope system: an appraisal and geochemical significance. *Geochim. Cosmochim. Acta* 66, 1881-1889.
- Miller, M. F., Franchi, I. A., Thiemens, M. H., Jackson, T. L., Brack, A., Kurat, G., Pillinger, C. T., 2002. Mass-independent fractionation of oxygen isotopes during thermal decomposition of carbonates. *Proc. Natl. Acad. Sci. USA* 99, 10988-10993.
- Pack, A., Toulouse, C., Przybilla, R., 2007. Determination of oxygen triple isotope ratios of silicates without cryogenic separation of NF_3 - technique with application to analyses of technical O_2 gas and meteorite classification. *Rapid Commun. Mass Spec.* 21, 3721-3728.
- Perri, M. J., Van Wyngarden, A. L., Boering, K. A., Lin, J. H., Lee, Y. T., 2003. Dynamics of the $\text{O}(^1\text{D})+\text{CO}_2$ oxygen isotope exchange reaction. *J. Chem. Phys.* 119, 8213-8216.
- Sharp, Z. D., 1990. A laser-based microanalytical method for the *in situ* determination of oxygen isotope ratios of silicates and oxides. *Geochim. Cosmochim. Acta* 54, 1353-1357.
- Thiemens, M. H., 2006. History and applications of mass-independent isotope effects. *Annu. Rev. Earth Planet. Sci.* 34, 217-262.
- Thiemens, M. H., Heidenreich, J. E. I., 1983. The mass-independent fractionation of oxygen: A novel isotope effect and its possible cosmochemical implications. *Science* 219, 1073-1075.
- Thiemens, M. H., Jackson, T., 1991. Oxygen isotope fractionation in stratospheric CO_2 . *Geophys. Res. Lett.* 18, 669-672.
- Thiemens, M. H., Jackson, T., Zipf, E. C., Erdman, P. W., van Egmond, C., 1995b. Carbon dioxide and oxygen isotope anomalies in the mesosphere and stratosphere. *Science* 270, 969-972.
- Young, E. D., Galy, A., Nagahara, H., 2002. Kinetic and equilibrium mass-dependent isotope fractionation laws in nature and their geochemical and cosmochemical significance. *Geochim. Cosmochim. Acta* 66, 1095-1104.
- Yung, Y. L., Demore, W. B., Pinto, J. P., 1991. Isotopic exchange between carbon dioxide and ozone via $\text{O}(^1\text{D})$ in the stratosphere. *Geophys. Res. Lett.* 18, 13-16.

3 Triple oxygen isotope equilibrium fractionation between carbon dioxide and water

Hofmann, M.E.G., Horváth, B. and Pack, A., 2012.

Triple oxygen isotope equilibrium fractionation between carbon dioxide and water.

Earth Planet. Sci. Lett. 319-320, 159-164

3.1 Abstract

The growing number of recent high precision triple oxygen isotope data of water and atmospheric gases requires the reinvestigation of the major isotope fractionation processes between the hydro-, bio- and atmosphere. Here we present the experimental triple oxygen isotope fractionation factor between CO₂ gas and water in the temperature range between 2 and 37 °C. We have determined the triple oxygen isotope fractionation factor, $\theta = \ln^{17}\alpha/\ln^{18}\alpha$, for CO₂–water equilibrium and found that $\theta_{\text{CO}_2\text{--water}} = 0.522 \pm 0.002$ ($t_{0.95} \times \text{SEM}$). No temperature dependence was resolved. Knowledge on the triple oxygen isotope equilibrium fractionation between CO₂ and water is crucial for estimating the triple oxygen isotope composition of tropospheric CO₂. Model predictions combined with high-precision $\Delta^{17}\text{O}$ analysis of tropospheric CO₂ might reveal new information on biosphere–atmosphere interactions or the influx of anomalous stratospheric CO₂.

3.2 Introduction

Oxygen isotope exchange between CO₂ and water is a ubiquitous process in the bio- and hydrosphere due to rapid hydration and dehydration of CO₂ in water. The steady exchange between CO₂ and water in leaves, soils and the ocean largely controls the ¹⁸O/¹⁶O ratio of tropospheric CO₂ (Ciais et al., 1997; Farquhar et al., 1993; Francey and Tans, 1987; Friedli et al., 1987; Yakir and Wang, 1996), and as a consequence, it also determines to a great extent the ¹⁷O/¹⁶O ratio of tropospheric CO₂.

Hoag et al. (2005) proposed that the triple oxygen isotope ratios (¹⁷O/¹⁶O, ¹⁸O/¹⁶O) of tropospheric CO₂ might be a tracer of bio-, hydro- and atmosphere interaction. According to their mass balance model, variations in the terrestrial biosphere productivity might induce seasonal variations in the triple oxygen isotope signature of tropospheric CO₂. Moreover, the influx of mass-independently fractionated stratospheric CO₂ (Lämmerzahl

et al., 2002; Thiemens et al., 1995a; Thiemens and Jackson, 1991) suggested to have a measurable impact on the oxygen isotope composition of tropospheric CO₂.

A comprehensive understanding of the triple oxygen isotope composition of tropospheric CO₂ requires the knowledge of the triple oxygen isotope fractionation between CO₂ and water. The triple oxygen isotope fractionation is expressed in terms of $\alpha_{\text{CO}_2\text{-water}}$ and $\theta_{\text{CO}_2\text{-water}}$ (Young et al., 2002) with:

$$^{17}\alpha_{\text{CO}_2\text{-water}} = \frac{\left(\frac{^{17}\text{O}}{^{16}\text{O}}\right)_{\text{CO}_2}}{\left(\frac{^{17}\text{O}}{^{16}\text{O}}\right)_{\text{water}}} \quad \text{and} \quad ^{18}\alpha_{\text{CO}_2\text{-water}} = \frac{\left(\frac{^{18}\text{O}}{^{16}\text{O}}\right)_{\text{CO}_2}}{\left(\frac{^{18}\text{O}}{^{16}\text{O}}\right)_{\text{water}}}. \quad \text{Eq. 3-1}$$

The relationship between the fractionation factors $^{17}\alpha$ and $^{18}\alpha$ is given by a power law function that can be expressed as

$$\ln ^{17}\alpha_{\text{CO}_2\text{-water}} = \theta_{\text{CO}_2\text{-water}} \times \ln ^{18}\alpha_{\text{CO}_2\text{-water}}. \quad \text{Eq. 3-2}$$

In the mass balance model for tropospheric CO₂, Hoag et al. (2005) assume that the exponent θ for CO₂–water equilibrium is equal to 0.516 without giving an explanation for the choice of their equilibrium θ value. However, the choice of $\theta_{\text{CO}_2\text{-water}}$ is crucial when modeling the triple oxygen isotope composition of tropospheric CO₂ because of the large ¹⁸O/¹⁶O equilibrium fractionation between CO₂ and water ($1000 \ln^{18}\alpha \approx +41$ at 20 °C).

Improvements in measurement precision of triple oxygen isotope ratios in CO₂ (Hofmann and Pack, 2010) provide the opportunity to determine experimentally the value $\theta_{\text{CO}_2\text{-water}}$ for equilibrium isotope exchange and to test if the triple oxygen isotope composition of tropospheric CO₂ can be used as an additional tracer of bio-, hydro- and atmosphere interaction (Hoag et al., 2005).

Here, we present the first experimental data on the triple oxygen isotope fractionation factor θ for equilibrium isotope exchange between CO₂ and water.

3.3 Methods

3.3.1 Definitions

All oxygen isotope data on $\delta^{17}\text{O}$ and $\delta^{18}\text{O}$ are reported relative to VSMOW. The δ values are defined as:

$$\delta^{17}\text{O} = \left[\frac{(^{17}\text{O} / ^{16}\text{O})_{\text{sample}}}{(^{17}\text{O} / ^{16}\text{O})_{\text{VSMOW}}} - 1 \right] \quad \text{and} \quad \delta^{18}\text{O} = \left[\frac{(^{18}\text{O} / ^{16}\text{O})_{\text{sample}}}{(^{18}\text{O} / ^{16}\text{O})_{\text{VSMOW}}} - 1 \right]. \quad \text{Eq. 3-3}$$

The $\delta'^{17}\text{O}$ and $\delta'^{18}\text{O}$ notation were introduced as the linearized version of the δ -notation, with $\delta'^{17}\text{O} = \ln(\delta^{17}\text{O} + 1)$ and $\delta'^{18}\text{O} = \ln(\delta^{18}\text{O} + 1)$ (Hulston and Thode, 1965; Miller, 2002; Young et al., 2002). $\Delta^{17}\text{O}_{\text{TFL}}$ values denote deviations in $\delta'^{17}\text{O}$ from the terrestrial fractionation line (TFL) of the form $\delta'^{17}\text{O} = \lambda_{\text{TFL}} \times \delta'^{18}\text{O}$. We are using the TFL as reference line because we are analyzing rocks. On the basis of >700 analyses of rocks and minerals, we determined a slope $\lambda_{\text{TFL}} = 0.5251 \pm 0.0014$ ($t_{0.95} \times \text{SEM}$). The slope λ_{TFL} is, within analytical uncertainty, identical to slopes reported for rocks and minerals in other studies (Kusakabe and Matsuhisa, 2008; Miller, 2002; Rumble et al., 2007). Literature data on MORB and NBS-28 suggest that the TFL passes through the origin within analytical uncertainty (Kusakabe and Matsuhisa, 2008; Robert et al., 1992), i.e. VSMOW falls on the TFL. Therefore, all $\Delta^{17}\text{O}$ analyses were corrected relative to NBS-28 quartz with $\Delta^{17}\text{O}_{\text{TFL}} = 0\text{‰}$. Errors of $\Delta^{17}\text{O}$ are given as standard errors of the mean (SEM) multiplied by Student's *t* factor for a 95% confidence limit.

3.3.2 Isotope exchange experiments between CO₂ and water

The CO₂–water equilibration experiments were carried out at 2, 23 and 37 °C within a bottle-shaped equilibration apparatus as shown in Fig. 3-1. The apparatus consists of a glass jar (~60 ml) for the water and a volume of about 350 ml for the CO₂ gas. The CO₂ and the water can be separated using a ball valve. The apparatus can be connected to a vacuum system. During the equilibration process, the molar H₂O(l)/CO₂ ratio exceeds 200, so that the oxygen isotopic composition of the water largely controls the triple oxygen isotope ratios of the CO₂. For the equilibration experiments, we used deionized tap water, which had been filled in a two-liter water tank, so that all experiments were conducted with isotopically identical water. The initial $\delta^{18}\text{O}_{\text{VSMOW}}$ value of the CO₂ gas varied between 15 and 28‰. We tested attainment of isotopic equilibrium by performing a set of time-dependent $\delta^{18}\text{O}$ analysis of equilibrated CO₂.

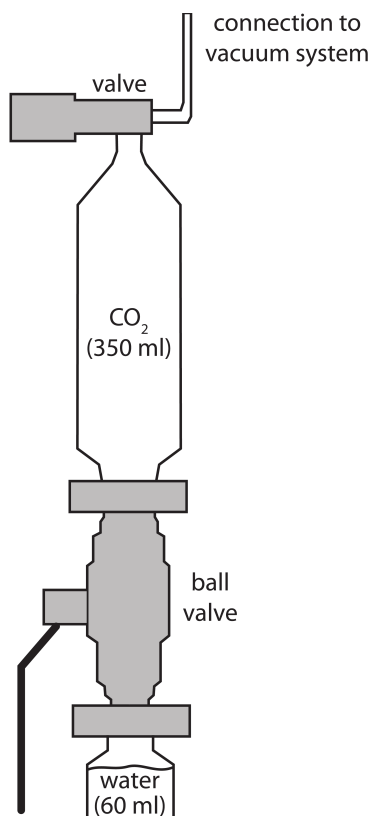


Fig. 3-1: The CO₂-water equilibration apparatus.

The experiments were conducted according to the following procedure: We first filled the bottom reservoir with 60 ml of water. The water was then frozen with liquid nitrogen. The freezing step took about 1 h. Next, the apparatus was evacuated to 3×10^{-3} mbar. We then closed the ball valve and expanded the CO₂ into the top part of the apparatus. The CO₂ pressure in the top part was ~ 1 bar in all experiments. Subsequent, we thawed the ice and brought the apparatus to the equilibration temperature. We then opened the ball valve to allow the CO₂ to equilibrate with the water. The 2 °C experiments were conducted in a fridge with a temperature stability of ± 2 °C. The 23 °C experiments were conducted in a temperature-controlled room with a stability of ± 2 °C. The 37 °C experiments were conducted in a drying oven with a stability of ± 3 °C.

After equilibration, we closed the ball valve and isolated the CO₂ from the water reservoir. The CO₂ was isolated from water vapor and other gaseous impurities using a Russian doll type cryogenic trap (Brenninkmeijer, 1991; Brenninkmeijer and Röckmann, 1996). An important issue was that the CO₂ had to be dried in order to avoid exchange of the sample CO₂ with condensed water. Therefore, sample CO₂ was passed through Mg(ClO₄)₂ before entering the cryogenic trap. For final drying, the CO₂ gas was brought in contact with P₂O₅ as drying agent for about 30 min.

3.3.3 Triple oxygen isotope analyses of CO₂ and water

The $\delta^{18}\text{O}$ analyses of CO₂ were carried out in dual inlet mode on a Finnigan Delta plus mass spectrometer. The $\delta^{18}\text{O}$ values were standardized by comparison with CO₂ generated by phosphoric acid decomposition of NBS-19 ($\delta^{18}\text{O}_{\text{VSMOW}} = +28.65\text{‰}$; $\delta^{13}\text{C}_{\text{PDB}} = +1.95\text{‰}$). The carbonate was reacted at 70 °C and the acid fractionation factor for calcite $\alpha_{\text{CO}_2\text{-calcite}} = 1.00871$ (Kim et al., 2007) was used. The mass spectrometric uncertainty in $\delta^{18}\text{O}$ is in the range of $\pm 0.03\text{‰}$ (1 σ , SD).

The $\Delta^{17}\text{O}$ analyses of CO₂ were performed using a CO₂–CeO₂ equilibration technique (Hofmann and Pack, 2010). For this purpose, about 13 mmol of CO₂ was equilibrated with 6 to 10 mg CeO₂ powder (0.04–0.06 mmol) at 685 °C. Subsequently, the CeO₂ was decomposed by infrared-laser fluorination and the liberated molecular oxygen was analyzed using a MAT 253 gas source mass spectrometer (details on the mass spectrometric analyses are given below). One analytical session generally contained 8–10 CeO₂ samples (0.6–3 mg per sample) and 5–8 NBS-28 quartz reference samples (0.2–1 mg per sample). The $\delta^{18}\text{O}$ and $\Delta^{17}\text{O}$ analyses of CeO₂ were corrected relative to NBS-28 quartz analyzed the same day ($\delta^{18}\text{O} = +9.6\text{‰}$ (Dargie et al., 2007), $\Delta^{17}\text{O}_{\text{TFL}} = 0\text{‰}$). In this way, $\Delta^{17}\text{O}$ analyses are recorded with high accuracy and precision relative to the TFL. The $\Delta^{17}\text{O}$ values of CO₂ were inferred from the $\Delta^{17}\text{O}$ values of CeO₂, with $\Delta^{17}\text{O}_{\text{CO}_2} = \Delta^{17}\text{O}_{\text{CeO}_2} + (\theta_{\text{CO}_2\text{-CeO}_2} - \lambda_{\text{TFL}}) \times 1000 \ln^{18}\alpha_{\text{CO}_2\text{-CeO}_2}$, where $^{18}\alpha_{\text{CO}_2\text{-CeO}_2}$ and $\theta_{\text{CO}_2\text{-CeO}_2}$ denote the fractionation factors for triple oxygen isotope exchange between CO₂ and CeO₂ (Hofmann and Pack, 2010).

Recently, (Cao and Liu, 2011) pointed out that the triple oxygen isotope fractionation exponent $\theta_{\text{CO}_2\text{-CeO}_2}$ published by Hofmann and Pack (2010) deviates significantly from their theoretical estimate for CO₂–CeO₂ exchange at 685 °C. Thus, it is important to note that the fractionation factor $^{18}\alpha_{\text{CO}_2\text{-CeO}_2}$ and the corresponding triple oxygen isotope fractionation exponent $\theta_{\text{CO}_2\text{-CeO}_2}$ given by Hofmann and Pack (2010) are steady-state values specific for the design of our apparatus and the experimental procedure. The temperature at the center of the equilibration tube, where the CeO₂ is placed, is 685 °C, whereas the two ends of the tube remain at room temperature. The thermal gradient within the tube leads to an isotope fractionation in the distribution of the CO₂ molecules: Light CO₂ isotopologues are enriched in the heated center part of the tube, whereas heavy CO₂ isotopologues are enriched near the tube ends (see Jones and Furry, 1946 and references therein). The fractionation related to thermal diffusion affects the triple oxygen isotope composition of the CO₂ that equilibrates with the CeO₂ because the diffusion process most likely proceeds with a θ value of ~ 0.509 (Young et al., 2002).

We redetermined the instrumental CO₂–CeO₂ fractionation for the design of our equilibration apparatus and obtained $1000 \ln^{18}\alpha_{\text{CO}_2\text{--CeO}_2} = 11.7 \pm 1.5$ (SD) and $\theta_{\text{CO}_2\text{--CeO}_2} = 0.523 \pm 0.001$ (SD) for a CO₂ pressure of ~600 mbar in the equilibration tube. For the calibration experiments, carbon dioxide with a known triple oxygen isotope composition was produced by combustion of carbon with O₂ ($\delta^{18}\text{O}_{\text{VSMOW}} = 13.473\text{‰}$, $\delta^{17}\text{O}_{\text{VSMOW}} = 6.649\text{‰}$) that was calibrated relative to VSMOW by E. Barkan (Institute of Earth Sciences, Hebrew University of Jerusalem). The current results on $^{18}\alpha_{\text{CO}_2\text{--CeO}_2}$ and $\theta_{\text{CO}_2\text{--CeO}_2}$ confirm previous results reported in Hofmann and Pack (2010).

The triple oxygen isotope analyses on the released O₂ were carried out on a Thermo MAT 253 mass spectrometer in continuous flow mode relative to an in-house reference O₂ gas. The in-house reference O₂ gas was calibrated relative to VSMOW by E. Barkan (Institute of Earth Sciences, Hebrew University of Jerusalem) with $\delta^{18}\text{O}_{\text{VSMOW}} = +13.473\text{‰}$ and $\delta^{17}\text{O}_{\text{VSMOW}} = +6.649\text{‰}$. The reference gas peaks were 15–25 V and the sample peaks 20–30 V ($m/z = 32$) high. The analytical uncertainty of $\Delta^{17}\text{O}$ for a single analysis is $\pm 0.05\text{‰}$ (1 σ , SD).

The triple oxygen isotope analyses of water were conducted by Amaelle Landais (*Laboratoire des Sciences du Climat et de l'Environnement*, Paris) using the CoF₃ fluorination method coupled with dual inlet mass spectrometry of O₂ (Baker et al., 2002; Barkan and Luz, 2005). The oxygen isotopic composition of the water was analyzed relative to a working standard that had been calibrated to VSMOW. The analytical uncertainty in $\delta^{18}\text{O}$ and $\Delta^{17}\text{O}$ is in the range of $\pm 0.05\text{‰}$ (SD) and $\pm 0.006\text{‰}$ (SD), respectively. A subsample of the water reservoir was analyzed before and after equilibration with CO₂ in order to verify that the CO₂–water equilibration process did not affect the isotopic composition of the water.

3.4 Results

First, we conducted three sets of time-dependent experiments at 2, 23 and 37 °C (Fig. 3-2). At 2 °C, the $\delta^{18}\text{O}$ value of equilibrated CO₂ converges to a limit value of +37.7‰ after 300 h of equilibration. This shows that isotopic equilibrium is reached within 300 h. At 23 and 37 °C, the equilibrium values of +33.0‰ and +30.0‰ are reached within 200 h. In order to ensure that isotopic equilibrium is reached in the subsequent experiments, we have chosen equilibration times of 312 h at 2 °C and 216 h at 23 and 37 °C.

The triple oxygen isotope composition of equilibrated CO₂ was analyzed for 12 CO₂–water equilibration experiments (Table 3-1). The $\Delta^{17}\text{O}_{\text{TFL}}$ value of the water-equilibrated CO₂

was determined with high precision to be $-0.17 \pm 0.03\text{‰}$ ($t_{0.95} \times \text{SEM}$) at 2 °C, $-0.08 \pm 0.02\text{‰}$ ($t_{0.95} \times \text{SEM}$) at 23 °C and $-0.10 \pm 0.03\text{‰}$ ($t_{0.95} \times \text{SEM}$) at 37 °C (Fig. 3-3).

The deionized tap water had a $\delta^{18}\text{O}$ value of -8.52‰ and a $\Delta^{17}\text{O}_{\text{TFL}}$ value of $+0.010 \pm 0.006\text{‰}$ prior to equilibration with CO₂ (Fig. 3-3). Recalculating the triple oxygen isotope composition relative to the global meteoric water line (GMWL) with $\delta^{17}\text{O} = 0.528 \times \delta^{18}\text{O} + 0.033\text{‰}$ (Luz and Barkan, 2010) gives $\Delta^{17}\text{O}_{\text{GMWL}} = +0.002 \pm 0.006\text{‰}$, i.e. the deionized tap water falls on the GMWL suggesting that it inherits its triple oxygen isotope signature from local meteoric water. For one equilibration experiment (Table 3-1, no. 1), the water was also analyzed after equilibration with CO₂ and these data indicate that the equilibration process did not affect the triple oxygen isotope composition of the water ($\delta^{18}\text{O} = -8.44\text{‰}$, $\Delta^{17}\text{O}_{\text{TFL}} = +0.019 \pm 0.006\text{‰}$).

Combining the oxygen isotope data of CO₂ and water, $\theta_{\text{CO}_2\text{-water}}$ is equal to 0.5211 ± 0.0015 ($t_{0.95} \times \text{SEM}$) at 2 °C, 0.5229 ± 0.0015 ($t_{0.95} \times \text{SEM}$) at 23 °C and 0.5223 ± 0.0016 ($t_{0.95} \times \text{SEM}$) at 37 °C. The weighted mean of $\theta_{\text{CO}_2\text{-water}}$ is 0.522 ± 0.002 ($t_{0.95} \times \text{SEM}$) in the temperature range of 2 to 37 °C. In addition, we calculated the fractionation factor $^{18}\alpha_{\text{CO}_2\text{-water}}$ for these equilibration experiments and found that $1000 \ln ^{18}\alpha_{\text{CO}_2\text{-water}}$ is equal to $45.3 \pm 0.5(\text{SD})$, 41.2 ± 0.8 and 38.5 ± 0.5 at 2, 23 and 37°C.

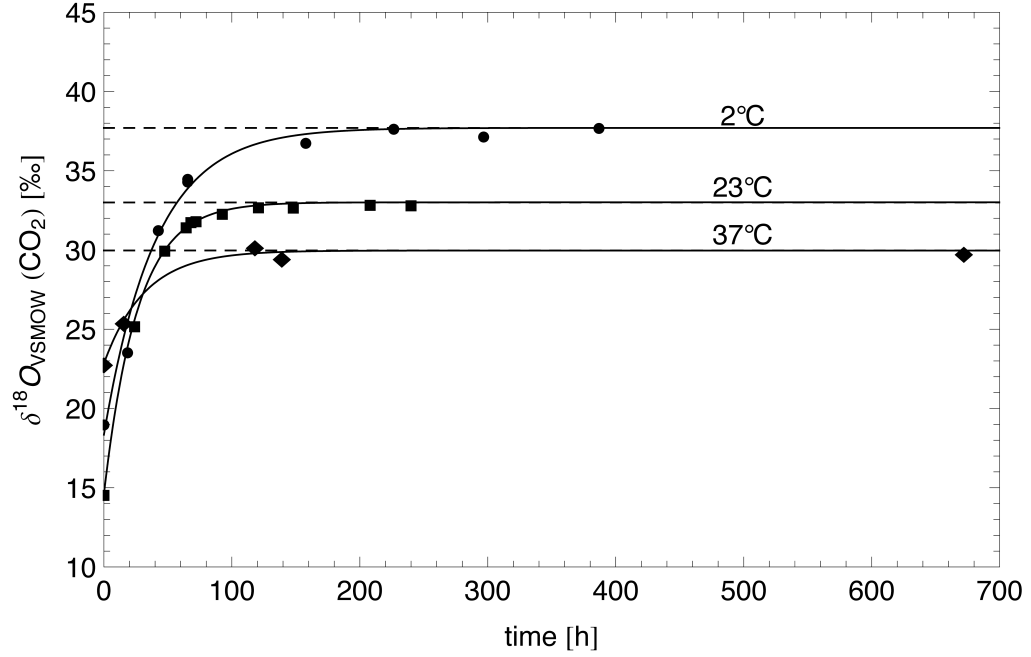


Fig. 3-2: Plot of $\delta^{18}\text{O}$ of CO₂ vs. equilibration time. Three sets of time-dependent equilibration experiments between CO₂ and water ($\delta^{18}\text{O} = -8.5\text{‰}$) at 2, 23 and 37 °C show that the $\delta^{18}\text{O}$ value of CO₂ reaches a limit value for an equilibration time >300 h at 2 °C and >200 h at 23 and 37 °C indicating that isotopic equilibrium is reached.

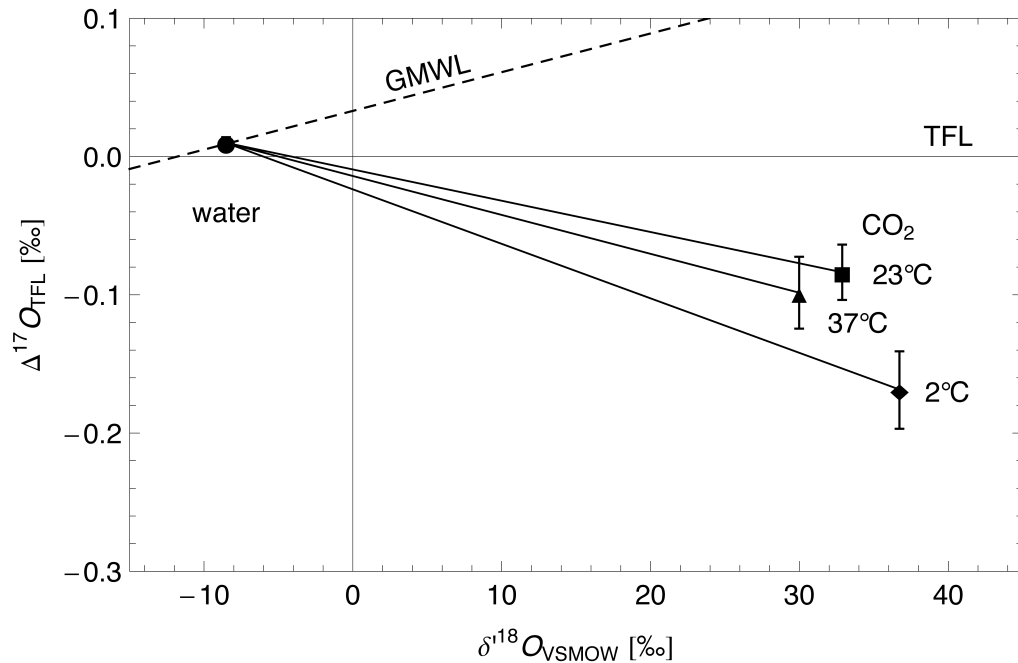


Fig. 3-3: Experimental determination of $\theta_{\text{CO}_2\text{-water}}$. The diamond, square and triangle represent triple oxygen isotope data of CO₂ equilibrated with water (•) at 2, 23 and 37 °C. Error bars represent the standard error of the mean multiplied by Student's t-factor for a 95% confidence limit. The dashed line illustrates the global meteoric water line (GMWL) determined by Luz and Barkan (2010).

Table 3-1: Isotopic data of water equilibrated CO₂ (12 equilibration experiments). The $\Delta^{17}\text{O}$ analyses are based on a CO₂-CeO₂ equilibration technique (Hofmann and Pack, 2010). Subsequent to the CO₂-CeO₂ equilibration, the CeO₂ is decomposed by infrared-laser fluorination and the liberated molecular oxygen is analyzed on a mass spectrometer. No systematic shift in $\delta^{18}\text{O}$ of the CO₂ was observed before and after equilibration with CeO₂.

No.	T [°C]	$\delta^{18}\text{O}_{\text{CeO}_2}$ [‰]	$\delta^{17}\text{O}_{\text{CeO}_2}$ [‰]	$\delta^{18}\text{O}_{\text{CO}_2}$ [‰] (before CeO_2 equilibration)	$\delta^{18}\text{O}_{\text{CO}_2}$ [‰] (after CeO_2 equilibration)	$\Delta^{17}\text{O}_{\text{CO}_2}$ [‰]	$\theta_{\text{CO}_2\text{-water}}$
1	2	27.325	14.096	38.6	37.4	-0.18	
		27.444	14.146			-0.19	
		27.781	14.28			-0.24	
		27.815	14.308			-0.22	
		27.851	14.34			-0.21	
2	2	24.548	12.686	37.0	36.9	-0.15	
		24.558	12.686			-0.16	
		24.646	12.76			-0.13	
		24.477	12.575			-0.23	
		23.685	12.345			-0.05	
3	2	24.439	12.68	37.2	37.2	-0.10	
		24.53	12.656			-0.17	
		23.762	12.247			-0.18	
		24.253	12.538			-0.15	
		24.376	12.595			-0.16	
Aver. $\pm t_{0.95}\times\text{SEM}$						-0.17 \pm 0.03	0.5211 \pm 0.0015
4	23	19.677	10.177	32.1	–	-0.13	
		19.708	10.173			-0.15	
		19.678	10.265			-0.05	
5	23	20.997	10.926	33.5	34.2	-0.07	
		21.04	10.964			-0.05	
		20.822	10.843			-0.06	
		21.136	10.936			-0.13	
6	23	20.495	10.643	32.5	32.5	-0.09	
		20.097	10.443			-0.08	
		20.204	10.516			-0.07	
7	23	20.184	10.428	34	33.4	-0.14	
		20.531	10.696			-0.06	
		20.509	10.707			-0.04	
8	23	21.623	11.241	33.7	33.6	-0.08	
		21.617	11.198			-0.12	
		21.652	11.294			-0.04	
		21.711	11.313			-0.05	
Aver. $\pm t_{0.95}\times\text{SEM}$						-0.08 \pm 0.02	0.5229 \pm 0.0015

No.	T [°C]	$\delta^{18}\text{O}_{\text{CeO}_2}$ [‰]	$\delta^{17}\text{O}_{\text{CeO}_2}$ [‰]	$\delta^{18}\text{O}_{\text{CO}_2}$ [‰] (before CeO_2 equilibration)	$\delta^{18}\text{O}_{\text{CO}_2}$ [‰] (after CeO_2 equilibration)	$\Delta^{17}\text{O}_{\text{CO}_2}$ [‰]	$\theta_{\text{CO}_2\text{-water}}$
9	37	18.932	9.846	29.9	30	-0.08	
		19.09	9.9			-0.10	
10	37	16.607	8.546	30.6	30.7	-0.16	
		16.712	8.684			-0.08	
		16.702	8.646			-0.11	
		16.633	8.628			-0.10	
11	37	18.528	9.66	31.1	30.9	-0.05	
		18.564	9.668			-0.06	
		18.455	9.633			-0.04	
		18.529	9.633			-0.08	
		18.53	9.64			-0.07	
12	37	21.483	11.04	30.3	30	-0.21	
		21.413	11.097			-0.11	
		21.65	11.219			-0.12	
Aver. $\pm t_{0.95} \times \text{SEM}$						-0.10 ± 0.03	0.5223 ± 0.0016

3.5 Discussion

3.5.1 The triple oxygen isotope equilibrium fractionation exponent $\theta_{\text{CO}_2\text{-water}}$ in the context of experimental and theoretical literature data

Our results show that the equilibrium fractionation exponent θ for CO₂–water exchange at low temperatures is significantly lower than the high-temperature limit of 0.530 (Cao and Liu, 2011; Young et al., 2002). We found that the equilibrium $\theta_{\text{CO}_2\text{-water}}$ value, within experimental uncertainty, is not temperature dependent in the temperature range between 2 and 37 °C, and thus, we suggest that CO₂–water exchange in the bio-, hydro- and atmosphere proceeds with a constant equilibrium $\theta_{\text{CO}_2\text{-water}}$ value of 0.522 ± 0.002 .

The fractionation in ¹⁸O/¹⁶O between CO₂ and water agrees well with literature data (Brenninkmeijer et al., 1983; O'Neil and Adami, 1969), see Fig. 3-4. This confirms that we have reached isotopic equilibrium in our experiments.

In order to test internal agreement between published data and our result on $\theta_{\text{CO}_2\text{-water}}$, we consider the relationship of $1000 \ln^{18}\alpha$ and θ for isotope exchange between CO₂ gas, water vapor and water. In a $\Delta^{17}\text{O}$ vs. $\delta^{18}\text{O}$ plot, the equilibrium fractionation factors between these three phases must form a triangle as illustrated in Fig. 3-5. The temperature-dependent equilibrium fractionation factor $1000 \ln^{18}\alpha$ is experimentally known for the systems CO₂–water (e.g. Brenninkmeijer et al., 1983) and water–water vapor (Friedman and O'Neil, 1977) and theoretically predicted for water vapor–CO₂ exchange (Richet et al., 1977). Barkan and Luz (2005) experimentally determined the equilibrium θ value for water–water vapor exchange and Matsuhisa et al. (1978) theoretically estimated the exponent θ for CO₂–water vapor equilibrium. Combining these literature data, we estimate that $\theta_{\text{CO}_2\text{-water}}$ should equal to 0.522 in the temperature range of 2 to 37 °C. The precision of this estimate is in the order of ± 0.001 because it mainly depends on the uncertainty of the experimental $\theta_{\text{water-water vapor}}$ value of 0.529 ± 0.001 (Barkan and Luz, 2005). The estimate of $\theta_{\text{CO}_2\text{-water}}$ is in excellent agreement with our experimentally determined θ value of 0.522 ± 0.002 .

Recently, Cao and Liu (2011) presented a data set on theoretical equilibrium θ values for oxygen isotope exchange. In Fig. 3-5, the light gray triangle illustrates their results on equilibrium θ values for the system CO₂–water–water vapor. The difference between their theoretical equilibrium θ value for CO₂–water vapor exchange and the previously published θ value from Matsuhisa et al. (1978) results from the calculation of the reduced partition function ratios of CO₂. Matsuhisa et al. (1978) applied the ‘rule of geometric

mean', where one would assume that the difference in bond energy between ¹⁸O–¹⁸O and ¹⁶O–¹⁶O is twice than the difference in bond energy between ¹⁸O–¹⁶O and ¹⁶O–¹⁶O (Bigeleisen, 1955; Eiler, 2007). In contrast, Cao and Liu (2011) conclude that the 'rule of geometric mean' is not a valid assumption for the calculation of equilibrium θ values at low temperatures, and as a consequence, calculate slightly different reduced partition function ratios of CO₂. As a result, the equilibrium $\theta_{\text{CO}_2\text{-water}}$ value from Cao and Liu (2011) of ~0.5245 in the temperature range from 2 to 37 °C is higher than what can be deduced from the reduced partition function ratios of carbon dioxide given by Matsuhisa et al. (1978). Our experimental value for $\theta_{\text{CO}_2\text{-water}}$, however, suggests that the theoretical estimate by Cao and Liu (2011) is slightly too high.¹

Theory suggests that equilibrium θ values at low temperatures show only a slight, if any temperature dependence (Cao and Liu, 2011; Matsuhisa et al., 1978). Cao and Liu (2011) predict that the $\theta_{\text{CO}_2\text{-water}}$ value increases from 0.5242 to 0.5247 in the temperature range from 2 to 37 °C as shown in Fig. 3-6. Our experimental data on the $\theta_{\text{CO}_2\text{-water}}$ value cannot resolve this small temperature dependence. For water–water vapor exchange, the experimental and theoretical equilibrium θ values do not show any temperature dependence at low temperatures, but coincide with the high temperature limit of 0.530 (Barkan and Luz, 2005; Cao and Liu, 2011), see Fig. 3-6.

¹ Yun Liu confirmed that the theoretical $\theta_{\text{CO}_2\text{-water}}$ value published in Cao and Liu (2011) is slightly too high and he calculated a revised $\theta_{\text{CO}_2\text{-water}}$ value of 0.523 at 25 °C (Y. Liu, pers. comm.).

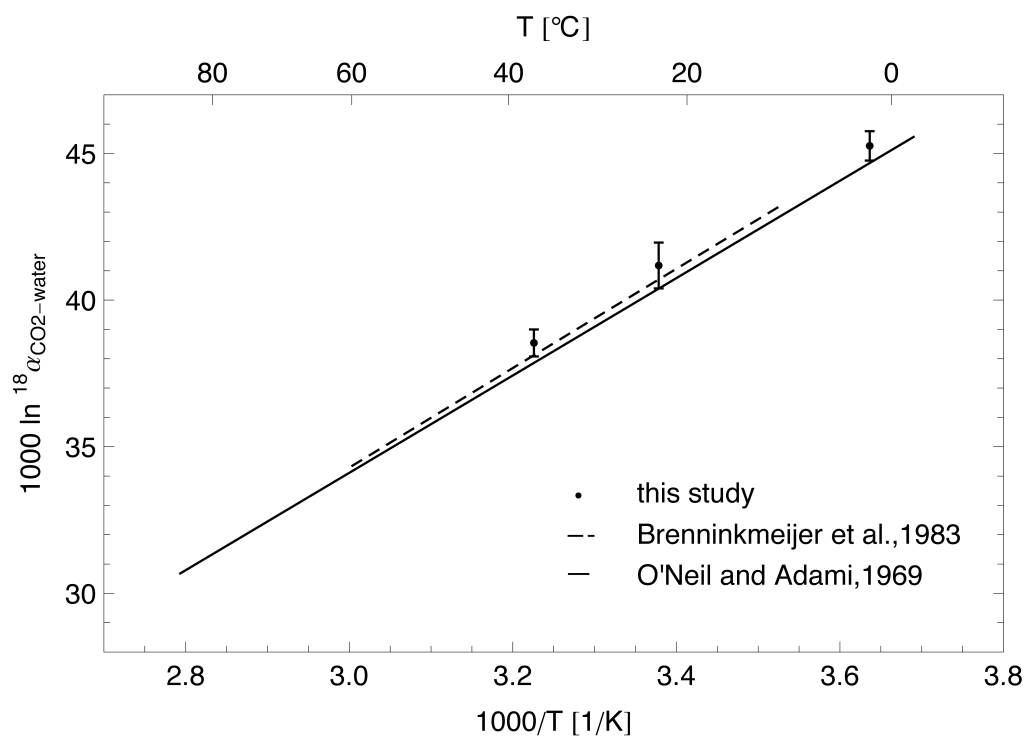


Fig. 3-4: Experimental determination of the fractionation factor $1000 \ln {}^{18}\alpha_{\text{CO}_2\text{-water}}$. The fractionation factor ${}^{18}\alpha$ determined in this study for 2, 23 and 37 °C agrees well with literature data on CO₂–water isotope exchange (Brenninkmeijer et al., 1983; O'Neil and Adami, 1969). Error bars denote the standard deviation.

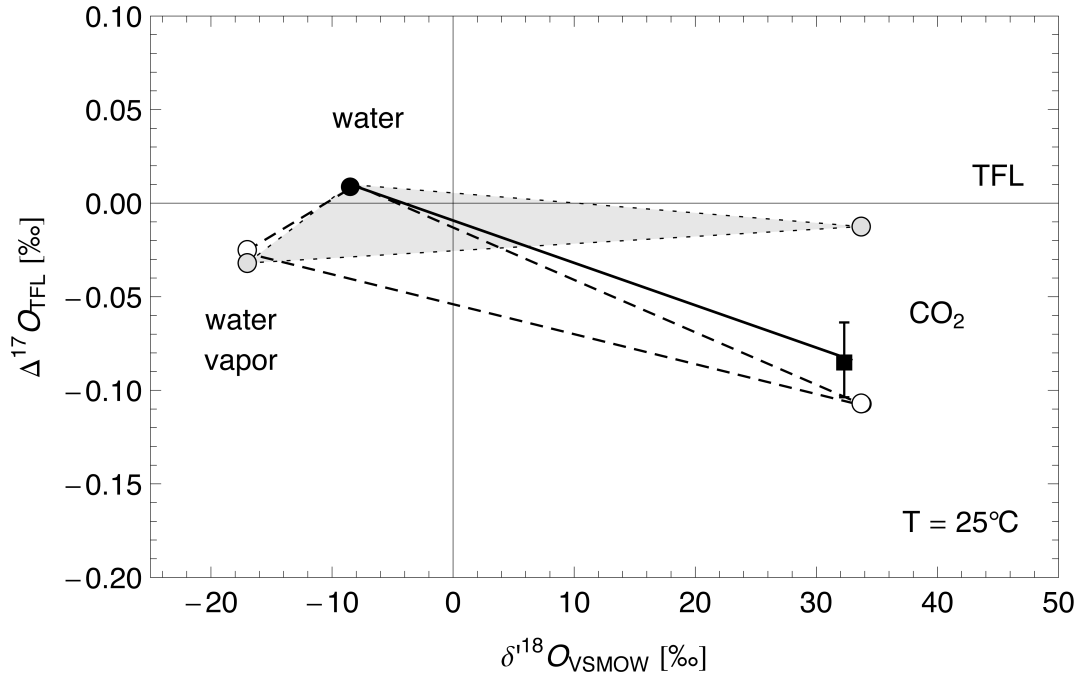


Fig. 3-5: Illustration of the equilibrium fractionation factors $1000 \ln^{18}\alpha$ and θ between CO₂ gas, water vapor and water at 25 °C. In a $\Delta^{17}\text{O}$ vs. $\delta^{18}\text{O}$ plot, the equilibrium fractionation factors between the three phases must form a triangle. Such a triangle can be used to test internal agreement between published data. Our experimental data on the triple oxygen isotope equilibrium fractionation between CO₂ and water are illustrated as a black line. The dashed triangle is based on compiled experimental and theoretical literature data: the fractionation factor $^{18}\alpha_{\text{CO}_2\text{-water}}$ was taken from Brenninkmeijer et al. (1983), the fractionation factor $^{18}\alpha_{\text{water-water vapor}}$ was taken from Friedman and O'Neil (1977), the fractionation factor $^{18}\alpha_{\text{CO}_2\text{-water vapor}}$ was taken from Richet et al. (1977), the $\theta_{\text{water-water vapor}}$ value was taken from Barkan and Luz (2005) and the $\theta_{\text{CO}_2\text{-water vapor}}$ value from Matsuhisa et al. (1978). From these literature data one can estimate a $\theta_{\text{CO}_2\text{-water}}$ value of 0.522 ± 0.001 ($2^\circ\text{C} \leq T \leq 37^\circ\text{C}$). The dotted, light gray triangle illustrates theoretical equilibrium fractionation factors from Cao and Liu (2011). Our data on water equilibrated CO₂ at 25 °C are consistent with theoretical data from Matsuhisa et al. (1978), but there is a slight discrepancy between our experimental $\theta_{\text{CO}_2\text{-water}}$ value and the theoretical estimate from Cao and Liu (2011).

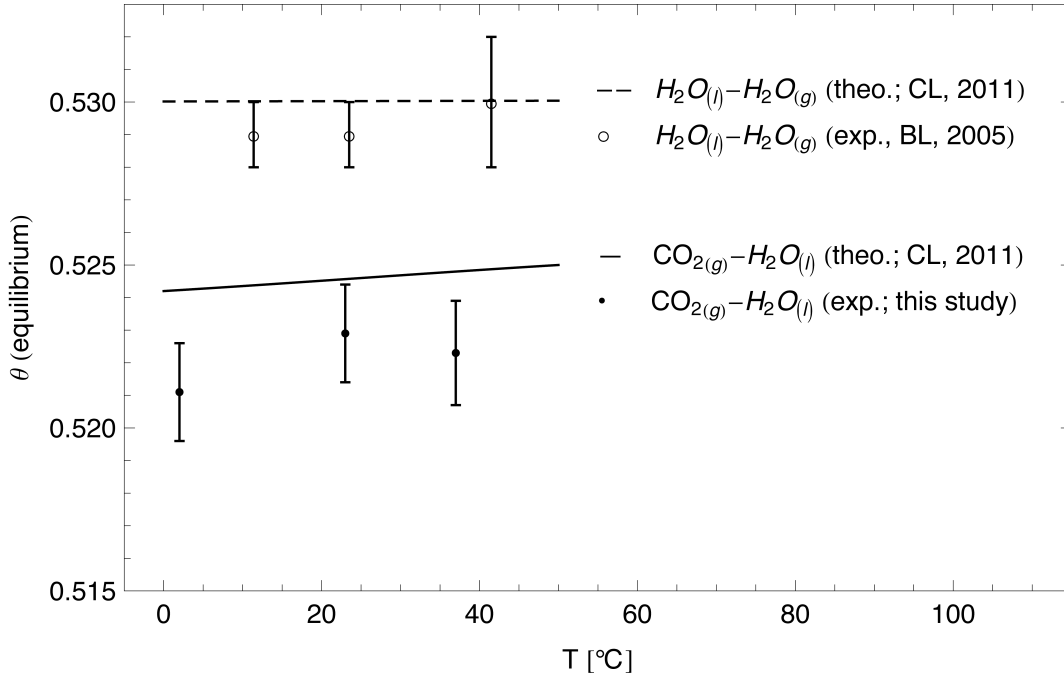


Fig. 3-6: Comparison of experimental and theoretical equilibrium θ values for water–water vapor and CO₂–water exchange at low temperatures. The theoretical θ value for water–water vapor exchange from Cao and Liu (2011) agrees well with experimental data from Barkan and Luz (2005). However, the theoretical θ value for CO₂–water exchange from Cao and Liu (2011) is slightly higher than experimental data determined in this study. Error bars denote the standard error of the mean multiplied by Student's t-factor for a 95% confidence limit.

3.5.2 Relevance of the $\theta_{CO_2\text{-}water}$ value for the identification of major CO₂ sources to the troposphere

Knowledge of the $\theta_{CO_2\text{-}water}$ value is essential when estimating the $\Delta^{17}O$ of tropospheric CO₂ (Hoag et al., 2005). This is because the triple oxygen isotope composition of tropospheric CO₂ is largely controlled by isotope exchange with water in the bio- and hydrosphere.

The main exchange reservoirs for tropospheric CO₂ are land plants (leaf water), soil water and the ocean surface waters. For leaf and ocean water exchange, an equilibrium fractionation exponent of $\theta_{CO_2\text{-}water} = 0.522$ is relevant. This value deviates significantly from the previously assumed $\theta_{CO_2\text{-}water}$ value of 0.516 (Hoag et al., 2005). For carbon dioxide emissions from soils, both equilibrium and kinetic fractionation play a role (Miller et al., 1999a); requiring a more complex model for understanding the $\Delta^{17}O$ of soil CO₂.

Isotope exchange between CO₂ and water in leaves and soils is catalyzed by the enzyme carbonic anhydrase (Gillon and Yakir, 2001; Gillon and Yakir, 2000; Seibt et al., 2006; Wingate et al., 2009). The influence of carbonic anhydrase on the $\theta_{CO_2\text{-}water}$ value is not

known. But as carbonic anhydrase has no influence on the $^{18}\text{O}/^{16}\text{O}$ fractionation, we suggest that it also does not have an influence on the $^{17}\text{O}/^{16}\text{O}$ fractionation, i.e. the $\theta_{\text{CO}_2\text{-water}}$. It is part of an ongoing study to verify this assumption.

To assess the potential of $\Delta^{17}\text{O}$ of tropospheric CO₂ as a tracer for the global carbon cycle, comprehensive model predictions on the $\Delta^{17}\text{O}$ value of tropospheric CO₂ should refine the model predictions from Hoag et al. (2005). We suggest that these model predictions should implement the experimentally determined equilibrium θ value for CO₂–water exchange. In doing so, the models could investigate both the gross carbon exchange between the bio- and hydrosphere and the influx of mass-independently fractionated CO₂ from the stratosphere to the troposphere more precisely.

3.6 Acknowledgment

We thank A. Landais for analyzing the triple oxygen isotope composition of our water samples and we thank E. Barkan for the calibration of our inhouse reference O₂ gas relative to VSMOW. We also thank two anonymous reviewers for helpful comments. This study was funded by the German Science Foundation (AP, project PA909/6-1, PA909/6-2).

3.7 References

- Baker, L., Franchi, I. A., Maynard, J., Wright, I. P., Pillinger, C. T., 2002. A technique for the determination of $^{18}\text{O}/^{16}\text{O}$ and $^{17}\text{O}/^{16}\text{O}$ isotopic ratios in water from small liquid and solid samples. *Anal. Chem.* 74, 1665-1673.
- Barkan, E., Luz, B., 2005. High precision measurements of $^{17}\text{O}/^{16}\text{O}$ and $^{18}\text{O}/^{16}\text{O}$ ratios in H₂O. *Rapid Commun. Mass Spec.* 19, 3737-3742.
- Bigeleisen, J., 1955. Statistical mechanics of isotopic systems with small quantum corrections. I. General considerations and the rule of the geometric mean. *J. Chem. Phys.* 23, 2264-2267.
- Brenninkmeijer, C. A. M., 1991. Robust, high-efficiency, high-capacity cryogenic trap. *Anal. Chem.* 63, 1182-1184.
- Brenninkmeijer, C. A. M., Kraft, P., Mook, W. G., 1983. Oxygen isotope fractionation between CO₂ and H₂O. *Isot. Geosci.* 1, 181-190.
- Brenninkmeijer, C. A. M., Röckmann, T., 1996. Russian doll type cryogenic traps: improved design and isotope separation effects. *Anal. Chem.* 68, 3050-3053.
- Cao, X., Liu, Y., 2011. Equilibrium mass-dependent fractionation relationships for triple oxygen isotopes. *Geochim. Cosmochim. Acta* 75, 7435-7445.
- Ciais, P., Denning, A. S., Tans, P. P., Berry, J. A., Randall, D., Collatz, J. G., Sellers, P. J., White, J. W., Troler, M., Meijer, H. A. J., Francey, R. J., Monfray, P., Heimann, M., 1997. A three-dimensional synthesis study of $\delta^{18}\text{O}$ in atmospheric CO₂: Part 1 Surface fluxes. *J. Geophys. Res.* 102, 5857-5872.
- Dargie, M., Winckler, G., Gröning, M., 2007. Reference sheet for reference materials. International Atomic Energy Agency (IAEA), Vienna.
- Eiler, J. M., 2007. "Clumped-isotope" geochemistry - The study of naturally-occurring, multiply-substituted isotopologues. *Earth Planet. Sci. Lett.* 262, 309-327.
- Farquhar, G. D., Lloyd, J., Taylor, J. A., Flanagan, L. B., Syvertsen, J. P., Hubick, K. T., Wong, S. C., Ehleringer, J. R., 1993. Vegetation effects on the isotope composition of oxygen in atmospheric CO₂. *Nature* 363, 439-443.
- Francey, R. J., Tans, P. P., 1987. Latitudinal variation in oxygen-18 of atmospheric CO₂. *Nature* 327, 495-497.
- Friedli, H., Siegenthaler, U., Rauber, D., Oeschger, H., 1987. Measurements of concentration, $^{13}\text{C}/^{12}\text{C}$ and $^{18}\text{O}/^{16}\text{O}$ ratios of tropospheric carbon dioxide over Switzerland. *Tellus B* 39B, 80-88.

- Friedman, I., O'Neil, J. R., 1977. Compilation of stable isotope fractionation factors of geochemical interest. *U.S. Geological Survey Prof. Paper* 440-KK.
- Gillon, J., Yakir, D., 2001. Influence of carbonic anhydrase activity in terrestrial vegetation on the ¹⁸O content of atmospheric CO₂. *Science* 291, 2584-2587.
- Gillon, J. S., Yakir, D., 2000. Naturally low carbonic anhydrase activity in C₄ and C₃ plants limits discrimination against C¹⁸OO during photosynthesis. *Plant Cell Environ.* 23, 903-915.
- Hoag, K. J., Still, C. J., Fung, I. Y., Boering, K. A., 2005. Triple oxygen isotope composition of tropospheric carbon dioxide as a tracer of terrestrial gross carbon fluxes. *Geophys. Res. Lett.* 32, 1-5.
- Hofmann, M. E. G., Pack, A., 2010. Technique for high-precision analysis of triple oxygen isotope ratios in carbon dioxide. *Anal. Chem.* 82, 4357-4361.
- Hulston, J. R., Thode, H. G., 1965. Variations in the S³³, S³⁴, and S³⁶ contents of meteorites and their relation to chemical and nuclear effects. *J. Geophys. Res.* 70, 3475-3484.
- Jones, R. C., Furry, W. H., 1946. The separation of isotopes by thermal diffusion. *Rev. Mod. Phys.* 18, 151-224.
- Kim, S.-T., Mucci, A., Taylor, B. E., 2007. Phosphoric acid fractionation factors for calcite and aragonite between 25 and 75 °C: Revisited. *Chem. Geol.* 246, 135-146.
- Kusakabe, M., Matsuhisa, Y., 2008. Oxygen three-isotope ratios of silicate reference materials determined by direct comparison with VSMOW-oxygen. *Geochem. J.* 42, 309-317.
- Lämmerzahl, P., Röckmann, T., Brenninkmeijer, C. A. M., Krankowsky, D., Mauersberger, K., 2002. Oxygen isotope composition of stratospheric carbon dioxide. *Geophys. Res. Lett.* 29, 1582.
- Luz, B., Barkan, E., 2010. Variations of ¹⁷O/¹⁶O and ¹⁸O/¹⁶O in meteoric waters. *Geochim. Cosmochim. Acta* 74, 6276-6286.
- Matsuhisa, Y., Goldsmith, J. R., Clayton, R. N., 1978. Mechanisms of hydrothermal crystallization of quartz at 250°C and 15kbar. *Geochim. Cosmochim. Acta* 42, 173-182.
- Miller, J. B., Yakir, D., White, J. W. C., Tans, P. P., 1999a. Measurement of ¹⁸O/¹⁶O in the soil-atmosphere CO₂ flux. *Global Biogeochem. Cy.* 13, 761-774.
- Miller, M. F., 2002. Isotopic fractionation and the quantification of ¹⁷O anomalies in the oxygen three-isotope system: an appraisal and geochemical significance. *Geochim. Cosmochim. Acta* 66, 1881-1889.

- O'Neil, J. R., Adami, L. H., 1969. Oxygen isotope partition function ratio of water and the structure of liquid water. *J. Phys. Chem.* 73, 1553-1558.
- Richet, P., Bottinga, Y., Javoy, M., 1977. A review of hydrogen, carbon, nitrogen, oxygen, sulphur, and chlorine stable isotope fractionation among gaseous molecules. *Annu. Rev. Earth Planet. Sci.* 5, 65-110.
- Robert, F., Rejou-Michel, A., Javoy, M., 1992. Oxygen isotopic homogeneity of the Earth: new evidence. *Earth Planet. Sci. Lett.* 108, 1-9.
- Rumble, D., Miller, M. F., Franchi, I. A., Greenwood, R. C., 2007. Oxygen three-isotope fractionation lines in terrestrial silicate minerals: An inter-laboratory comparison of hydrothermal quartz and eclogitic garnet. *Geochim. Cosmochim. Acta* 71, 3592-3600.
- Seibt, U., Wingate, L., Lloyd, J., Berry, J. A., 2006. Diurnally variable $\delta^{18}\text{O}$ signatures of soil CO₂ fluxes indicate carbonic anhydrase activity in a forest soil. *J. Geophys. Res.* 111, G04005.
- Thiemens, M., Jackson, T., Brenninkmeijer, C. A. M., 1995a. Observation of a mass independent oxygen isotopic composition in terrestrial stratospheric CO₂, the link to ozone chemistry, and the possible occurrence in the Martian atmosphere. *Geophys. Res. Lett.* 22, 255-257.
- Thiemens, M. H., Jackson, T., 1991. Oxygen isotope fractionation in stratospheric CO₂. *Geophys. Res. Lett.* 18, 669-672.
- Wingate, L., Ogée, J., Cuntz, M., Genty, B., Reiter, I., Seibt, U., Yakir, D., Maseyk, K., Pendall, E. G., Barbour, M. M., Mortazavi, B., Burlett, R. g., Peylin, P., Miller, J., Mencuccini, M., Shim, J. H., Hunt, J., Grace, J., 2009. The impact of soil microorganisms on the global budget of $\delta^{18}\text{O}$ in atmospheric CO₂. *Proc. Natl. Acad. Sci.* 106, 22411-22415.
- Yakir, D., Wang, X. F., 1996. Fluxes of CO₂ and water between terrestrial vegetation and the atmosphere estimated from isotope measurements. *Nature* 380, 515-517.
- Young, E. D., Galy, A., Nagahara, H., 2002. Kinetic and equilibrium mass-dependent isotope fractionation laws in nature and their geochemical and cosmochemical significance. *Geochim. Cosmochim. Acta* 66, 1095-1104.

4 On the triple oxygen isotope composition of carbon dioxide from some combustion processes

Horváth, B., Hofmann, M.E.G. and Pack, A.,

On the triple oxygen isotope composition of carbon dioxide from some combustion processes, *Geochim. Cosmochim. Acta*, in press.

4.1 Abstract

The triple oxygen isotope composition ($\Delta^{17}\text{O}$) of CO₂ from different sources is gaining in importance as possible tracer of gross carbon exchanges between major reservoirs. Here we present the $\Delta^{17}\text{O}$ of CO₂ from natural gas and propane–butane combustion, wood chips burning, car exhaust and human breath. All investigated CO₂ samples had negative $\Delta^{17}\text{O}$ value compared to the CO₂–water equilibration line (slope $\theta = 0.522$; zero intercept), which was inherited from the oxidant air O₂. However, for all combustion experiments, the $\Delta^{17}\text{O}$ value of CO₂ was significantly higher than the $\Delta^{17}\text{O}$ value of air O₂. The oxygen isotope composition of CO₂ from natural gas ($\delta^{18}\text{O} = 21.6 \pm 0.7\text{‰}$; $\Delta^{17}\text{O} = -0.30 \pm 0.02\text{‰}$) and from propane–butane ($\delta^{18}\text{O} = 22.5 \pm 0.8\text{‰}$; $\Delta^{17}\text{O} = -0.32 \pm 0.02\text{‰}$) combustion is explained by kinetic fractionation of ambient air O₂. In case of wood chips burning ($\delta^{18}\text{O} = 19.4 \pm 1.0\text{‰}$; $\Delta^{17}\text{O} = -0.21 \pm 0.02\text{‰}$) the wood inherent O also affected the triple oxygen isotope composition of the CO₂. Car exhaust CO₂ ($\delta^{18}\text{O} = 32.6 \pm 3.0\text{‰}$; $\Delta^{17}\text{O} = -0.32 \pm 0.03\text{‰}$) might have likely equilibrated with the condensed water in the exhaust line. The isotope composition of breath CO₂ ($\delta^{18}\text{O} = 35.1 \pm 1.0\text{‰}$; $\Delta^{17}\text{O} = -0.03 \pm 0.03\text{‰}$) was controlled by equilibration with body water. We assess the $\Delta^{17}\text{O}$ value of CO₂ as a potential tracer for anthropogenic CO₂ emission.

4.2 Introduction

In order to predict possible consequences of anthropogenic carbon dioxide (CO₂) emissions it is important to understand the global carbon cycle. One powerful tool for investigating the interactions between the major carbon reservoirs (geosphere, hydrosphere, biosphere) is the stable isotope geochemistry. The ¹³C/¹²C and ¹⁸O/¹⁶O isotope ratios of tropospheric CO₂ are established tracers in studies on the global carbon cycles (e.g. Cuntz et al., 2003b; Francey and Tans, 1987; Gruber, 2001; Keeling, 1958; Keeling, 1961).

The carbon isotope composition of atmospheric CO₂ (expressed in form of the $\delta^{13}\text{C}$ value, see section 4.3) gives information on the net carbon exchange between atmosphere and biosphere (e.g. Ciais et al., 1995). The oxygen isotope composition of tropospheric CO₂ (expressed as $\delta^{18}\text{O}$ for the $^{18}\text{O}/^{16}\text{O}$ ratio) is controlled by isotope exchange with different water reservoirs; namely leaf, soil and surface water (e.g. Francey and Tans, 1987). The $\delta^{18}\text{O}$ value of CO₂ that has equilibrated with leaf water is different from the $\delta^{18}\text{O}$ of CO₂ that has equilibrated with soil water (e.g. Cuntz et al., 2003b). Thus, the $\delta^{18}\text{O}$ value of tropospheric CO₂ can be used as a tracer for the gross flux of carbon between troposphere and biosphere (e.g. Ciais et al., 1997; Farquhar et al., 1993).

Hoag et al. (2005) suggested that the triple oxygen isotope composition of CO₂ (expressed in form of $\Delta^{17}\text{O}$, which is the deviation in $\delta^{17}\text{O}$ from a reference line; for definition see section 4.3) provides a more robust tracer for the global carbon cycle than $\delta^{18}\text{O}$ alone. The $\Delta^{17}\text{O}$ value of tropospheric CO₂ is controlled by the influx of stratospheric CO₂ with a large $\Delta^{17}\text{O}$ excess and resetting of the $\Delta^{17}\text{O}$ excess by exchange with water in oceans, in soil and most importantly in leaves. Assuming a constant flux and a constant $\Delta^{17}\text{O}$ value of stratospheric CO₂ and a constant exchange with ocean water, the $\Delta^{17}\text{O}$ value of tropospheric CO₂ has been suggested as a tracer for global primary production (Hoag et al., 2005).

Apart from stratospheric CO₂, the CO₂ from the combustion of fossil and modern organic matter (fossil fuels, wood) is likely also a source of CO₂ with non-zero $\Delta^{17}\text{O}$. Hoag et al. (2005) proposed that CO₂ from combustion is another source of “anomalous” oxygen with a deficit in ^{17}O . The deficit is thought to be inherited from tropospheric O₂, which carries a negative $\Delta^{17}\text{O}$ value (Barkan and Luz, 2005; Pack et al., 2007). It is hypothesized that during combustion, the anomaly is transferred from the O₂ to CO₂ making combustion CO₂ clearly distinguishable from ambient background CO₂. According to Hoag et al. (2005) “anomalous” CO₂ from anthropogenic sources has little effect on a global scale, but can be an important source in urban regions (Newman et al., 2008; Pataki et al., 2007; Widory and Javoy, 2003; Yanes and Yapp, 2010).

The $^{13}\text{C}/^{12}\text{C}$ and $^{18}\text{O}/^{16}\text{O}$ ratios of CO₂ alone are insufficient for unambiguous determination of different fluxes (e.g. Demény and Haszpra, 2002; Djuricin, 2010). For example, CO₂ from soil respiration has a similar $\delta^{13}\text{C}$ value to CO₂ from fossil fuel combustion. Other tracers were also tested. Levin et al. (2003) successfully applied cost intensive ^{14}C analyses for determination of the mixing ratio of CO₂ from fossil fuel

combustion. In a promising approach, Affek et al. (2007) suggested using the mass-47 anomaly of CO₂ (Δ_{47}) for tracing combustion CO₂ in air.

In this contribution, we present the first data on the triple oxygen isotope composition of CO₂ from combustion processes. We test the hypothesis from Hoag et al. (2005) that the $\Delta^{17}\text{O}$ value of combustion CO₂ is inherited from tropospheric O₂.

4.3 Materials and methods

4.3.1 Definitions

Variations in stable isotope ratios are expressed in form of the δ notation relative to a standard. The $\delta^{13}\text{C}$ value is defined as:

$$\delta^{13}\text{C} = \left(\frac{\left(\frac{^{13}\text{C}}{^{12}\text{C}} \right)_{\text{sample}}}{\left(\frac{^{13}\text{C}}{^{12}\text{C}} \right)_{\text{VPDB}}} - 1 \right) \quad \text{Eq. 4-1}$$

with VPDB as standard. The variations in the $^{17}\text{O}/^{16}\text{O}$ and $^{18}\text{O}/^{16}\text{O}$ ratios are expressed in the same way with the only difference that VSMOW is used as standard. For correct description of the effect of fractionation processes on the $^{17}/^{16}\text{O}$ to $^{18}/^{16}\text{O}$ relation, the linearized version of δ' notation was introduced. The δ' values are defined as $\delta'^{17}\text{O} = \ln(\delta^{17}\text{O} + 1)$ and $\delta'^{18}\text{O} = \ln(\delta^{18}\text{O} + 1)$ (Hulston and Thode, 1965; Miller, 2002; Young et al., 2002).

The triple oxygen isotope composition is given as $\Delta^{17}\text{O}$ values, which denote the deviation from a reference line (RL) with: $\Delta^{17}\text{O} = \delta'^{17}\text{O} - \lambda_{\text{RL}} \times \delta'^{18}\text{O} - \gamma_{\text{RL}}$

We use the equilibrium slope for CO₂–water equilibration of 0.522 (Hofmann et al., 2012b) as λ_{RL} and a zero intercept ($\gamma_{\text{RL}} = 0$) for our study. We point out, however, that any other line could be chosen, as long as it is well defined and as long as it is helpful for the scientific problem being addressed (Assonov and Brenninkmeijer, 2005).

4.3.2 Sampling

We have produced CO₂ by combustion of four different combustibles: (i) In-house laboratory gas (natural gas) originated from production sites in Russia and Norway (according to information from the local supplier, the Stadtwerke Göttingen AG). It is composed of >90 mol% methane. (ii) A propane-butane gas mixture was supplied in small

(220 g), pressurized bottles (Apragas, France) for use in a camping stove. (iii) Air dried wood chips were prepared from dry Norway spruce (*Picea abies*) wood from Göttingen. The chips were 2–8 cm long, ca. 1 cm wide, and 0.5 mm thin. (iv) The CO₂ in the exhaust gas of a gasoline engine car (VW POLO, 2010, 1400 cm³ engine displacement) was sampled. The samples were taken after the engine reached the normal operating temperature of 90 °C for the cooling water.

In addition to the inorganic combustion processes, we studied CO₂ exhaled by two humans (female, 25; male, 35).

Ambient air oxygen was the oxidant in all cases.

4.3.3 Experimental procedures

Natural gas was combusted by means of a laboratory Bunsen burner. The bottled propane–butane mixture was combusted using a Markill “Devil” camping stove with pre-adjusted and optimized air/fuel ratios. Wood chips were dried at 60 °C for 24 h before using. They were burned in an open fire under a fume hood. The temperature of the natural gas and propane butane flame were above the measurement range of the thermometer, i.e., >1200 °C. The temperature of the wood chips flame was between 600 and 700 °C. The flame temperatures were measured with a digital thermometer (Extech Instruments, 421501) with a K-Type thermocouple, and an accuracy of ±3 K. The combustion gases were collected directly above the flame, through a ¼” stainless steel tube. The sampling rate was set to ~0.3 L min⁻¹. The combustion gases were first pumped through a 2 µm particle filter (Swagelok) and then dried at sub-atmospheric pressure by pumping through a 20 cm long tube with an inner diameter of 1 cm, which was filled with magnesium perchlorate (Mg(ClO₄)₂). As combustion gases were pumped through the filter and the Mg(ClO₄)₂ trap within a second and no condensed water was observed in any of the experiments, we exclude that the isotope composition of CO₂ was modified by exchange with liquid water. After filtering and drying, sample CO₂ was isolated from the non-condensable gases with a “Russian doll”-type cryogenic trap (Brenninkmeijer and Röckmann, 1996) that was submerged in liquid nitrogen (–196 °C). Any remaining water was removed from the sample CO₂ in a second drying step by expanding the gas for 30–60 min into a glass volume that contained a few grams of P₂O₅.

The exhaust gas of the Volkswagen Polo was sampled at a flow rate of 0.2 L min⁻¹ through a 2 µm particle filter (Swagelok) and a Mg(ClO₄)₂ water trap into a pre-evacuated 3.5 L glass flask. The ¼” stainless steel sampling tube was inserted 5–10 cm into the tail pipe, where the temperature was 55–65 °C. The CO₂ was extracted from the pre-dried gas

mixture as described above. As for the gas and wood combustibles, no liquid water was observed in the sampling apparatus at any of the experiments.

Human breath was sampled by exhaling through a Mg(ClO₄)₂ water trap directly into the cryogenic trap. After deep inhalation, air was exhaled for ~30–40 s. The flow into the trap was ~0.3 L min⁻¹. About 7 L of respired breath was collected for one sample.

4.3.4 Analytical procedures

The CO₂ concentration in the combustion gases was measured with an electronic pressure gauge in a calibrated volume. The concentrations ranged between 1.5 (exhaled breath) and 15 vol.% (car exhaust). Open flame combustion yielded 2.5–17 vol.% CO₂. Contamination by air from the laboratory was negligible as the laboratory was kept well-vented during the experiments.

The $\delta^{13}\text{C}$ and $\delta^{18}\text{O}$ values of the extracted CO₂ were measured by dual inlet gas source mass spectrometry using a Finnigan Delta Plus isotope ratio mass spectrometer. The in-house reference CO₂ was calibrated relative to CO₂ generated by phosphoric acid decomposition of NBS-19 ($T = 70\text{ }^{\circ}\text{C}$; $\delta^{18}\text{O}_{\text{VSMOW}} = +28.65\text{‰}$; $\delta^{13}\text{C}_{\text{PDB}} = +1.95\text{‰}$ (Coplen et al., 2002)). We applied the acid fractionation factor $^{18}\alpha_{\text{CO}_2\text{-calcite}} = 1.00871$ (Kim et al., 2007) to calculate the composition of the CO₂ gas.

The external reproducibility for $\delta^{13}\text{C}$ and $\delta^{18}\text{O}$ was $\pm 0.1\text{‰}$. We measured the N₂O mixing ratios on He diluted subsamples with a gas chromatograph (Carlo Erba, Hofheim, Germany). As the measured N₂O/CO₂ ratios were $< 1/10,000$ in all cases, no correction for N₂O was necessary (Assonov and Brenninkmeijer, 2006).

The $\Delta^{17}\text{O}$ value of the CO₂ was measured with the CO₂–CeO₂ equilibration method (Hofmann et al., 2012b; Hofmann and Pack, 2010). An excess of CO₂ was equilibrated with CeO₂ powder at 685 °C. It was shown by Assonov and Brenninkmeijer (2001) and confirmed by Hofmann and Pack (2010) and Hofmann et al. (2012b) that CO₂ and CeO₂ fully exchange at these conditions. The equilibrated CeO₂ was analyzed for its triple oxygen isotope ratios by infrared-laser fluorination coupled with continuous flow gas chromatograph isotope ratio monitoring mass spectrometry (CF-GCirmMS). Samples were loaded along with NBS-28 quartz into an 18-pit Ni sample holder. One analytical session generally contained 8–12 CeO₂ samples (0.6–3 mg per sample) and 6–8 NBS-28 quartz standards (0.2–1 mg per sample). Purified F₂ gas was used as oxidation agent. The sample O₂ was cleaned from excess F₂ by passing through a NaCl trap. The liberated Cl₂ was trapped in a cold trap at –196 °C. The interfering NF₃ (Pack et al., 2007) was separated in a

5 Å molecular sieve type GC Column (Thermo Gasbench II) before introduction of the sample gas into the source of a Thermo MAT 253 gas mass spectrometer. The in-house reference O₂ gas was calibrated relative to VSMOW by E. Barkan (Institute of Earth Sciences, Hebrew University of Jerusalem) with $\delta^{18}\text{O}_{\text{VSMOW}} = 13.473 \pm 0.015\text{‰}$ ($t_{0.95} \times \text{SEM}$) and $\delta^{17}\text{O}_{\text{VSMOW}} = 6.649 \pm 0.009\text{‰}$ ($t_{0.95} \times \text{SEM}$). The $\Delta^{17}\text{O}$ value of CO₂ was calculated as follows:

$$\Delta^{17}\text{O}_{\text{CO}_2} = \Delta^{17}\text{O}_{\text{CeO}_2} + (\lambda_{\text{CO}_2-\text{CeO}_2} - \lambda_{\text{RL}}) \times 10^3 \ln^{18} \alpha_{\text{CO}_2-\text{CeO}_2} \quad \text{Eq. 4-2}$$

where $^{18}\alpha_{\text{CO}_2-\text{CeO}_2}$ and $\lambda_{\text{CO}_2-\text{CeO}_2}$ are the fractionation factor and the triple oxygen isotope fractionation exponent for oxygen isotope exchange between CO₂ and CeO₂ in our apparatus. Note that α and λ are *not* equilibrium values of a simple equilibration reaction between CO₂ and CeO₂. Instead, they are due to equilibrium and kinetic fractionation and are a function of the geometry of the equilibration apparatus and the CO₂ pressure in the equilibration tube. The data presented here were obtained using the same apparatus and pressure range as calibration experiments with CO₂ with known isotope composition (Hofmann et al., 2012b; Hofmann and Pack, 2010).

Each CO₂-equilibrated CeO₂ sample was divided into 2–6 aliquots, which were measured separately. The $\Delta^{17}\text{O}$ values of CeO₂ were corrected relative to NBS-28 analyzed the same day. The analytical uncertainty of $\Delta^{17}\text{O}$ for a single analysis was $\leq \pm 0.05\text{‰}$ (1σ , SD). This value was calculated based on the error propagation for Eq. 4-2 (Gehler et al., 2011; Hofmann et al., 2012b; Hofmann and Pack, 2010). An example for the precision of the measurements from one analytical session is displayed in Fig. 4-1.

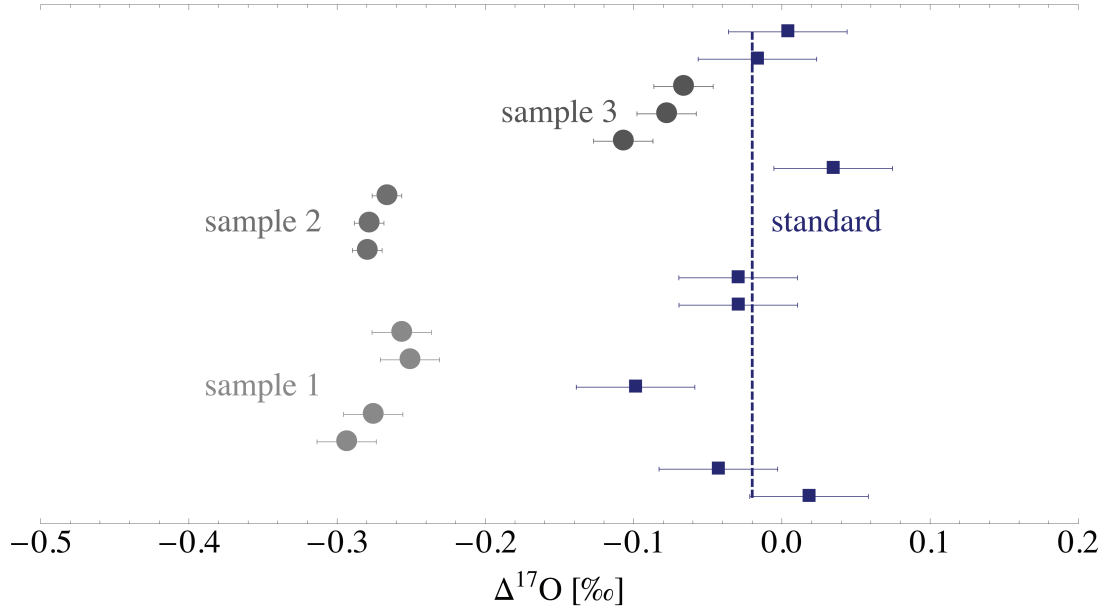


Fig. 4-1: With the method described by Hofmann and Pack (2010), the $\Delta^{17}\text{O}$ value of CO_2 can be measured with a precision of 0.05‰ (SD) or better. This variation diagram depicts the results of $\Delta^{17}\text{O}$ measurements for one analytical session. The data points are vertically arranged in the order they have been obtained (from bottom to top). The bars indicate the 1σ standard deviation. Solid squares indicate the silicate and rock standards (NBS-28 quartz and mid-ocean ridge basalt). The standard deviation of the measured values was 0.04‰ ($n = 8$, SE 0.015‰). Three CO_2 equilibrated CeO_2 samples (dots) were analyzed. The standard deviations of the measurements were 0.02‰, 0.01‰ and 0.02‰, respectively.

4.4 Results

Carbon and oxygen isotope ratios of CO_2 from the experiments are listed in Table 4-1.

The $\delta^{13}\text{C}$ value of CO_2 from our natural gas combustion was $-29.6 \pm 0.8\text{‰}$ and $-30.7 \pm 0.1\text{‰}$ from the propane-butane combustion. The oxygen isotope composition of CO_2 from combustion of natural gas and propane-butane were similar in $\delta^{18}\text{O} \sim 22\text{‰}$ (Table 4-1). The $\Delta^{17}\text{O}$ values showed a significant deficit in ^{17}O with $\Delta^{17}\text{O} = -0.30 \pm 0.02\text{‰}$ for natural gas and $-0.32 \pm 0.02\text{‰}$ for the propane-butane mixture.

The $\delta^{13}\text{C}$ value of CO_2 that was extracted from the wood combustion gases was $-26.4 \pm 1.0\text{‰}$. The corresponding $\delta^{18}\text{O}$ and $\Delta^{17}\text{O}$ values were $19.4 \pm 1.0\text{‰}$ and $-0.21 \pm 0.02\text{‰}$, respectively.

The oxygen isotope composition of CO_2 from the car exhaust gases was $\delta^{18}\text{O} = 32.6 \pm 3.0\text{‰}$. The $\Delta^{17}\text{O}$ value of the car exhaust gas was $-0.32 \pm 0.03\text{‰}$.

The $\delta^{13}\text{C}$ value of human breath CO₂ was $-24.5 \pm 1.0\text{‰}$ and the $\delta^{18}\text{O}$ value was $35.1 \pm 1.0\text{‰}$. The corresponding $\Delta^{17}\text{O}$ value was $-0.03 \pm 0.03\text{‰}$. No significant difference was observed between CO₂ from the two individuals (Table 4-1).

Table 4-1: Carbon and oxygen isotope compositions of CO₂ from different anthropogenic sources. For the mean values 95% confidence limits are given (standard error of the mean multiplied by Student's t-factor).

Sample	N ^a	$\delta^{13}\text{C}_{\text{VPDB}}$	$\delta^{18}\text{O}_{\text{VSMOW}}$	$\Delta^{17}\text{O}_{\text{RL}}^{\text{b}}$
		[‰]		
Natural gas	1	−29.6	22.2	−0.29
				−0.25
				−0.25
	2	−29.1	21.3	−0.33
				−0.33
				−0.34
				−0.32
	3	−29.4	21.5	−0.27
				−0.31
	4	−30.2	21.4	−0.31
				−0.33
				−0.29
Average±t _{0.95} ×SEM		−29.6 ± 0.8	21.6 ± 0.7	−0.30 ± 0.02
Propane−butane	1	−30.6	22.4	−0.31
				−0.38
				−0.30
	2	−30.7	22.5	−0.29
				−0.32
				−0.32
	3	−30.6	22.0	−0.32
				−0.34
	4	−30.8	23.2	−0.32
				−0.30
				−0.32
	Average±t _{0.95} ×SEM		−30.7 ± 0.1	22.5 ± 0.8
Wood chips	1	−25.5	19.3	−0.23
				−0.21
				−0.19
				−0.18
	2	−26.5	18.6	−0.21
				−0.21
				−0.19
				−0.18
	3	−26.6	19.9	−0.27
				−0.17
				−0.18
				−0.21
	4	−26.9	19.9	−0.22
				−0.23
				−0.21
				−0.23
Average±t _{0.95} ×SEM		−26.4 ± 1.0	19.4 ± 1.0	−0.21 ± 0.02

Sample	N ^a	$\delta^{13}\text{C}_{\text{VPDB}}$	$\delta^{18}\text{O}_{\text{VSMOW}}$	$\Delta^{17}\text{O}_{\text{RL}}^{\text{b}}$
————— [‰] —————				
Car exhaust	1	−27.7	35.4	−0.27
				−0.29
				−0.30
	2	−27.7	31.5	−0.31
				−0.43
				−0.38
	3	−27.8	31.4	−0.28
				−0.36
				−0.30
	4	−28.9	32.1	−0.37
				−0.34
				−0.31
				−0.32
				−0.33
				−0.24
Average±t _{0.95} ×SEM		−28.0 ± 0.9	32.6 ± 3.0	−0.32 ± 0.03
Human breath	1	−25.5	35.2	−0.01
				−0.07
				0.04
	2	−24.3	34.9	−0.07
				−0.07
				−0.07
	3	−24.0	36.0	0.04
				−0.06
				−0.01
	4	−24.3	34.5	−0.01
				−0.04
	Average±t _{0.95} ×SEM		−24.5 ± 1.0	35.1 ± 1.0

^a N denotes the number of independent experiments. The $\delta^{13}\text{C}$ and $\delta^{18}\text{O}$ values were measured once per experiment in dual-inlet mode (5 cycles). In contrast, the $\Delta^{17}\text{O}$ values were determined on 2–6 aliquots in continuous flow mode (see section 4.3).

^b $\Delta^{17}\text{O}$ values are given as a deviation from the reference line, with a slope (λ) 0.522 and 0 intercept (γ). λ refers to the CO₂–water equilibration line, determined by Hofmann et al. (2012b).

4.5 Discussion

4.5.1 Carbon isotope ratios

The carbon isotope composition of the CO₂ samples from different combustion processes was within the range of literature data given for the respective combustibles. This is expected as the entire carbon is converted to CO₂.

The $\delta^{13}\text{C}$ value of CO₂ from our natural gas combustion ($-29.6 \pm 0.8\text{‰}$) is within the range reported for natural methane of -20‰ to -75‰ (Yakir, 2003). It agrees well with the range measured recently by Schumacher et al. (2011) for natural gas combustion CO₂ (-31.8 to -29.7‰).

The $\delta^{13}\text{C}$ value of CO₂ from the propane–butane combustion was $-30.7 \pm 0.1\text{‰}$, which is consistent with the range given by Rooney et al. (1995) for propane (-26‰ to -32‰). The $\delta^{13}\text{C}$ value of CO₂ that was extracted from the wood combustion gases ($-26.4 \pm 1.0\text{‰}$) is in the range of -22‰ to -28‰ reported for wood by Craig (1953). Our values are very similar to the values measured on spruce wood from Switzerland (-25‰) (Jäggi et al., 2002) and from Norway (-25‰) (Saurer et al., 2004). For comparison, Schumacher et al. (2011) measured a $\delta^{13}\text{C}$ value of -27.1‰ for CO₂ from spruce wood combustion.

The $\delta^{13}\text{C}$ value of CO₂ from car exhaust ($-28.0 \pm 0.9\text{‰}$) is consistent with the values reported by Pataki et al. (2003) (-28‰) and Newman (2008) (-26‰) for gasoline. The $\delta^{13}\text{C}$ of CO₂ from the car exhaust agrees with the measured value of Schumacher et al. (2011) (-27‰). Affek and Eiler (2006) reported a $\delta^{13}\text{C}$ value of -25‰ for CO₂ from car exhausts.

Our data and the data by Schumacher et al. (2011) and Affek and Eiler (2006) demonstrate that no large fractionation in $\delta^{13}\text{C}$ occurs between the fuels and the combustion CO₂.

4.5.2 Oxygen isotope ratios

Air O₂

Air O₂ was the oxidant in all experiments. The isotope composition of air O₂ has been analyzed relative to VSMOW to $\delta^{18}\text{O} = 23.88\text{‰}$ and $\delta^{17}\text{O} = 12.08\text{‰}$ with $\Delta^{17}\text{O} = -0.31\text{‰}$ (Barkan and Luz, 2005). This value has been suggested of being incorrect and has recently been revised to $\Delta^{17}\text{O} = -0.37\text{‰}$ (letter to the editor, Barkan and Luz (2011)). Pack et al. (2007) report the isotope composition of technical O₂. Their dataset includes a number of

gases with $\delta^{18}\text{O}$ values equal to air O₂. As technical O₂ is made of air O₂, it is assumed to be unfractionated in $\Delta^{17}\text{O}$ relative to air O₂ as well. Pack et al. (2007) reported their data with respect to the terrestrial fractionation line with a slope of 0.5237 and zero intercept with NBS-28 quartz having $\Delta^{17}\text{O} = 0\text{‰}$. Recent high-precision analyses of NBS-28 quartz relative to VSMOW give $\Delta^{17}\text{O} = 0\text{‰}$ when using a line with a slope of 0.527 and an intercept of -0.07‰ (Tanaka and Nakamura, 2012). Recalculating the data reported in Pack et al. (2007) and taking in account the newly reported $\Delta^{17}\text{O}$ of NBS-28 from Tanaka and Nakamura (2012) with respect to a reference line with slope 0.522 and zero intercept gives a $\Delta^{17}\text{O}$ of air O₂ of -0.34‰ .

Combustion CO₂ obtains its oxygen from air O₂. Thus combustion CO₂ should have an oxygen isotope composition that is related to the composition of air O₂.

Natural gas combustion

The $\delta^{18}\text{O}$ of CO₂ from the open-flame combustion experiments for natural gas were $\sim 2\text{‰}$ lower than the $\delta^{18}\text{O}$ of air O₂. The small fractionation in $\delta^{18}\text{O}$ may be explained by means of a slight preference of ¹⁶O relative to ¹⁸O during the combustion process. Isotope exchange between CO₂ and water at $T < 100\text{ °C}$ is unlikely to have occurred because one would expect higher $\delta^{18}\text{O}$ of CO₂. If CO₂ and water initially inherited the isotope composition of air O₂ ($+23.88\text{‰}$), exchange between these reservoirs at any temperature would lead to $\delta^{18}\text{O} > 23.88\text{‰}$ in the CO₂ and $\delta^{18}\text{O} < 23.88\text{‰}$ for the H₂O (see fractionation factors, e.g. in Brenninkmeijer et al., 1983). Instead, a $\delta^{18}\text{O}$ value slightly lower than 23.88‰ was measured for the combustion CO₂. Also, no water was observed in any part of the extraction apparatus during sampling and storage. We therefore conclude that equilibration between CO₂ and water did not play any role.

We calculated the kinetic fractionation factor for O₂ according to Craig (1954) and Young et al. (2002):

$$\lambda_{\text{O}_2}^{\text{kin}} = \frac{\ln^{17}\alpha_{\text{O}_2}^{\text{kin}}}{\ln^{18}\alpha_{\text{O}_2}^{\text{kin}}} = \frac{\ln\left[\frac{29 \times 32}{29 + 32} \times \frac{29 + 33}{29 \times 33}\right]}{\ln\left[\frac{29 \times 32}{29 + 32} \times \frac{29 + 34}{29 \times 34}\right]} = 0.512 \quad \text{Eq. 4-3}$$

A -2‰ shift in $\delta^{18}\text{O}$ results in a 0.02‰ shift in $\Delta^{17}\text{O}$, giving an expected value for the CO₂ of -0.32‰ , which is close to the observed $\Delta^{17}\text{O}$ value of $-0.30 \pm 0.02\text{‰}$ for CO₂ from natural gas combustion (Fig. 4-2).

Schumacher et al. (2011) measured in natural gas combustion CO₂ a $\delta^{18}\text{O}$ depletion between 13.5‰ and 16.8‰ compared to the oxidant, which is in stark contrast to the depletion of 2.4‰ measured in this study. We assume that this difference partially arises from the difference in the oxidant. Schumacher et al. (2011) used pure oxygen, where $^{18}\alpha^{\text{kin}}_{\text{O}_2}$ is 0.970, while in this study the oxygen source was air, where the $^{18}\alpha^{\text{kin}}_{\text{O}_2}$ is 0.986.

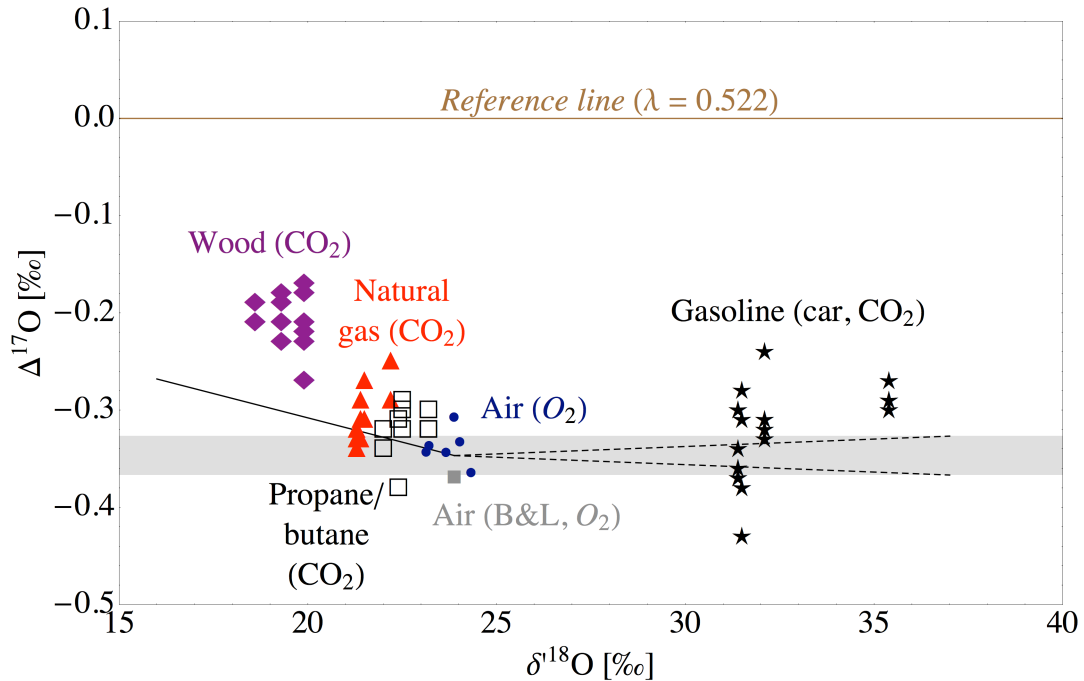


Fig. 4-2: The triple oxygen isotope compositions of CO₂ from fossil fuel combustion reflect a small fractionation in diffusion of O₂ to the combustion site (^{18}O depletion). Triangles and open squares depict CO₂ from natural gas and propane–butane combustion, respectively. In case of biomass combustion (diamonds) intrinsic O, in case of car exhaust CO₂ (stars) equilibration between condensed water and CO₂ plays a significant role, too. Dots depict the triple oxygen isotope composition of air O₂ measured by Pack et al. (2007); the gray band represents the 95% confidence interval of these measurements. The solid gray square shows air O₂ measured by Barkan and Luz (2011). Black line indicates the kinetic fractionation trajectory for diffusion of O₂ in air ($\lambda^{\text{kin}}_{\text{O}_2} = 0.512$); dashed lines show the 95% confidence interval of the CO₂–water equilibration line (0.522 ± 0.002 , Hofmann et al., 2012b).

Propane–butane combustion

For the propane–butane mixture, a $\delta^{18}\text{O}$ value was observed that was only 1.4‰ lower than the $\delta^{18}\text{O}$ of air O₂. This demonstrates that very little fractionation occurs during the combustion process. The corresponding $\Delta^{17}\text{O}$ value is –0.32‰. Considering a kinetic diffusive effect on $\Delta^{17}\text{O}$ of 0.01‰ (Eq. 4-3) the expected $\Delta^{17}\text{O}$ value of CO₂ is –0.33‰, which is in agreement with our observation of -0.32 ± 0.02 ‰ (Fig. 4-2).

The gas combustion experiments show that only very little oxygen isotope fractionation occurs between O₂ in the educts and CO₂ in the products in the flame and that post-combustion exchange with vapor is negligible. A small kinetic effect may be suggested by the observed slightly lower $\delta^{18}\text{O}$ value of combustion CO₂ relative to the $\delta^{18}\text{O}$ value of air O₂.

Wood combustion

Unlike fossil fuels, a considerable amount of oxygen is contained in wood. Average spruce contains 70 mol% cellulose and hemi cellulose ($[\text{C}_6\text{H}_{10}\text{O}_5]_n$) and 30 mol% lignin ($\text{C}_{10}\text{H}_{12}\text{O}$) (Sjostrom, 1993). Assuming combustion of water-free wood, 22% of the oxygen in the combustion is intrinsic oxygen and only 78% sources from ambient air O₂.

Therefore, at least ~22% of the oxygen in combustion gases (CO₂, H₂O) originated not from isotopically anomalous air O₂, but from intrinsic “normal” oxygen cellulose, hemi cellulose, and lignin. The $\Delta^{17}\text{O}$ value of CO₂ from our wood combustion experiments clearly indicates the presence of an isotopically “normal” (i.e., without large negative anomaly as air O₂) component in the combustion gases as the $\Delta^{17}\text{O}$ value of CO₂ is higher than the $\Delta^{17}\text{O}$ value of air O₂ (Fig. 4-2).

The $\delta^{18}\text{O}$ value of spruce wood (i.e., cellulose, hemi cellulose and lignin) grown in a similar environment is 25‰ (Jäggi et al., 2003). The high $\delta^{18}\text{O}$ value of wood is due to equilibrium fractionation between leaf water and cellulose, which is ~27‰ (DeNiro and Epstein, 1979; Yakir and DeNiro, 1990). Leaf water in temperate regions is enriched in $\delta^{18}\text{O}$ relative to meteoric water ($\delta^{18}\text{O} \sim -8$ ‰) by $\sim 8 \pm 5$ ‰ (Landais et al., 2006) giving a $\delta^{18}\text{O}$ of leaf water of $\sim 0 \pm 5$ ‰. The $\Delta^{17}\text{O}$ value of wood has not yet been analyzed. Assuming that a triple oxygen isotope fractionation exponent for cellulose–water falls within the range of the published low-T oxygen isotope equilibrium exponents (Barkan and Luz, 2005; Hofmann et al., 2012b) $0.522 \leq \lambda_{\text{cellulose–water}} \leq 0.529$, a $\Delta^{17}\text{O}$ of cellulose of $\sim 0 \pm 0.1$ ‰ is estimated (Fig. 4-3). Remaining moisture in wood is assumed to be kinetically

fractionated relative to the original stem water with $\lambda = 0.516$ (see Landais et al., 2006) resulting in $\delta^{18}\text{O} \approx 0\text{‰}$ and $\Delta^{17}\text{O} \approx -0.06\text{‰}$ (Fig. 4-3).

Our rough estimate on the triple isotope composition of possible oxygen sources in the combustion gases of wood show that $\sim 2/3$ of oxygen in combustion CO₂ sources from air O₂ and $\sim 1/3$ sources from oxygen intrinsic to wood, i.e., cellulose, hemi cellulose and remaining moisture.

In case of wood chips combustion, Schumacher et al. (2011) measured a $\delta^{18}\text{O}$ depletion of 15.5‰ compared to the oxidant. This value is in contrast to our measured depletion of 4.4‰. Similar to natural gas combustion, we assume that this difference arises from the different oxidant (pure O₂ vs. O₂ in air) and different experimental set up (closed chamber with ignition through heating vs. open flame). Open flame combustion of charcoal and peat coal by Schumacher et al. (2011) resulted in a much smaller (1.3 and 4.5‰) $\delta^{18}\text{O}$ depletion of the oxygen source, similar to our observations.

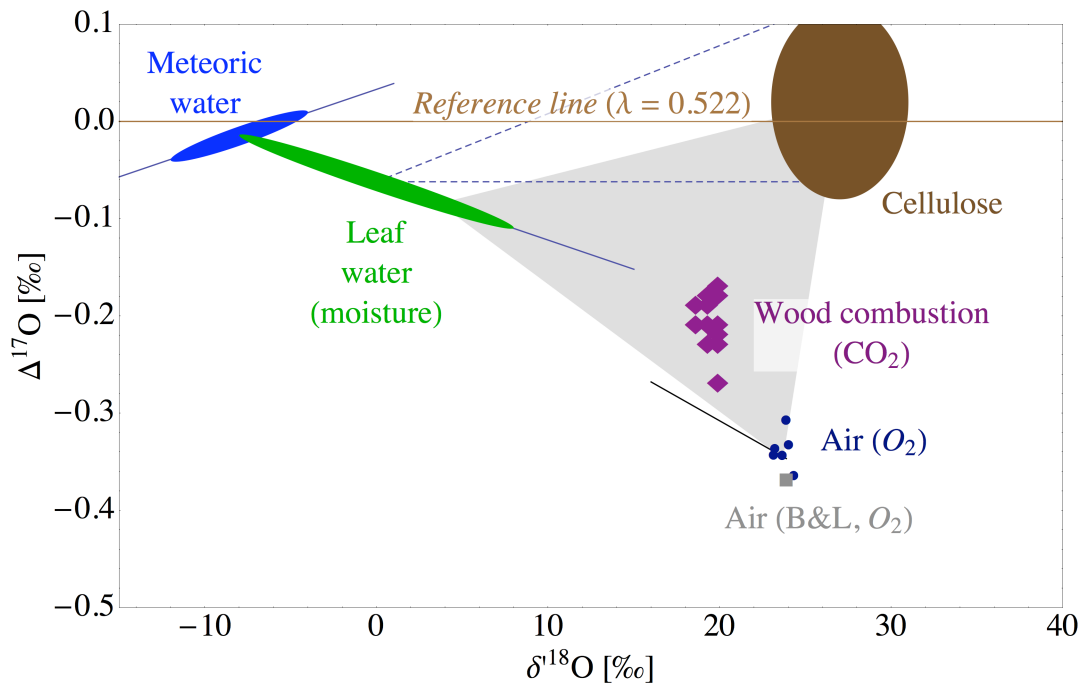


Fig. 4-3: The CO₂ from wood combustion may have three sources of O: (i) tropospheric O₂ (small dots, measurements from Pack et al., 2007; solid gray square from Barkan and Luz, 2011) which can be depleted along a kinetic fractionation trajectory (black line) (ii) intrinsic O from cellulose (brown ellipse) (iii) remaining moisture in wood. (See text for details on estimates for each oxygen source). Global meteoric water line (GMWL, $\lambda = 0.528$ and $\gamma = 0.033\text{‰}$, Luz and Barkan, 2010) and the evaporation line of water ($\lambda = 0.516$, Landais et al., 2006) are depicted.

Car exhaust

The $\delta^{18}\text{O}$ value of CO₂ collected from the car exhaust is by ~9‰ higher than the $\delta^{18}\text{O}$ value of air O₂. The CO₂ was sampled from the exhaust pipe where temperatures were about 60 °C and CO₂–water oxygen isotope exchange may be the cause for the observed $\delta^{18}\text{O}$ value.

The $\Delta^{17}\text{O}$ value of the CO₂ from the exhaust pipe ($-0.32 \pm 0.03\text{‰}$) is only slightly higher than the $\Delta^{17}\text{O}$ of air O₂ (-0.37‰ , by Barkan and Luz, 2011; -0.34‰ by Pack et al., 2007). Hofmann et al. (2012b) gave an uncertainty ($t_{0.95} \times \text{SEM}$) of ± 0.002 for the CO₂–water equilibrium isotope fractionation exponent. Considering the fractionation in $\delta^{18}\text{O}$ of 9‰, this uncertainty introduces an intrinsic uncertainty of 0.02‰, giving an expected $\Delta^{17}\text{O}$ of CO₂ of $-0.37 \pm 0.02\text{‰}$ (for $\Delta^{17}\text{O}$ of O₂ from Barkan and Luz, 2011) and of $-0.34 \pm 0.02\text{‰}$ (for $\Delta^{17}\text{O}$ of O₂ from Pack et al., 2007), respectively. As in the case of gas combustion, our $\Delta^{17}\text{O}$ of CO₂ is slightly higher than expected when using the revised value for air O₂, but is in good agreement when using the value $\Delta^{17}\text{O}$ of air O₂ measured by Pack et al. (2007) (Fig. 4-2).

Alternatively, CO₂ may have exchanged with vapor within the exhaust pipe as suggested by the clumped isotope analyses by Affek and Eiler (2006). In such a scenario, metal walls within the pipe, large surfaces within the silencers or the Pt coated surface in the catalysts may have catalyzed the exchange reaction. There is no strong evidence, however, for fast oxygen isotope exchange between CO₂ and water vapor, thus the partial equilibration between CO₂ and the condensed water in the exhaust pipe line seems to be a more plausible explanation for our results.

Human respiration CO₂

We demonstrate that the triple oxygen isotope composition of CO₂ from abiotic combustion processes is partly controlled by the isotope composition of air O₂, and thus, shows significant negative $\Delta^{17}\text{O}$ values. Exchange with water is the second important factor controlling $\delta^{18}\text{O}$ and $\Delta^{17}\text{O}$ of combustion CO₂. Although CO₂ from human breath does not influence the isotope composition of atmospheric CO₂, it is a model for biogenic “combustion” CO₂ that has extensively exchanged with water. Exchange with water is expected for CO₂ that is emitted by any kind of heterotrophic organisms, e.g. in soils. Soil CO₂ is an important source of CO₂ in the atmosphere. CO₂ that equilibrated with seawater is another important source for the atmosphere.

The $\delta^{13}\text{C}$ value of CO₂ from human respiration of two individuals was $-24.5 \pm 1.0\text{‰}$. This value largely reflects the $\delta^{13}\text{C}$ of the diet. Both individuals live in Germany and have similar $\delta^{13}\text{C}$ as the individuals from France that were studied by Widory and Javoy (2003) ($\delta^{13}\text{C} = -24.5\text{‰}$). In contrast, respired CO₂ of US Americans had $\delta^{13}\text{C}$ -values that were 1 to 6 ‰ higher than in our study (Affek and Eiler, 2006; Epstein and Zeiri, 1988; Yanes and Yapp, 2010). As noted by Affek and Eiler (2006), a possible explanation is the larger contribution of C₄ plants (e.g. corn) with a higher $\delta^{13}\text{C}$ value to the diet of people from North America compared to the Mid-European individuals.

We observed a mean $\delta^{18}\text{O}$ value of $35.1 \pm 1.0\text{‰}$ in the exhaled breath CO₂. This is similar to the value of exhaled CO₂ reported by Affek and Eiler (2006) ($34.3 \pm 0.3\text{‰}$). The $\delta^{18}\text{O}$ value of exhaled CO₂ is controlled by equilibration with body water (Luz et al., 1984), which, in turn, is largely controlled by drinking water (Longinelli, 1984). According to Brenninkmeijer et al. (1983) the $^{18}\text{O}/^{16}\text{O}$ fractionation of CO₂ relative to water is $^{18}\alpha_{\text{CO}_2\text{-water}} = 1.03865$ at 37°C. This gives a $\delta^{18}\text{O}$ value of -3.4‰ for the body water of the two individuals in this study (Fig. 4-4). This value is somewhat lower than the value (-2.6‰) measured by Luz et al. (1984).

As for $\delta^{18}\text{O}$, the $\Delta^{17}\text{O}$ value of exhaled CO₂ of -0.03‰ is also controlled by the composition of body water. Hofmann et al. (2012b) experimentally determined a $\theta_{\text{CO}_2\text{-water}}$ value of 0.522 ± 0.002 ($t_{0.95} \times \text{SE}$) for a temperature range of 2–37 °C. This, along with the $^{18}\alpha_{\text{CO}_2\text{-water}}$ value (Brenninkmeijer et al., 1983) gives a $\Delta^{17}\text{O}$ value of body water of the two individuals of $-0.03 \pm 0.08\text{‰}$ (Fig. 4-4). Local drinking water has $\delta^{18}\text{O} = -8.5\text{‰}$ and a $\Delta^{17}\text{O}$ value of -0.02‰ (Hofmann et al., 2012b). Considering that the isotope composition of body water of medium sized mammals (e.g. humans) is largely controlled by drinking water, our data are in good agreement with the expectation.

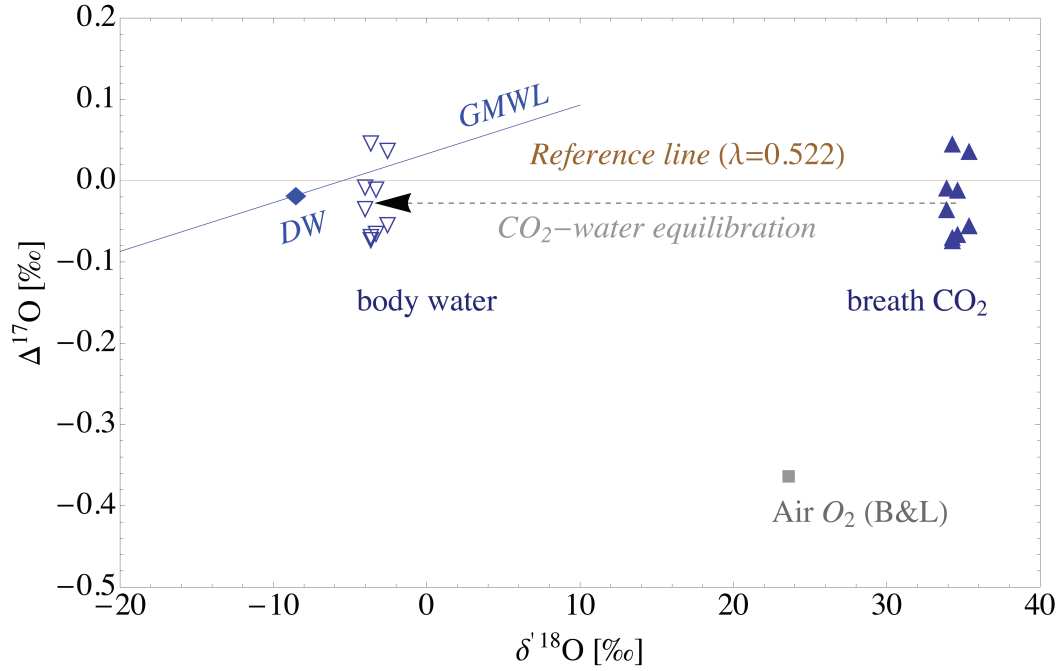


Fig. 4-4: From the triple oxygen isotope composition of CO₂ from human respiration (filled triangles) the isotopic composition of body water (open triangles) can be inferred. The $\theta_{\text{CO}_2\text{-water}}$ is 0.522 (Hofmann et al., 2012b), the fractionation factor $^{18}\alpha_{\text{CO}_2\text{-water}}$ at 37°C is 1.03879 (Brenninkmeijer et al., 1983). The two main O sources of human body water are displayed: local drinking water (DW, diamond) (Hofmann et al., 2012b) and air O₂ (solid gray square) (Barkan and Luz, 2011). The line labeled with GMWL represents the global meteoric water line ($\lambda = 0.528$ and $\gamma = 0.033\text{‰}$, Luz and Barkan, 2010).

4.5.3 Can the $\Delta^{17}\text{O}$ value of CO₂ be used as a tracer to distinguish between different CO₂ sources?

Our data show that with our current technique, $\Delta^{17}\text{O}$ value of CO₂ from gas combustion, combustion of wood and from respiration can be well distinguished.

The background CO₂ concentration level is 390 ppm (NOAA, 2012). The $\delta^{18}\text{O}$ value of background CO₂ is $\sim 41.5\text{‰}$ (e.g. Francey and Tans, 1987) and the $\Delta^{17}\text{O}$ is 0.01‰ (Hofmann et al., 2012a). We assume an average $\Delta^{17}\text{O}$ value of anthropogenic CO₂ of -0.33‰ . Considering a necessary analytical resolution of $\pm 0.05\text{‰}$, a detection limit for anthropogenic CO₂ is at ~ 60 ppm above background level. Such levels can, indeed, be observed in urban environments (Affek and Eiler, 2006; Pataki et al., 2007; Widory and Javoy, 2003) making identification of anthropogenic CO₂ on basis of $\Delta^{17}\text{O}$ conceivable. For the case of anthropogenic emissions in urban environment, however, $\delta^{13}\text{C}$ may be a better proxy than $\Delta^{17}\text{O}$.

For cases, where high atmospheric CO₂ levels are either due to anthropogenic emissions or soil respiration, $\Delta^{17}\text{O}$ can be used as an additional proxy to $\delta^{13}\text{C}$ and $\delta^{18}\text{O}$ values, because the traditional tracers ($\delta^{13}\text{C}$ and $\delta^{18}\text{O}$) cannot distinguish between anthropogenic and soil emissions (Djuricin, 2010).

4.6 Conclusions

We demonstrate that CO₂ from combustion of natural gas and propane–butane gas largely inherits the isotope composition of air O₂ and has an anomaly of $\Delta^{17}\text{O} = -0.30$ to -0.32‰ . Carbon dioxide from wood combustion contains a mixture of oxygen from atmospheric O₂ and oxygen intrinsic to wood with a $\Delta^{17}\text{O} = -0.21\text{‰}$. The isotope composition of CO₂ from car exhaust inherits the $\Delta^{17}\text{O}$ of air O₂, but has likely exchanged with similarly anomalous combustion water at $T < 100\text{ °C}$. Our experiments demonstrate that the isotope composition of respired CO₂ is controlled by ambient water and does not carry a large anomaly in $\Delta^{17}\text{O}$.

We have given constraints on the $\Delta^{17}\text{O}$ value of selected CO₂ sources that may be used as additional proxy when modeling the isotope composition of tropospheric CO₂.

4.7 Acknowledgments

We thank E. Barkan for the calibration of our in-house reference O₂ gas relative to VSMOW. We thank two reviewers (S. S. Assonov and an anonymous reviewer) whose comments led to considerable improvement of the manuscript. The German Science Foundation supported this project financially (AP, project PA909/6-1, PA909/6-2).

4.8 References

- Affek, H. P., Eiler, J. M., 2006. Abundance of mass 47 CO₂ in urban air, car exhaust, and human breath. *Geochim. Cosmochim. Acta* 70, 1-12.
- Affek, H. P., Xu, X., Eiler, J. M., 2007. Seasonal and diurnal variations of ¹³C¹⁸O¹⁶O in air: Initial observations from Pasadena, CA. *Geochim. Cosmochim. Acta* 71, 5033-5043.
- Assonov, S., Brenninkmeijer, C., 2006. On the N₂O correction used for mass spectrometric analysis of atmospheric CO₂. *Rapid Commun. Mass Spec.* 20, 1809-1819.
- Assonov, S. S., Brenninkmeijer, C. A. M., 2001. A new method to determine the ¹⁷O isotopic abundance in CO₂ using oxygen isotope exchange with a solid oxide. *Rapid Commun. Mass Spec.* 15, 2426-2437.
- Assonov, S. S., Brenninkmeijer, C. A. M., 2005. Reporting small Δ¹⁷O values: existing definitions and concepts. *Rapid Commun. Mass Spec.* 19, 627-636.
- Barkan, A., Luz, B., 2011. The relationship among the three stable isotopes of oxygen in air, seawater and marine photosynthesis. *Rapid Commun. Mass Spec.* 25, 2367-2369.
- Barkan, E., Luz, B., 2005. High precision measurements of ¹⁷O/¹⁶O and ¹⁸O/¹⁶O ratios in H₂O. *Rapid Commun. Mass Spec.* 19, 3737-3742.
- Brenninkmeijer, C. A. M., Kraft, P., Mook, W. G., 1983. Oxygen isotope fractionation between CO₂ and H₂O. *Isot. Geosci.* 1, 181-190.
- Brenninkmeijer, C. A. M., Röckmann, T., 1996. Russian doll type cryogenic traps: improved design and isotope separation effects. *Anal. Chem.* 68, 3050-3053.
- Ciais, P., Denning, A. S., Tans, P. P., Berry, J. A., Randall, D., Collatz, J. G., Sellers, P. J., White, J. W., Troler, M., Meijer, H. A. J., Francey, R. J., Monfray, P., Heimann, M., 1997. A three-dimensional synthesis study of δ¹⁸O in atmospheric CO₂: Part 1 Surface fluxes. *J. Geophys. Res.* 102, 5857-5872.
- Ciais, P., Tans, P. P., Troler, M., White, J. W. C., Francey, R. J., 1995. A large northern hemisphere terrestrial CO₂ sink indicated by the ¹³C/¹²C ratio of atmospheric CO₂. *Science* 269, 1098-1102.
- Coplen, T. B., Hopple, J. A., Böhlke, J. K., Peiser, H. S., Rieder, S. E., Krouse, H. R., Rosman, K. J. R., Ding, T., Jr. Vocke, R. D., Révész, K. M., Lamberty, A., Taylor, P., De Bièvre, P., 2002. Compilation of minimum and maximum isotope ratios of selected elements in naturally occurring terrestrial materials and reagents. *Water-Resources Investigations Report* U.S. Geological Survey, Reston, Virginia.

- Craig, H., 1953. The geochemistry of the stable carbon isotopes. *Geochim. Cosmochim. Acta* 3, 53-92.
- Craig, H., 1954. Carbon 13 in plants and the relationships between carbon 13 and carbon 14 variations in nature. *The Journal of Geology* 62, 115-149.
- Cuntz, M., Ciais, P., Hoffmann, G., Knorr, W., 2003b. A comprehensive global three-dimensional model of $\delta^{18}\text{O}$ in atmospheric CO₂: 1. Validation of surface processes. *J. Geophys. Res.* 108, ACH1-ACH23.
- Demény, A., Haszpra, L., 2002. Stable isotope compositions of CO₂ in background air and at polluted sites in Hungary. *Rapid Commun. Mass Spectrom.* 16, 797-804.
- DeNiro, M. J., Epstein, S., 1979. Relationship between the oxygen isotope ratios of terrestrial plant cellulose, carbon dioxide, and water. *Science* 204, 51-53.
- Djuricin, S., 2010. A comparison of tracer methods for quantifying CO₂ sources in an urban region. *J. Geophys. Res.* 115, D11303.
- Epstein, S., Zeiri, L., 1988. Oxygen and Carbon Isotopic Compositions of Gases Respired by Humans. *Proc. Natl. Acad. Sci. USA* 85, 1727-1731.
- Farquhar, G. D., Lloyd, J., Taylor, J. A., Flanagan, L. B., Syvertsen, J. P., Hubick, K. T., Wong, S. C., Ehleringer, J. R., 1993. Vegetation effects on the isotope composition of oxygen in atmospheric CO₂. *Nature* 363, 439-443.
- Francey, R. J., Tans, P. P., 1987. Latitudinal variation in oxygen-18 of atmospheric CO₂. *Nature* 327, 495-497.
- Gehler, A., Tütken, T., Pack, A., 2011. Triple oxygen isotope analysis of bioapatite as tracer for diagenetic alteration of bones and teeth. *Palaeogeography, Palaeoclimatology, Palaeoecology* 310, 84-91.
- Gruber, N., 2001. An improved estimate of the isotopic air-sea disequilibrium of CO₂: Implications for the oceanic uptake of anthropogenic CO₂. *Geophys. Res. Lett.* 28, 555.
- Hoag, K. J., Still, C. J., Fung, I. Y., Boering, K. A., 2005. Triple oxygen isotope composition of tropospheric carbon dioxide as a tracer of terrestrial gross carbon fluxes. *Geophys. Res. Lett.* 32, 1-5.
- Hofmann, M. E. G., Horváth, B., Pack, A., 2012a. Global long-term mean triple oxygen isotope composition of tropospheric CO₂. Sixth International Symposium on Isotopomers, Washington DC.

- Hofmann, M. E. G., Horváth, B., Pack, A., 2012b. Triple oxygen isotope equilibrium fractionation between carbon dioxide and water. *Earth Planet. Sci. Lett.* 319-320, 159-164.
- Hofmann, M. E. G., Pack, A., 2010. Technique for high-precision analysis of triple oxygen isotope ratios in carbon dioxide. *Anal. Chem.* 82, 4357-4361.
- Hulston, J. R., Thode, H. G., 1965. Variations in the S³³, S³⁴, and S³⁶ contents of meteorites and their relation to chemical and nuclear effects. *J. Geophys. Res.* 70, 3475-3484.
- Jäggi, M., Saurer, M., Fuhrer, J., Siegwolf, R., 2003. Seasonality of δ¹⁸O in needles and wood of *Picea abies*. *New Phytologist* 158, 51-59.
- Jäggi, M. J., Saurer, M. S., Fuhrer, J. F., Siegwolf, R. S., 2002. The relationship between the stable carbon isotope composition of needle bulk material, starch, and tree rings in *Picea abies*. *Oecologia* 131, 325-332.
- Keeling, C. D., 1958. The concentration and isotopic abundances of atmospheric carbon dioxide in rural areas. *Geochim. Cosmochim. Acta* 13, 322-334.
- Keeling, C. D., 1961. The concentration and isotopic abundances of carbon dioxide in rural and marine air. *Geochim. Cosmochim. Acta* 24, 277-298.
- Kim, S.-T., Mucci, A., Taylor, B. E., 2007. Phosphoric acid fractionation factors for calcite and aragonite between 25 and 75 °C: Revisited. *Chem. Geol.* 246, 135-146.
- Landais, A., Barkan, E., Yakir, D., Luz, B., 2006. The triple isotopic composition of oxygen in leaf water. *Geochim. Cosmochim. Acta* 70, 4105-4115.
- Levin, I., 2003. A novel approach for independent budgeting of fossil fuel CO₂ over Europe by ¹⁴CO₂ observations. *Geophys. Res. Lett.* 30, 2194.
- Longinelli, A., 1984. Oxygen isotopes in mammal bone phosphate: A new tool for paleohydrological and paleoclimatological research? *Geochim. Cosmochim. Acta* 48, 385-390.
- Luz, B., Barkan, E., 2010. Variations of ¹⁷O/¹⁶O and ¹⁸O/¹⁶O in meteoric waters. *Geochim. Cosmochim. Acta* 74, 6276-6286.
- Luz, B., Kolodny, Y., Horowitz, M., 1984. Fractionation of oxygen isotopes between mammalian bone-phosphate and environmental drinking water. *Geochim. Cosmochim. Acta* 48, 1689-1693.
- Miller, M. F., 2002. Isotopic fractionation and the quantification of ¹⁷O anomalies in the oxygen three-isotope system: an appraisal and geochemical significance. *Geochim. Cosmochim. Acta* 66, 1881-1889.

- Newman, S., Xu, X., Affek, H. P., Stolper, E., Epstein, S., 2008. Changes in mixing ratio and isotopic composition of CO₂ in urban air from the Los Angeles basin, California, between 1972 and 2003. *J. Geophys. Res.* 113, D23304.
- NOAA, U. S. D. o. C., National Oceanic and Atmospheric Administration, Earth System Research Laboratory, Global Monitoring Division 2012. Mauna Loa, Hawaii United States (MLO). In-situ CO₂ monthly averages.
- Pack, A., Toulouse, C., Przybilla, R., 2007. Determination of oxygen triple isotope ratios of silicates without cryogenic separation of NF₃ - technique with application to analyses of technical O₂ gas and meteorite classification. *Rapid Commun. Mass Spec.* 21, 3721-3728.
- Pataki, D., Xu, T., Luo, Y., Ehleringer, J., 2007. Inferring biogenic and anthropogenic carbon dioxide sources across an urban to rural gradient. *Oecologia* 152, 307-322.
- Pataki, D. E., Bowling, D. R., Ehleringer, J. R., 2003. Seasonal cycle of carbon dioxide and its isotopic composition in an urban atmosphere: Anthropogenic and biogenic effects. *J. Geophys. Res.* 108, 4735.
- Rooney, M. A., Claypool, G. E., Moses Chung, H., 1995. Modeling thermogenic gas generation using carbon isotope ratios of natural gas hydrocarbons. *Chem. Geol.* 126, 219-232.
- Saurer, M., Siegwolf, R. T. W., Schweingruber, F. H., 2004. Carbon isotope discrimination indicates improving water-use efficiency of trees in northern Eurasia over the last 100 years. *Global Change Biology* 10, 2109-2120.
- Schumacher, M., Werner, R. A., Meijer, H. A. J., Jansen, H. G., Brand, W. A., Geilmann, H., Neubert, R. E. M., 2011. Oxygen isotopic signature of CO₂ from combustion processes. *Atmos. Chem. Phys.* 11, 1473-1490.
- Sjostrom, E., 1993. *Wood Chemistry. Fundamentals and Applications*. Academic press., San Diego.
- Tanaka, R., Nakamura, E., 2012. Kinetic isotope fractionation effect observed in oxygen triple isotope ratios in terrestrial silicate minerals. Sixth International Symposium on Isotopomers, Washington DC.
- Widory, D., Javoy, M., 2003. The carbon isotope composition of atmospheric CO₂ in Paris. *Earth Planet. Sci. Lett.* 215, 289-298.
- Yakir, D., 2003. The stable isotopic composition of atmospheric CO₂. In: Keeling, R. F. (Ed.), *The Atmosphere*. Elsevier-Pergamon, Oxford.
- Yakir, D., DeNiro, M. J., 1990. Oxygen and hydrogen isotope fractionation during cellulose metabolism in *Lemna gibba* L. *Plant Physiology* 93, 325.

- Yanes, Y., Yapp, C. J., 2010. Indoor and outdoor urban atmospheric CO₂: Stable carbon isotope constraints on mixing and mass balance. *Appl. Geochem.* 25, 1339-1349.
- Young, E. D., Galy, A., Nagahara, H., 2002. Kinetic and equilibrium mass-dependent isotope fractionation laws in nature and their geochemical and cosmochemical significance. *Geochim. Cosmochim. Acta* 66, 1095-1104.

5 Triple oxygen isotope composition of tropospheric CO₂: Observational data and model simulation

Hofmann, M.E.G., Horváth, B. and Pack, A.,

Triple oxygen isotope composition of tropospheric CO₂: Observational data and model
simulation, in preparation

5.1 Abstract

In recent years, modeling results suggested that the triple oxygen isotope composition of tropospheric CO₂ might be a promising new tracer for terrestrial gross carbon fluxes. Here, we present high-precision triple oxygen isotope data of ambient air CO₂ sampled in Göttingen (NW Germany) over the course of 2 years and on top of the Brocken Mountain (1140 m, NW Germany). We compare our observational data to a revised triple oxygen isotope mass balance model of tropospheric CO₂ where we reconcile both ¹⁸O/¹⁶O and ¹⁷O/¹⁶O fractionation processes. All triple oxygen isotope data are reported as $\Delta^{17}\text{O}$ values relative to a CO₂-water equilibration line with $\Delta^{17}\text{O} = \ln(\delta^{17}\text{O}+1) - 0.522 \times \ln(\delta^{18}\text{O}+1)$. Carbon dioxide sampled in Göttingen has a long-term mean triple oxygen isotope composition with $\delta^{18}\text{O}_{\text{VSMOW}} = 41.6 \pm 0.9\text{‰}$ (SD) and $\Delta^{17}\text{O} = -0.03 \pm 0.07\text{‰}$ (SD). The $\Delta^{17}\text{O}$ signal shows a temporal variation with a peak-to-peak range of about 0.25‰ that parallels the seasonal $\delta^{18}\text{O}$ cycle from summer 2010 to winter 2011, but deviates from the seasonal pattern in 2012. Three samples from the Brocken Mountain fall within the range observed in Göttingen. Overall, the observational data are slightly lower than the prediction for the global troposphere of +0.06‰. A Monte Carlo simulation gives an uncertainty estimate intrinsic to our model of $\pm 0.05\text{‰}$ (SD). The revised global mass balance model shows a sensitivity of $\Delta^{17}\text{O}$ of tropospheric CO₂ to variations in the terrestrial gross primary production, which is only slightly lower than previously predicted. However, the discrepancy between the observed and predicted mean $\Delta^{17}\text{O}$ and the large interannual variation in $\Delta^{17}\text{O}$ requires future investigations.

5.2 Introduction

The triple oxygen isotope composition of strato- and mesospheric CO₂ is characterized by a large oxygen isotope anomaly (Boering et al., 2004; Kawagucci et al., 2008; Lämmerzahl et al., 2002; Thiemens et al., 1995b). This anomaly has its origin in the formation of ozone in the stratosphere and is passed on to stratospheric CO₂ via exchange with O(¹D) (Yung et al., 1991). As stratospheric CO₂ enters the troposphere, the anomaly is lost due to dilution with mass-dependently fractionated CO₂ and isotopic exchange with water in the hydro- and biosphere.

To date, extensive data on the triple oxygen isotope composition of stratospheric CO₂ were reported in the literature (Boering et al., 2004; Kawagucci et al., 2008; Lämmerzahl et al., 2002; Thiemens et al., 1995b), but no high-precision data on tropospheric CO₂ have been published so far. The lack of high-precision data on $\Delta^{17}\text{O}$ of tropospheric CO₂ motivated Hoag et al. (2005) to set up a model that characterizes the triple oxygen isotope composition of tropospheric CO₂. The authors predict that tropospheric CO₂ should have an oxygen isotope anomaly of $\sim 0.15\text{‰}$ relative to a reference line with a slope of 0.516 in a $\delta^{18}\text{O}$ vs. $\delta^{17}\text{O}$ plot (corresponding to $\Delta^{17}\text{O} = 0.11\text{‰}$ relative to a reference line with a slope of 0.522 in a $\ln(\delta^{18}\text{O}+1)$ vs. $\ln(\delta^{17}\text{O}+1)$ plot, see section 5.3.1 for definition of δ and $\Delta^{17}\text{O}$ values) and they postulate that high-precision $\Delta^{17}\text{O}$ analyses of tropospheric CO₂ should constrain estimates on terrestrial gross primary productivity. However, the model prediction is based on several simplified assumptions for biosphere-atmosphere interaction, e.g. the authors assume that the exponent θ , where $\alpha^{17/16} = (\alpha^{18/16})^\theta$, for CO₂-water equilibrium isotope exchange is 0.516. Recently, Hofmann et al. (2012b) determined an exponent of 0.522 ± 0.002 for CO₂-water equilibrium exchange, and thus, a revised model prediction of $\Delta^{17}\text{O}$ of tropospheric CO₂ becomes necessary.

Here, we present a revised global mass balance model for the triple oxygen isotope composition of tropospheric CO₂, where we reconcile the assumptions for $^{18}\text{O}/^{16}\text{O}$ and $^{17}\text{O}/^{16}\text{O}$ fractionation of atmospheric CO₂: (i) we implement the experimental results for the exponent θ for CO₂-water equilibrium (Hofmann et al., 2012b), (ii) we take into account that the main water reservoirs that exchange with atmospheric CO₂ (ocean, soil and leaf water) have a distinct triple oxygen isotope signature (Landaïs et al., 2006; Luz and Barkan, 2010) and (iii) we assume that CO₂ sinks can also fractionate the triple oxygen isotope composition.

Subsequent, we compare the revised model prediction to high-precision triple oxygen isotope data of tropospheric CO₂ from Göttingen, a medium-sized town located in the center of Germany, and triple oxygen isotope data of CO₂ sampled on top of the nearby Brocken Mountain.

5.3 Method

5.3.1 Triple oxygen isotope notation

Oxygen isotope ratios (¹⁷O/¹⁶O and ¹⁸O/¹⁶O) are traditionally reported as δ-values relative to VSMOW:

$$\delta^{17}\text{O} = \left[\frac{\left(\frac{{}^{17}\text{O}}{{}^{16}\text{O}} \right)_{\text{sample}}}{\left(\frac{{}^{17}\text{O}}{{}^{16}\text{O}} \right)_{\text{VSMOW}}} - 1 \right] \quad \text{Eq. 5-1}$$

and

$$\delta^{18}\text{O} = \left[\frac{\left(\frac{{}^{18}\text{O}}{{}^{16}\text{O}} \right)_{\text{sample}}}{\left(\frac{{}^{18}\text{O}}{{}^{16}\text{O}} \right)_{\text{VSMOW}}} - 1 \right] \quad \text{Eq. 5-2}$$

Small variations in the triple oxygen isotope composition are reported as deviations from a mass-dependent reference line in a triple oxygen isotope plot with logarithmic δ-coordinates (Hulston and Thode, 1965; Miller, 2002; Young et al., 2002):

$$\Delta^{17}\text{O}_{\text{RL}} = \ln(\delta^{17}\text{O} + 1) - \lambda_{\text{RL}} \times \ln(\delta^{18}\text{O} + 1) - \gamma_{\text{RL}} \quad \text{Eq. 5-3}$$

In this study, we take a CO₂-water equilibration line as reference line (RL) with a slope $\lambda_{\text{RL}} = 0.522$ and zero intercept, e.g. $\gamma_{\text{RL}} = 0\text{‰}$. The slope is based on the exponent θ for equilibrium exchange between CO₂ and water (Hofmann et al., 2012b); the zero intercept was chosen for simplicity. The logarithmic δ-values are abbreviated as δ'-values with $\delta'^{17}\text{O} = \ln(\delta^{17}\text{O} + 1)$ and $\delta'^{18}\text{O} = \ln(\delta^{18}\text{O} + 1)$. For the ¹⁸O/¹⁶O mass balance calculation, all oxygen isotope ratios are reported as δ¹⁸O values.

5.3.2 Model description

Various CO₂ sources and sinks characterize the triple oxygen isotope signature of tropospheric CO₂. We consider the following gross fluxes F that affect the tropospheric CO₂ reservoir:

$$dM / dt = F_A(t) + F_{resp}(t) + F_{OA}(t) + F_{AO}(t) + F_{SA}(t) + F_{AS}(t) + F_{SIA}(t) + F_{ASI}(t) + F_{ff} + F_{fire} \quad \text{Eq. 5-4}$$

with

- dM/dt = rate of increase of tropospheric CO₂ reservoir (in PgC/yr)
- F_A = terrestrial assimilation flux (in PgC/yr)
- F_{resp} = CO₂ emitted from terrestrial respiration (in PgC/yr)
- F_{OA} = CO₂ emitted from the oceans (in PgC/yr)
- F_{AO} = CO₂ taken up by oceans (in PgC/yr)
- F_{SA} = stratospheric CO₂ entering the troposphere (in PgC/yr)
- F_{AS} = tropospheric CO₂ entering the stratosphere (in PgC/yr)
- F_{SIA} = soil invasion flux to troposphere (in PgC/yr)
- F_{ASI} = soil invasion flux from troposphere (in PgC/yr)
- F_{ff} = CO₂ emitted from fossil fuel burning (in PgC/yr)
- F_{fire} = CO₂ emitted from biomass burning (in PgC/yr)

We use an initial size of 830 PgC (= M_0) for the tropospheric CO₂ reservoir and an increase rate of 4 PgC/yr (= dM/dt) (Canadell et al., 2007; Le Quéré et al., 2009). Note that the size of the CO₂ fluxes (except F_{ff} and F_{fire}) increases as the CO₂ concentration in the atmosphere increases. The initial magnitudes of the carbon sources and sinks are listed in Table 5-1 and will be discussed in detail below.

In order to model the global $\delta^{18}\text{O}$ composition of tropospheric CO₂ ($= \delta_a$), we consider the following global mass balance equation according to previous studies (e.g. Ciais et al., 1997; Cuntz et al., 2003a; Cuntz et al., 2003b; Welp et al., 2011):

$$\frac{d\delta_a}{dt} = \frac{1}{M_0 + (dM/dt)t} \times [F_A(t) D_A + F_{resp}(t) (\delta_{resp} - \delta_a) + F_{OA}(t) (\delta_O - \delta_a) + F_{SA}(t) (\delta_{strat} - \delta_a) + F_{SIA}(t) (\delta_{SI} - \delta_a) + F_{ff}(t) (\delta_{ff} - \delta_a) + F_{fire}(t) (\delta_{fire} - \delta_a)] \quad \text{Eq. 5-5}$$

with

- M_0 = initial size of tropospheric CO₂ reservoir (in PgC)
- D_A = $\delta^{18}\text{O}$ isotope discrimination due to assimilation (in ‰), i.e. kinetic fractionation during diffusion into and out of leaf stomata and CO₂-water equilibration in the stomata
- δ_{resp} = $\delta^{18}\text{O}$ value of CO₂ emitted from terrestrial respiration (in ‰)
- δ_O = $\delta^{18}\text{O}$ value of CO₂ emitted from the ocean (in ‰)
- δ_{strat} = $\delta^{18}\text{O}$ value of CO₂ from the lower stratosphere (in ‰)
- δ_{SI} = $\delta^{18}\text{O}$ value of CO₂ in equilibrium with soil water (in ‰)
- δ_{ff} = $\delta^{18}\text{O}$ value of CO₂ from fossil fuel burning (in ‰)
- δ_{fire} = $\delta^{18}\text{O}$ value of CO₂ from biomass burning (in ‰)

For the mass balance equations we abbreviate $\delta^{18}\text{O}$ values with δ . The isotopic signatures are listed in Table 5-2 and will also be discussed in detail below. In Eq. 5-5, we can omit the carbon sinks F_{AO} , F_{AS} and F_{ASI} because the δ -values of the transported CO₂ are identical to δ_a .

In accordance with the global budget equation for the $\delta^{18}\text{O}$ composition of the troposphere (Eq. 5-5), we calculate the $\Delta^{17}\text{O}$ signature of tropospheric CO₂ ($= \Delta^{17}_a$):

$$\frac{d\Delta_a^{17}}{dt} = \frac{1}{M_0 + (dM/dt)t} \times [F_A(t) D_A^{17} + F_{resp}(t) (\Delta_{resp}^{17} - \Delta_a^{17}) + F_{OA}(t) (\Delta_O^{17} - \Delta_a^{17}) + F_{SA}(t) (\Delta_{strat}^{17} - \Delta_a^{17}) + F_{SIA}(t) (\Delta_{SI}^{17} - \Delta_a^{17}) + F_{ff}(t) (\Delta_{ff}^{17} - \Delta_a^{17}) + F_{fire}(t) (\Delta_{fire}^{17} - \Delta_a^{17})] \quad \text{Eq. 5-6}$$

with

D_A^{17} = $\Delta^{17}\text{O}$ isotope discrimination due to assimilation (in ‰), i.e. kinetic fractionation during diffusion into and out of leaf stomata and CO₂-water equilibration in the stomata

Δ_{resp}^{17} = $\Delta^{17}\text{O}$ value of CO₂ emitted from terrestrial respiration (in ‰)

Δ_O^{17} = $\Delta^{17}\text{O}$ value of CO₂ in equilibrium with ocean water (in ‰)

Δ_{strat}^{17} = $\Delta^{17}\text{O}$ value of CO₂ from the lower stratosphere (in ‰)

Δ_{SI}^{17} = $\Delta^{17}\text{O}$ value of CO₂ in equilibrium with soil water (in ‰)

Δ_{ff}^{17} = $\Delta^{17}\text{O}$ value of CO₂ from fossil fuel burning (in ‰)

Δ_{fire}^{17} = $\Delta^{17}\text{O}$ value of CO₂ from biomass burning (in ‰)

$\lambda_{kinetic}$ = triple oxygen isotope exponent for kinetic fractionation

For the model description, we abbreviate $\Delta^{17}\text{O}$ values with Δ^{17} . Both mass balance equations reach a quasi steady-state after a few years, and thus, all model results are given for $t = 50$ yr.

Note that strictly speaking the $\Delta^{17}\text{O}$ mass balance formulation gives only an approximation for Δ^{17}_a . To be precise, a $\delta^{17}\text{O}$ mass balance equation would be more appropriate, however, our approximation with $\Delta^{17}\text{O}$ values changes the final outcome by less than 0.002‰.

Terrestrial assimilation

The terrestrial biosphere fixes about 120 PgC per year (Beer et al., 2010). This rate of carbon fixation by the biosphere is generally termed gross primary production (GPP). Ciais et al. (1997) estimate that about 12% of the annual GPP are consumed by leaf respiration. Furthermore, we assume that the rate of assimilation increases as the CO₂ concentration increases:

$$F_A(t) = 0.88 \text{ GPP} \left(1 + \frac{dM/dt}{M_0} t \right) \quad \text{Eq. 5-7}$$

The assimilation rate of the terrestrial biosphere is driven by the difference in CO₂ concentration in the leaf stomata (C_{cs}) and the atmosphere (C_a) (Farquhar et al., 1993):

$$F_A = \frac{C_a}{C_a - C_{cs}} F_A - \frac{C_{cs}}{C_a - C_{cs}} F_A = -(F_{LA} + F_{AL}) \quad \text{Eq. 5-8}$$

where F_{LA} denotes the amount of CO₂ that is released per year from the stomata to the atmosphere and F_{AL} is the amount of CO₂ diffusing into terrestrial leaf stomata. The C_{cs}/C_a ratio varies between C₃ and C₄ plants because the latter fix carbon dioxide more effectively due to a different photosynthetic pathway (Pearcy and Ehleringer, 1984). For the mass balance calculation we assume an overall C_{cs}/C_a ratio of 0.70 (Ciais et al., 1997; Cuntz et al., 2003a; Cuntz et al., 2003b), which takes into account that about 77% of the global GPP can be traced back to C₃ plants (f_{C3}) and the remaining to C₄ plants (f_{C4}) (Lloyd and Farquhar, 1994; Still et al., 2003).

The CO₂ diffusing into the leaf stomata rapidly exchanges its oxygen isotopes with the leaf water. For C₃ plants, about 93% of the CO₂ diffusing out of the stomata is in isotopic equilibrium with leaf water ($\Theta_{C3}=0.93$) and for C₄ plants about 38% of the CO₂ is in isotopic equilibrium ($\Theta_{C4}=0.38$) (Gillon and Yakir, 2001; Gillon and Yakir, 2000). Thus, we can estimate the fraction of CO₂ that is in equilibrium with leaf water (F_{LAequ}) and the fraction of CO₂ that is not affected by exchange with leaf water (F_{LAnequ}):

$$F_{LAequ} = (f_{C3} \times \Theta_{C3} + f_{C4} \times \Theta_{C4}) \times F_{LA} \quad \text{Eq. 5-9}$$

and

$$F_{LAnequ} = (f_{C3} \times (1 - \Theta_{C3}) + f_{C4} \times (1 - \Theta_{C4})) \times F_{LA} \quad \text{Eq. 5-10}$$

The ¹⁸O/¹⁶O ratio of CO₂ in equilibrium with leaf water (δ_L) depends on (i) the isotopic composition of the soil and stem water ($\delta_{SW} = -7.5\%$, Ciais et al. 1997), (ii) the degree of kinetic fractionation due to evapotranspiration in the leaves ($\alpha_{transpiration} = 0.9917$, West et al., 2008) and (iii) the equilibration temperature ($T_{leaf} = 285 \text{ K}$, Ciais et al., 1997):

$$\delta_L = (\delta_{SW} + 1) \frac{\alpha_{CO2-water}(T_{leaf})}{\alpha_{transpiration}} \quad \text{Eq. 5-11}$$

where $\alpha_{\text{CO}_2\text{-water}}$ is the temperature dependent $^{18}\text{O}/^{16}\text{O}$ fractionation factor for CO₂-water exchange according to Brenninkmeijer et al. (1983).

The $^{18}\text{O}/^{16}\text{O}$ isoflux for carbon assimilation during photosynthesis (in ‰PgC/yr) can then be expressed as:

$$F_A \times D_A = (\alpha_L - 1) \times (F_{AL} + F_{LA\text{nonequ}}) + ((\delta_L + 1) \times \alpha_L - 1 - \delta'_a) \times F_{LA\text{equ}} \quad \text{Eq. 5-12}$$

where $\alpha_L = 0.9926$ describes the kinetic fractionation factor for diffusion into and out of the stomata (Farquhar et al., 1993).

Similar to $^{18}\text{O}/^{16}\text{O}$, the triple oxygen isotope composition of CO₂ emitted from plants depends on the oxygen isotope signature of soil water. We assume that the triple oxygen isotope composition of soil water (Δ^{17}_{SW}) at the depth where plant roots take up water is not affected by evaporation and that it falls on the global meteoric water line (GMWL) with a slope $\lambda_{\text{GMWL}} = 0.528$ and an intercept $\gamma_{\text{GMWL}} = 0.033\text{‰}$ (Luz and Barkan, 2010):

$$\Delta^{17}_{\text{SW}} = (\lambda_{\text{GMWL}} - \lambda_{\text{RL}}) \times \ln(\delta_{\text{SW}} + 1) + \gamma_{\text{GMWL}} \quad \text{Eq. 5-13}$$

Given this relationship, soil water with $\delta_{\text{SW}} = -7.5\text{‰}$ has a Δ^{17}_{SW} value of -0.01‰ .

The triple oxygen isotope composition of CO₂ in equilibrium with leaf water (Δ^{17}_{L}) depends on (i) the isotopic composition of the soil water, (ii) the degree of evapotranspiration and (iii) the oxygen isotope exchange between CO₂ and water in the stomata (see Fig. 5-1):

$$\Delta^{17}_{\text{L}} = \Delta^{17}_{\text{SW}} + (\lambda_{\text{RL}} - \lambda_{\text{transpiration}}) \times \ln(\alpha_{\text{transpiration}}) + (\lambda_{\text{RL}} - \theta_{\text{CO}_2\text{-water}}) \times \ln(\alpha_{\text{CO}_2\text{-water}}(T_{\text{leaf}})) \quad \text{Eq. 5-14}$$

where $\theta_{\text{CO}_2\text{-water}}$ is the exponent for triple oxygen isotope exchange between CO₂ and water and $\lambda_{\text{transpiration}}$ the exponent for transpiration in plant leaves. In a previous study, we determined an exponent $\theta_{\text{CO}_2\text{-water}}$ of 0.522 ± 0.002 for the temperature range of 2 to 37°C (Hofmann et al., 2012b). For the exponent $\lambda_{\text{transpiration}}$, Landais et al. (2006) showed that it depends on the mean humidity h above the leaf stomata: $\lambda_{\text{transpiration}} = 0.522 - 0.008 \times h$. Note that the slope of the reference line λ_{RL} is equal to the exponent $\theta_{\text{CO}_2\text{-water}}$ and for this particular case the last term becomes zero.

The ¹⁷O/¹⁶O isoflux for photosynthetic activity of terrestrial plants (in ‰PgC/yr) can be calculated according to the ¹⁸O/¹⁶O isoflux (see Eq. 5-12):

$$F_A \times \Delta_A^{17} = \left(\ln(\alpha_L) \times (\lambda_{kinetic} - \lambda_{RL}) \right) \times (F_{AL} + F_{LAnequ}) + \left(\Delta_L^{17} + (\lambda_{kinetic} - \lambda_{RL}) \times \ln(\alpha_L) - \Delta_a^{17} \right) \times F_{LAequ} \quad \text{Eq. 5-15}$$

Equation 5-15 illustrates that all the CO₂ diffusing into and out of the stomata is kinetically fractionated, but only a part of the CO₂ equilibrates with leaf water before retro-diffusing into the atmosphere.

Respiration and soil invasion

Most of the carbon assimilated by terrestrial photosynthesis is eventually released back to the atmosphere as CO₂ due to soil respiration. The net carbon sink due to terrestrial carbon assimilation is about 3 PgC/yr (Canadell et al., 2007; Le Quéré et al., 2009):

$$F_{resp}(t) = A(t) - 3 \text{ PgC/yr} \quad \text{Eq. 5-16}$$

Based on our assumption on GPP and the relationship given above, the flux from terrestrial respiration is 102.6 PgC/yr.

Carbon dioxide produced by soil respiration rapidly equilibrates with soil water at a global mean temperature of 12°C (Ciais et al., 1997). Subsequently, it is kinetically fractionated during the diffusion process out of the soil column with $\alpha_s = 0.9928$ (Miller et al., 1999a):

$$\delta_{resp} = (\delta_{SW} + 1) \alpha_{CO2-water}(T_{soil}) \alpha_s - 1 \quad \text{Eq. 5-17}$$

Analogous to δ_{resp} , we estimate the triple oxygen isotope composition of soil respired CO₂:

$$\Delta_{resp}^{17} = \Delta_{SW}^{17} - (\lambda_{RL} - \theta_{CO2-water}) \times \ln(\alpha_{CO2-water}(T_{soil})) - (\lambda_{RL} - \lambda_{kinetic}) \times \ln(\alpha_s) \quad \text{Eq. 5-18}$$

CO₂ diffusing into the uppermost soil column equilibrates with soil water and diffuses back to the atmosphere. This process is known as the soil invasion flux (Miller et al., 1999a; Tans, 1998). We take a soil invasion flux F_{SI} of 30 PgC per year (Stern et al., 2001). Recently, Wingate et al. (2009) suggested that the soil invasion flux might account for up to 450 PgC/yr and we considered this estimate as an upper limited for the soil invasion flux in the Monte Carlo simulation (see below section on the Monte Carlo simulation).

The isotopic composition of the soil invasion flux depends on the global mean soil water isotope composition and on the equilibration temperature in the soils:

$$\delta_{SI} = (\delta_{SW} + 1) \times \alpha_{CO_2-water}(T_{soil}) - 1 \quad \text{Eq. 5-19}$$

Analog to δ_{SI} , we estimate the triple oxygen isotope signature of the soil invasion flux:

$$\Delta_{SI}^{17} = \Delta_{SW}^{17} - (\lambda_{RL} - \theta_{CO_2-water}) \times \ln(\alpha_{CO_2-water}(T_{soil})) \quad \text{Eq. 5-20}$$

Ocean gross fluxes

We assume that the gross CO₂ flux from the oceans to the troposphere is about 90 PgC/yr (Heimann and Maier-Reimer, 1996):

$$F_{OA}(t) = 90 \text{ PgC/yr} \left(1 + \frac{dM/dt}{M_0} t \right) \quad \text{Eq. 5-21}$$

Global carbon models generally consider a constant net ocean sink of 2 PgC/yr (Canadell et al., 2007; Le Quéré et al., 2009). However, we omit the carbon sink flux for triple oxygen isotope calculations because the oxygen isotope fractionation occurring at the air-sea interface is negligible (e.g. Ciais et al., 2005).

The mean oxygen isotope composition of ocean water is $\delta_{ocean} = 0\text{‰}$ and $\Delta_{ocean}^{17} = -0.005\text{‰}$ (Luz and Barkan, 2010). The CO₂ diffusing into the ocean surface water equilibrates rapidly with the ocean water at a global mean temperature of 18°C (Ciais et al., 1997). It follows from the above that

$$\delta_O = (\delta_{ocean} + 1) \times \alpha_{CO_2-water}(T_{ocean}) - 1 \quad \text{Eq. 5-22}$$

and

$$\Delta_O^{17} = \Delta_{ocean}^{17} - (\lambda_{RL} - \theta_{CO_2-water}) \times \ln(\alpha_{CO_2-water}(T_{soil})). \quad \text{Eq. 5-23}$$

Stratosphere-troposphere exchange fluxes

The CO₂ fluxes from the troposphere into the stratosphere and vice versa are 100 PgC/yr and –100 PgC/yr, respectively (Appenzeller et al., 1996). Because the CO₂ flux leaving the troposphere is not fractionated, we only have to consider the CO₂ source entering the troposphere:

$$F_{SA}(t) = 100 \text{ PgC/yr} \left(1 + \frac{dM/dt}{M_0} t \right) \quad \text{Eq. 5-24}$$

Carbon dioxide from the stratosphere is enriched in ¹⁸O due to isotopic exchange with stratospheric ozone (Gamo et al., 1989). Kawagucci et al. (2008) estimate the oxygen isotope fluxes for stratospheric carbon dioxide to the troposphere based on a linear correlation between the N₂O mixing ratio and the δ¹⁸O composition of CO₂. For δ¹⁸O, the authors give +38 ‰PgC/yr. Combining their data with an estimate for the CO₂ flux size of 100 PgC/yr (Appenzeller et al., 1996), we assume that stratospheric CO₂ is enriched relative to tropospheric CO₂ by 0.4‰:

$$\delta_{strat} = \delta_a + 0.4 \text{ ‰} \quad \text{Eq. 5-25}$$

Similar to δ¹⁸O, the ¹⁷O enrichment of the stratospheric CO₂ flux to the troposphere can be estimated on combined Δ¹⁷O (CO₂) and N₂O measurements of stratospheric air masses (Boering et al., 2004; Kawagucci et al., 2008). Boering et al. (2004) determined a net CO₂ flux from the stratosphere of 42.9 ‰PgC/yr and Kawagucci et al. (2008) determined a value of 48 ‰PgC/yr. Recasting these literature data relative to our reference line with λ_{RL} = 0.522 in a triple oxygen isotope plot with logarithmic δ-coordinates gives 42 ‰PgC/yr and 47 ‰PgC/yr, respectively. We take an average value of 44.5 ‰PgC/yr and combine it with the stratospheric flux size of 100 PgC/yr (Appenzeller et al., 1996) to estimate the Δ¹⁷O value of stratospheric CO₂ entering the troposphere:

$$\Delta_{strat}^{17} = \Delta_a^{17} + 0.445 \text{ ‰} \quad \text{Eq. 5-26}$$

Anthropogenic emissions and biomass burning

Carbon dioxide from anthropogenic emissions and biomass burning are minor carbon fluxes on a global scale compared to the large gross carbon fluxes from the terrestrial biosphere. Anthropogenic CO₂ emissions from fossil fuel burning amount to about 8 PgC/yr (Canadell et al., 2007; Le Quéré et al., 2009). Global fire emissions are estimated to contribute about 1 PgC/yr to global CO₂ sources (Canadell et al., 2007; Le Quéré et al., 2009; van der Werf et al., 2004).

It may be assumed that CO₂ from fossil fuel combustion or biomass burning largely inherits its triple oxygen isotope composition from atmospheric O₂. Barkan and Luz (2011) determined the triple oxygen isotope composition of tropospheric O₂ with $\delta^{18}\text{O} = 23.881\text{‰}$ and $\Delta^{17}\text{O} = -0.365\text{‰}$ (relative to a reference line with $\lambda_{\text{RL}} = 0.522$). Horváth et al. (in press) show that CO₂ from high-temperature combustion, indeed, produces CO₂ with a triple oxygen isotope composition that is close to that of ambient air O₂ ($\delta^{18}\text{O} \approx \sim 22\text{‰}$ and $\Delta^{17}\text{O} \approx -0.31\text{‰}$). However, car exhaust is significantly enriched in ¹⁸O ($\delta^{18}\text{O} = 33\text{‰}$), but it also inherits the oxygen isotope anomaly of air O₂ ($\Delta^{17}\text{O} = -0.32\text{‰}$) (Horváth et al., in press). For this study, we assume that anthropogenic CO₂ from fossil fuel burning has $\delta_{\text{ff}} = 25\text{‰}$ and $\Delta^{17}_{\text{ff}} = -0.32\text{‰}$. The triple oxygen isotope composition of carbon dioxide from low temperature combustion, such as wood combustion, is affected by equilibration with water or other oxygen sources, e.g. wood inherent oxygen (Horváth et al., in press). Thus, we assume that CO₂ produced from biomass burning has $\delta_{\text{fire}} = 19\text{‰}$ and $\Delta^{17}_{\text{fire}} = -0.21\text{‰}$ (Horváth et al., in press).

Monte Carlo simulation

We carried out a Monte Carlo simulation in order to obtain an uncertainty estimate of the $\delta^{18}\text{O}$ and $\Delta^{17}\text{O}$ mass balance output. The input parameters that were considered for the Monte Carlo simulation are listed in Table 5-3. The parameters were independently varied using a random function that produces values according to a normal distribution. The mean, standard deviation and maximum-minimum values were chosen according to the literature. For all parameters, the range of variation represents the broadest reasonable distribution. The simulation was carried out with 500 random numbers for each variable. Additionally, we tested the sensitivity of $\Delta^{17}\text{O}$ of tropospheric CO₂ to the size of terrestrial gross primary productivity.

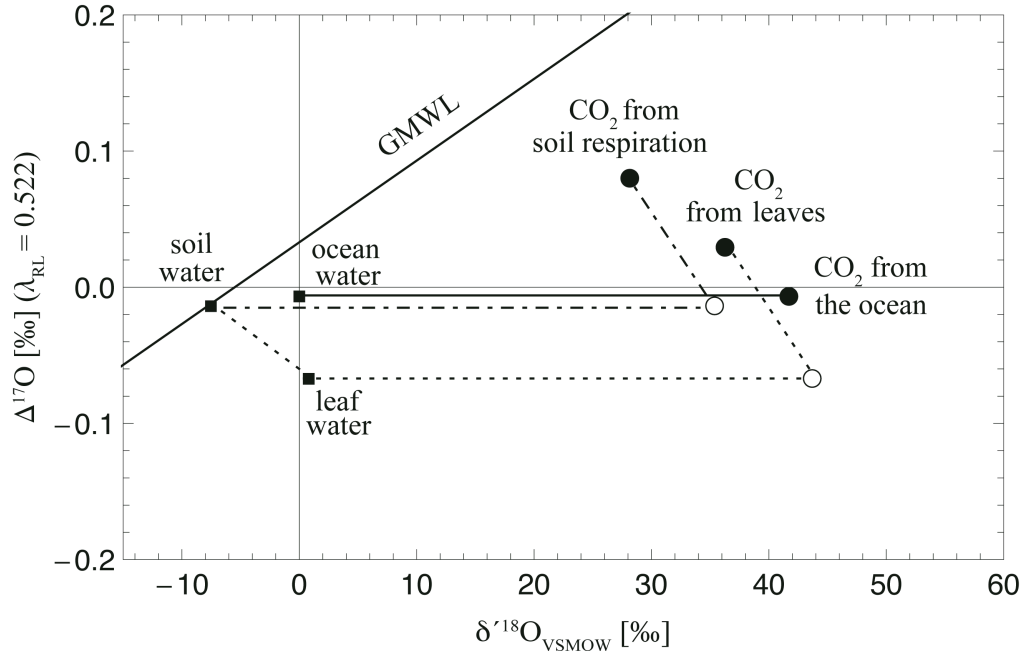


Fig. 5-1: Triple oxygen isotope signature of the main mass-dependently fractionated CO₂ sources to the troposphere. The closed squares illustrate the triple oxygen isotope composition of the main water reservoirs (ocean, soil and leaf water); the closed circles illustrate the isotopic composition of the CO₂ emitted from ocean, soils and terrestrial plants. We assume that equilibration between carbon dioxide and the three water reservoirs takes place with $\theta_{\text{CO}_2\text{-water}} = 0.522 \pm 0.002$ (Hofmann et al., 2012b), i.e. parallel to the slope of our reference line λ_{RL} . Carbon dioxide released from the oceans is in isotopic equilibrium with ocean surface water. Carbon dioxide released from plant leaves is in isotopic equilibrium with leaf water which deviates from the global meteoric water line (GMWL, Luz and Barkan, 2010) due to kinetic fractionation during evapotranspiration (Landais et al., 2006). Carbon dioxide produced in soils equilibrates with soil water (open circle), but subsequently the CO₂ is kinetically fractionated due to diffusion out of the soil column (Miller et al., 1999a).

Table 5-1: Mass balance variables: carbon fluxes and related parameters.

Parameter	Description	Estimate	Units	References
M_0	CO ₂ inventory troposphere	830	PgC	(Canadell et al., 2007; Le Quéré et al., 2009)
dM/dt	rate of increase of tropospheric CO ₂ reservoir	4	PgC/yr	(Canadell et al., 2007; Le Quéré et al., 2009)
GPP	gross primary production	120	PgC/yr	(Beer et al., 2010)
$F_A = 0.88 \times GPP$	terrestrial assimilation rate	106	PgC/yr	(Ciais et al., 1997)
F_{LA} $= A \times C_{cs} / (C_a - C_{cs})$	from leaves	246	PgC/yr	(Farquhar et al., 1993)
F_{LAequ} $= \Theta \times F_{LA}$	CO ₂ fraction from leaves that is in equilibrium with leaf water	197	PgC/yr	(Gillon and Yakir, 2001; Gillon and Yakir, 2000)
$F_{LAnonequ}$ $= (1 - \Theta) \times F_{LA}$	CO ₂ fraction from leaves that is not in equilibrium with leaf water	49	PgC/yr	(Gillon and Yakir, 2001; Gillon and Yakir, 2000)
F_{AL} $= -A \times C_a / (C_a - C_{cs})$	to leaves	-352	PgC/yr	(Farquhar et al., 1993)
F_{resp} $= A - 3$	from terrestrial respiration	103	PgC/yr	(Canadell et al., 2007; Le Quéré et al., 2009)
F_{SA}	from stratosphere	100	PgC/yr	(Appenzeller et al., 1996)
F_{AS}	to stratosphere	-100	PgC/yr	(Appenzeller et al., 1996)
F_{OA}	from ocean	90	PgC/yr	(Heimann and Maier-Reimer, 1996)

Parameter	Description	Estimate	Units	References
F_{AO}	to ocean	-92	PgC/yr	(Canadell et al., 2007; Le Quéré et al., 2009)
F_{SIA}	soil invasion (CO ₂ source)	30	PgC/yr	(Stern et al., 2001)
F_{ASI}	soil invasion (CO ₂ sink)	-30	PgC/yr	(Stern et al., 2001)
F_{ff}	fossil fuels	8	PgC/yr	(Boden et al., 2011)
F_{fire}	fire emissions	1	PgC/yr	(Canadell et al., 2007; Le Quéré et al., 2009; van der Werf et al., 2004)
Θ $= f_{C3}\Theta_{C3} + f_{C4}\Theta_{C4}$	degree of CO ₂ -water equilibration in plant leaves	0.80	—	(Gillon and Yakir, 2001; Gillon and Yakir, 2000)
Θ_{C3}	degree of CO ₂ -water equilibration in C ₃ plants	0.93	—	(Gillon and Yakir, 2001; Gillon and Yakir, 2000)
Θ_{C4}	degree of CO ₂ -water equilibration in C ₄ plants	0.38	—	(Gillon and Yakir, 2001; Gillon and Yakir, 2000)
f_{C3}	fraction of C ₃ plants	0.77	—	(Still et al., 2003)
$f_{C4} = (1 - f_{C3})$	fraction of C ₄ plants	0.23	—	(Still et al., 2003)
C_{cs}/C_a	CO ₂ concentration gradient between chloroplasts and atmosphere	0.70	—	(Ciais et al., 1997; Cuntz et al., 2003a; Cuntz et al., 2003b)

Table 5-2: Mass balance variables: isotopic signatures, fractionation factors and related parameters. For the model description, $\delta^{18}\text{O}$ values are abbreviated with δ and $\Delta^{17}\text{O}$ values are abbreviated with Δ^{17} .

Parameter	Description	Estimate	Units	References
δ_a	modeled $\delta^{18}\text{O}$ value of global tropospheric CO ₂		‰	
D_A	$\delta^{18}\text{O}$ isotope discrimination of CO ₂ due to assimilation		‰	
δ_L	$\delta^{18}\text{O}$ value of CO ₂ in equilibrium with leaf water	44.7	‰	(Ciais et al., 1997)
δ_{SW}	$\delta^{18}\text{O}$ value of soil water	-7.5	‰	(Ciais et al., 1997)
δ_{resp}	$\delta^{18}\text{O}$ value of CO ₂ emitted from terrestrial respiration	28.6	‰	(Ciais et al., 2005; Ciais et al., 1997; Cuntz et al., 2003a; Cuntz et al., 2003b)
δ_{ocean}	$\delta^{18}\text{O}$ value of ocean surface water	0	‰	(Ciais et al., 2005; Ciais et al., 1997; Cuntz et al., 2003a; Cuntz et al., 2003b)
δ_O	$\delta^{18}\text{O}$ value of CO ₂ in equilibrium with ocean water	42.6	‰	(Ciais et al., 2005; Ciais et al., 1997; Cuntz et al., 2003a; Cuntz et al., 2003b)
δ_{strat}	$\delta^{18}\text{O}$ value of CO ₂ from the lower stratosphere	$\delta_a + 0.4\text{‰}$	‰	(Kawagucci et al., 2008)
δ_{SI}	$\delta^{18}\text{O}$ value of CO ₂ in equilibrium with soil water	36.0	‰	(Wingate et al., 2009)
δ_{ff}	$\delta^{18}\text{O}$ value of CO ₂ from fossil fuel burning	25	‰	(Horváth et al., in press)

Parameter	Description	Estimate	Units	References
δ_{fire}	$\delta^{18}\text{O}$ value of CO ₂ from biomass burning	19	‰	(Horváth et al., in press)
Δ^{17}_{a}	modeled $\Delta^{17}\text{O}$ value of global tropospheric CO ₂		‰	
D^{17}_{A}	$\Delta^{17}\text{O}$ isotope discrimination due to assimilation		‰	
Δ^{17}_{L}	$\Delta^{17}\text{O}$ value of CO ₂ in equilibrium with leaf water	-0.07	‰	
Δ^{17}_{sw}	$\Delta^{17}\text{O}$ value of soil water	-0.01	‰	
$\Delta^{17}_{\text{resp}}$	$\Delta^{17}\text{O}$ value of CO ₂ emitted from terrestrial respiration	0.08	‰	
$\Delta^{17}_{\text{ocean}}$	$\Delta^{17}\text{O}$ value of ocean surface water	-0.01	‰	(Luz and Barkan, 2010)
Δ^{17}_{O}	$\Delta^{17}\text{O}$ value of CO ₂ in equilibrium with ocean water	-0.01	‰	
$\Delta^{17}_{\text{strat}}$	$\Delta^{17}\text{O}$ value of CO ₂ from the lower stratosphere	$\Delta^{17}_{\text{a}} + 0.445\text{‰}$	‰	(Boering et al., 2004; Kawagucci et al., 2008)
Δ^{17}_{SI}	$\Delta^{17}\text{O}$ value of CO ₂ in equilibrium with soil water	-0.01	‰	
Δ^{17}_{ff}	$\Delta^{17}\text{O}$ value of CO ₂ from fossil fuel burning	-0.32	‰	(Horváth et al., in press)
$\Delta^{17}_{\text{fire}}$	$\Delta^{17}\text{O}$ value of CO ₂ from biomass burning	-0.21	‰	(Horváth et al., in press)
$\alpha_{\text{CO}_2\text{-water}}$	temperature dependent equilibrium fractionation factor for $^{18}\text{O}/^{16}\text{O}$ isotope exchange between CO ₂ and water	$(17.604/T - 0.01793) + 1$	—	(Brenninkmeijer et al., 1983)

Parameter	Description	Estimate	Units	References
$\theta_{\text{CO}_2\text{-water}}$	triple oxygen isotope equilibrium fractionation factor (2°C≤T≤37°C)	0.522	–	(Hofmann et al., 2012b)
$\alpha_{\text{transpiration}}$	leaf water enrichment in ¹⁸ O due to evapotranspiration	0.9917	–	(West et al., 2008)
$\lambda_{\text{transpiration}}$	triple oxygen isotope fractionation factor for transpiration in plant leaves	0.522– 0.008×h	–	(Landais et al., 2006)
h	mean humidity above leaf stomata	0.8	–	(Ciais et al., 1997)
α_L	kinetic fractionation factor (¹⁸ O/ ¹⁶ O) for diffusion into and out of stomata	0.9926	–	(Farquhar et al., 1993)
α_S	kinetic fractionation factor (¹⁸ O/ ¹⁶ O) for diffusion out of soils	0.9928	–	(Miller et al., 1999a)
λ_{kinetic}	triple oxygen isotope factor for kinetic fractionation	0.509	–	(Young et al., 2002)
λ_{RL}	slope of reference line (CO ₂ -water equilibration line)	0.522	–	(Hofmann et al., 2012b)
λ_{GMWL}	slope of the global meteoric water line	0.528	–	(Luz and Barkan, 2010)
γ_{GMWL}	intercept of the global meteoric water line	0.033	‰	(Luz and Barkan, 2010)
T _{soil}	global mean soil temperature	285	K	(Ciais et al., 1997)
T _{leaf}	global mean leaf temperature	285	K	(Ciais et al., 1997)
T _{ocean}	global mean sea surface temperature	291	K	(Ciais et al., 1997)

Table 5-3: Input parameters for the Monte Carlo simulation.

Parameter	Mean	SD	Min	Max	Units	References
GPP	120	30	100	180	PgC/yr	(Beer et al., 2010; Welp et al., 2011)
C_{CS}/C_a	0.70	0.13	0.56	0.77	–	(Ciais et al., 1997; Cuntz et al., 2003b; Welp et al., 2011)
Θ	0.8	0.1	0.6	1	–	(Gillon and Yakir, 2001; Gillon and Yakir, 2000)
α_L	0.9926	0.0030	0.9912	0.9941	–	(Farquhar et al., 1993)
α_S	0.9928	0.0030	0.9912	0.9941	–	(Miller et al., 1999a)
T_{soil}	288	2	285	293	K	(Ciais et al., 1997; Cuntz et al., 2003b)
T_{leaf}	291	2	286	296	K	(Ciais et al., 1997; Cuntz et al., 2003b)
T_{ocean}	291	2	286	296	K	(Ciais et al., 1997; Cuntz et al., 2003b)
δ_{SW}	–7.5	3	–9	0	‰	(Ciais et al., 1997; Cuntz et al., 2003b)
$\alpha_{transpiration}$	0.9917	0.0010	0.9900	0.9940	–	(West et al., 2008)
h	0.8	0.1	0.6	1	–	(Ciais et al., 1997)
$\theta_{CO_2-water}$	0.522	0.001	0.50	0.53	–	(Hofmann et al., 2012b)
$\lambda_{kinetic}$	0.509	0.001	0.50	0.53	–	(Young et al., 2002)
F_{OA}	90	10	70	100	PgC/yr	(Naegler et al., 2006)
F_{SA}	100	30	25	175	PgC/yr	(Appenzeller et al., 1996)
F_{SI}	30	120	0	450	PgC/yr	(Wingate et al., 2009)

5.3.3 Sampling of tropospheric CO₂ and isotope analyses

We sampled ambient air CO₂ in two-week intervals from June 2010 to July 2012 from the fourth floor of the Geoscience Department in Göttingen. The department is situated at the outskirts of the medium-sized town Göttingen with moderate traffic density (130,000 inhabitants, 51.5569°N, 9.9468°E).

Additionally, we sampled two air samples on top of the nearby Brocken Mountain, the highest peak of the Harz Mountain range with an elevation of about 1140 m (51.7987°N, 10.6185°E). The mountain range stands out of the surrounding lowlands and the Mt. Brocken is mostly exposed to low tropospheric winds from west/southwest. The Brocken air was sampled on 2nd and 28th March and 17th July 2012 in order to check if the air samples from Göttingen were significantly affected by elevated anthropogenic CO₂ influx (Horváth et al., in press) or local CO₂ sources from the biosphere.

In Göttingen, the CO₂ was directly extracted from ambient air using a Russian doll type cryogenic trap with borosilicate-glass filters (Brenninkmeijer, 1991; Brenninkmeijer and Röckmann, 1996). A tube was installed at the building so that ambient air was collected with 1-2 meter distance to the building. First, the ambient air passed through magnesium perchlorate, Mg(ClO₄)₂, to remove water vapor. Then, the CO₂ was separated from all non-condensable gases by means of the cryogenic trap at a flow rate of 2-3 L/min. In order to analyze the $\Delta^{17}\text{O}$ of CO₂ we use our CO₂-CeO₂ equilibration technique which requires at least 3.5 mmol of CO₂ (corresponding to about 400 L of ambient air at STP) (Hofmann et al., 2012b; Hofmann and Pack, 2010).

Subsequent to the collection of CO₂ in the Russian doll type cryogenic trap, the cold trap is slowly warmed to room temperature. Simultaneously, a second trap is held at -70°C (with a mixture of liquid nitrogen and ethanol) to hold back remaining water vapor. Next, the CO₂ gas is exposed for about 30 minutes to P₂O₅ for final drying. A subsample of the CO₂ (~50 μmol) is separated for conventional $\delta^{13}\text{C}$ and $\delta^{18}\text{O}$ analyses. The remaining CO₂ sample is then immediately transferred to the CO₂-CeO₂ equilibration apparatus, so that no storage of the sample CO₂ becomes necessary.

Air sampling on top of the Brocken Mountain was carried out with an oil-free, high-pressure compressor from Rix Industries with a gas engine drive (model SA-3G). The air inlet was held at about 4 m above ground. The air stream passed through two Mg(ClO₄)₂

units in order to effectively remove water vapor. Before entering the compressor, the flow rate was controlled with a mass flow controller, which was set to 2-3 L/min. The dried air was compressed into a 5 L pressure cylinder, which was filled up to 100 bar. A 3 m long exhaust pipe was attached to the compressor to ensure that the exhaust fumes were directed away from the air inlet system. Additionally, the compressor and the exhaust pipe were placed downwind so that the air samples were not contaminated with exhaust gases. The CO₂ extraction from the compressed air and the sample preparation was carried out analog to the procedure described above.

The $\delta^{18}\text{O}$ analyses of CO₂ were carried out on a Finnigan Delta plus mass spectrometer. The $\delta^{18}\text{O}$ values were standardized by comparison with CO₂ generated by phosphoric acid decomposition of NBS-19 ($\delta^{18}\text{O}_{\text{VSMOW}} = +28.65\text{‰}$). The carbonate was reacted at 70 °C and the acid fractionation factor for calcite $\alpha_{\text{CO}_2\text{-calcite}} = 1.00871$ (Kim et al., 2007) was used. The mass spectrometric uncertainty in $\delta^{18}\text{O}$ is in the range of $\pm 0.03\text{‰}$ (1 σ , SD).

We measured CO₂ and N₂O concentrations of the air samples with a gas chromatograph (Carlo Erba) in order to correct the $\delta^{18}\text{O}$ values for interferences with N₂O (Assonov et al., 2009). All $\delta^{18}\text{O}$ data of ambient air CO₂ were corrected with $-0.29 \pm 0.03\text{‰}$ (SD).

The $\Delta^{17}\text{O}$ analyses were carried out using the CO₂-CeO₂ exchange method (Hofmann et al., 2012b; Hofmann and Pack, 2010). The method was calibrated by producing CO₂ with a known triple oxygen isotope composition by combustion of graphite with O₂ ($\delta^{18}\text{O}_{\text{VSMOW}} = 13.473\text{‰}$, $\delta^{17}\text{O}_{\text{VSMOW}} = 6.649\text{‰}$) that was analyzed relative to VSMOW by E. Barkan (Institute of Earth Sciences, Hebrew University of Jerusalem).

5.4 Results and discussion

5.4.1 Modeled triple oxygen isotope composition of tropospheric CO₂

The mass balance calculation and the Monte Carlo simulation give a global annual mean of tropospheric CO₂ of $\Delta^{17}\text{O} = +0.06 \pm 0.05\text{‰}$ (SD). The model prediction is slightly lower than the former prediction from Hoag et al. (2005) with $\Delta^{17}\text{O} \approx +0.11\text{‰}$ (relative to a reference line with a slope of 0.522 in a $\ln(\delta^{18}\text{O}+1)$ vs. $\ln(\delta^{17}\text{O}+1)$ plot). Our model prediction is the most sensitive to assumption on the exponent $\theta_{\text{CO}_2\text{-water}}$, the magnitude of stratospheric CO₂ influx, the $C_{\text{cs}}/C_{\text{a}}$ ratio (the ratio of CO₂ concentration in chloroplasts to atmospheric CO₂ concentration), the magnitude of the soil invasion flux and the magnitude of the terrestrial gross primary production (see section 5.4.2 and 5.4.3).

For the $\delta^{18}\text{O}$ mass balance calculation, the base scenario (see Table 5-1 and Table 5-2) results in $\delta^{18}\text{O} = 41.3\text{‰}$ and the Monte Carlo simulation (see Table 5-3) in $\delta^{18}\text{O} = 40.9 \pm 1.9\text{‰}$ (SD). The modeled mean $\delta^{18}\text{O}$ value is in good agreement with the observed global mean of about 41.5‰ (e.g. Farquhar et al., 1993). The large uncertainty in the $\delta^{18}\text{O}$ model prediction gives a very conservative estimate for the global troposphere, in order to test the maximum effect of the model assumptions on the $\Delta^{17}\text{O}$ prediction of tropospheric CO₂.

5.4.2 Impact of the major CO₂ sources and sinks on the global mean $\Delta^{17}\text{O}$ value of tropospheric CO₂

The effect of the various carbon sources and sinks on the global triple oxygen isotope composition of tropospheric CO₂ is best illustrated by comparing the $\delta^{18}\text{O}$ and $\Delta^{17}\text{O}$ isofluxes (Fig. 5-2). The term isoflux refers to the multiplication of the carbon flux size F and the difference in the isotopic composition of the respective carbon flux and the isotopic composition of tropospheric CO₂, e.g. $F_{\text{SA}}(\delta^{18}\text{O}_{\text{SA}} - \delta^{18}\text{O}_{\text{a}})$.

The $\delta^{18}\text{O}$ isofluxes of our mass balance model were chosen in accordance with previous modeling studies (see e.g. Ciais et al., 2005). In doing so, the $^{18}\text{O}/^{16}\text{O}$ ratio of tropospheric CO₂ is mainly controlled by assimilation and respiration but the range for the assimilation and respiration isoflux was slightly extended compared to the ranges given by Ciais et al. (2005), see Fig. 5-2a. This is mainly due to the large variation in the CO₂ concentration gradient between chloroplasts and atmosphere ($0.56 < C_{\text{cs}}/C_{\text{a}} < 0.77$) and in the terrestrial

gross primary production ($100 \text{ PgC/yr} < \text{GPP} < 180 \text{ PgC/yr}$) that were considered for the Monte Carlo simulation.

It is well known that stratospheric CO₂ is enriched in ¹⁸O relative to tropospheric CO₂, and as a consequence, the influx of stratospheric CO₂ must go along with a positive $\delta^{18}\text{O}$ isoflux. However, $\delta^{18}\text{O}$ modeling studies generally neglect the influx of stratospheric CO₂ (Cuntz et al., 2003a; Cuntz et al., 2003b; Peylin et al., 1996; Welp et al., 2011). Here, we consider the estimate of stratospheric CO₂ influx from Kawagucci et al. (2008) and conclude that stratospheric CO₂ influx indeed does not have a significant impact on the $\delta^{18}\text{O}$ composition of tropospheric CO₂ (see Fig. 5-2a).

For the soil invasion flux, we considered recent findings from Wingate et al. (2009) that the abiotic CO₂ flux from soils might have a much larger effect on the oxygen isotope composition of tropospheric CO₂ than previously assumed ($0 \text{ PgC/yr} < F_{\text{SI}} < 450 \text{ PgC/yr}$).

The large scatter in $\delta^{18}\text{O}$ isofluxes illustrates that modeling the $\delta^{18}\text{O}$ value of tropospheric CO₂ is very sensitive to various assumptions. Thus, comprehensive bio- and atmosphere models are required to simulate spatial and temporal variations in $\delta^{18}\text{O}$ of tropospheric CO₂ (Ciais et al., 1997; Cuntz et al., 2003a; Cuntz et al., 2003b; Peylin et al., 1996; Welp et al., 2011). That is why Hoag et al. (2005) suggested that $\Delta^{17}\text{O}$ of tropospheric CO₂ might be a more straightforward tracer of variations in assimilation and respiration.

The modeled $\Delta^{17}\text{O}$ isofluxes suggest that the $\Delta^{17}\text{O}$ value of tropospheric CO₂ is mainly controlled by terrestrial assimilation, respiration, stratospheric influx and soil invasion (see Fig. 5-2b). However, in contrast to the previous $\Delta^{17}\text{O}$ model from Hoag et al. (2005), assimilation has a negative effect on $\Delta^{17}\text{O}$ of tropospheric CO₂, whereas both respiratory CO₂ and stratospheric influx have a positive effect on $\Delta^{17}\text{O}$ of tropospheric CO₂. The negative $\Delta^{17}\text{O}$ isoflux for assimilation is mainly a result of kinetic fractionation during CO₂ diffusion into the stomata. The positive effect of respiratory CO₂ on the $\Delta^{17}\text{O}$ composition of tropospheric CO₂ results from the kinetic fractionation during diffusion out of the soil column (see Fig. 5-1). For the stratospheric CO₂ influx, we combine the estimates from Boering et al. (2004) and Kawagucci et al. (2008) on the ¹⁷O enrichment of stratospheric CO₂ influx, and thus, we obtain a slightly higher $\Delta^{17}\text{O}$ isoflux for stratospheric CO₂ compared to the previous $\Delta^{17}\text{O}$ model from Hoag et al. (2005). The assumption on the size of the soil invasion flux also has a considerable effect on the modeled $\Delta^{17}\text{O}$ value, whereas fossil fuel emissions and biomass burning do not have a significant impact on the $\Delta^{17}\text{O}$ composition of global tropospheric CO₂.

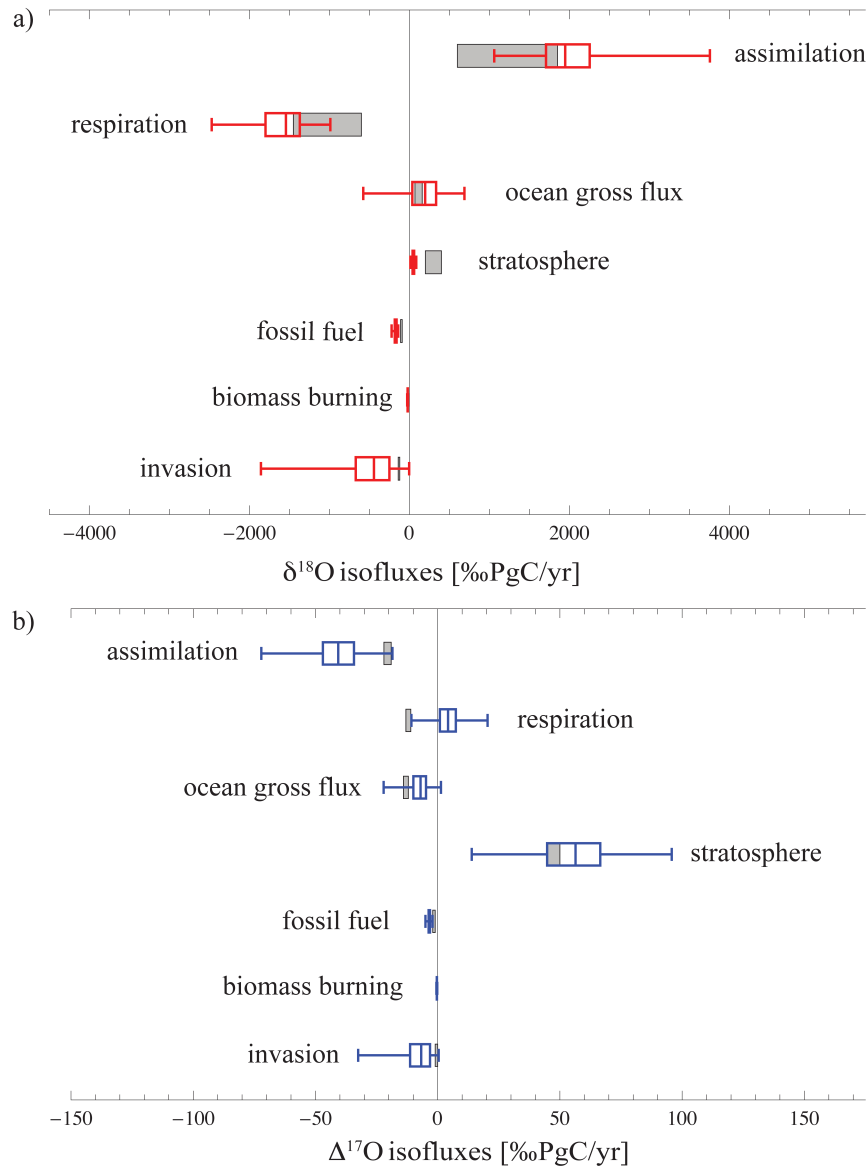


Fig. 5-2: Box plots showing the main isofluxes controlling the triple oxygen isotope composition of tropospheric CO₂. The boxes indicate the median, 25th and 75th percentiles of the Monte Carlo simulation. The whisker caps indicate 5th and 95th percentiles. a) $\delta^{18}\text{O}$ isofluxes: The $\delta^{18}\text{O}$ composition of tropospheric CO₂ is mainly controlled by two opponents: assimilation and respiration. Our $\delta^{18}\text{O}$ model assumptions are in good agreement with previous $\delta^{18}\text{O}$ isofluxes from Ciais et al. (2005) (gray rectangles). The only major modification is the assumption on the soil invasion flux: We implemented a mean of 30 PgC/yr in the Monte Carlo simulation, but extended the possible range up to 450 PgC/yr as suggested by Wingate et al. (2009). b) $\Delta^{17}\text{O}$ isofluxes: The model suggests that the $\Delta^{17}\text{O}$ value of tropospheric CO₂ is mainly controlled by assimilation, respiration, soil invasion and stratospheric influx. However, in contrast to the model from Hoag et al. (2005) (gray rectangles), our modeling results suggest that both respiratory CO₂ and stratospheric influx have a positive effect on $\Delta^{17}\text{O}$ of tropospheric CO₂ and the soil invasion flux might also significantly affect the triple oxygen isotope composition of tropospheric CO₂.

5.4.3 Is $\Delta^{17}\text{O}$ of tropospheric CO₂ a potential tracer for the terrestrial gross primary production?

We tested the sensitivity of $\Delta^{17}\text{O}$ of tropospheric CO₂ to GPP. The model predicts that a 3-fold change from 50 to 150 PgC/yr results in a $\Delta^{17}\text{O}$ decrease of about -0.08‰ (Fig. 5-3). This sensitivity to GPP is slightly lower than the prediction of -0.11‰ for a decrease from 50 to 150 PgC/yr from Hoag et al. (2005). However, the $\Delta^{17}\text{O}$ composition of tropospheric CO₂ is also significantly affected by the $C_{\text{cs}}/C_{\text{a}}$ ratio, and as a consequence by the distribution of C₃ and C₄ plants, the magnitude of stratospheric CO₂ influx and soil invasion CO₂. Thus, in order to use $\Delta^{17}\text{O}$ of CO₂ as a tracer for GPP better constrains for these parameters are required.

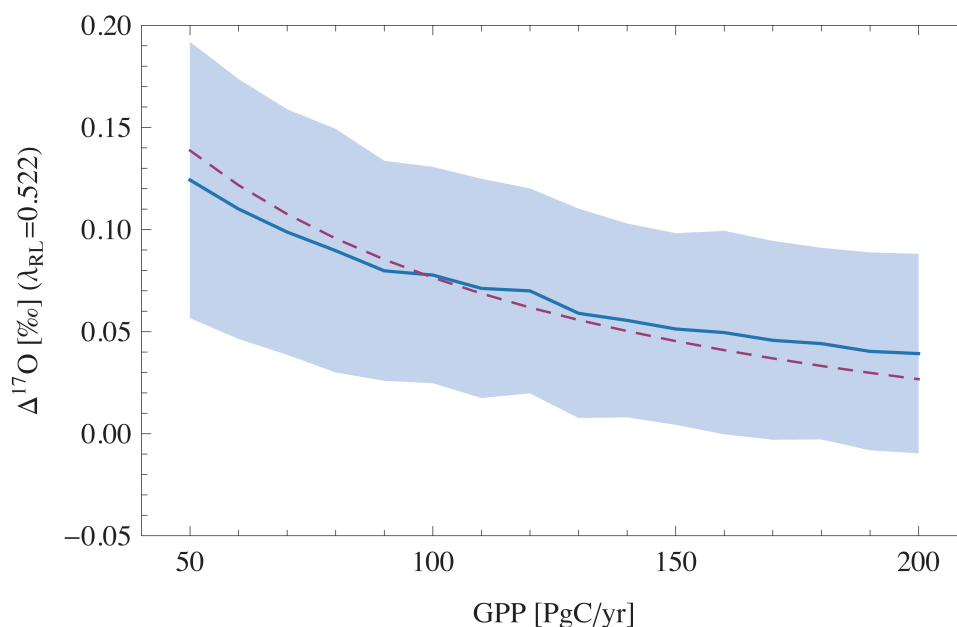


Fig. 5-3: Modeled sensitivity of $\Delta^{17}\text{O}$ of tropospheric CO₂ to variations in the terrestrial gross primary production (GPP). The dashed curve shows the sensitivity of $\Delta^{17}\text{O}$ for the base scenario (see Table 5-1 and Table 5-2) and the solid curve shows the result from the Monte Carlo simulation (see Table 5-3). The error envelope denotes the standard deviation obtained from the Monte Carlo simulation and reflects all uncertainties in $\Delta^{17}\text{O}$ modeling, most notably, the $C_{\text{cs}}/C_{\text{a}}$ ratio, the magnitude of stratospheric CO₂ influx and the amount of soil invasion CO₂.

5.4.4 Observational triple oxygen isotope data of tropospheric CO₂

Ambient air CO₂ sampled in Göttingen has a mean $\Delta^{17}\text{O}$ value of $-0.03 \pm 0.07\text{‰}$ (SD) and a corresponding $\delta^{18}\text{O}$ value of $41.6 \pm 0.9\text{‰}$ (SD). In contrast to stratospheric CO₂, the observational data do not show any correlation between $\delta^{18}\text{O}$ and $\Delta^{17}\text{O}$ (Fig. 5-4).

The Mt. Brocken CO₂ data fall within the range observed in Göttingen: The CO₂ sampled on 2nd and 28th March and on 17th July 2012 have $\Delta^{17}\text{O}$ values of $0.00 \pm 0.02\text{‰}$ (SE), $-0.08 \pm 0.02\text{‰}$ (SE) and $-0.06 \pm 0.03\text{‰}$ (SE) and $\delta^{18}\text{O}$ values of 40.4‰, 40.7‰ and 40.6‰ (Fig. 5-4 and Fig. 5-5). Thus, the triple oxygen isotope composition of ambient air CO₂ from Göttingen is not significantly affected by local anthropogenic CO₂ emissions.

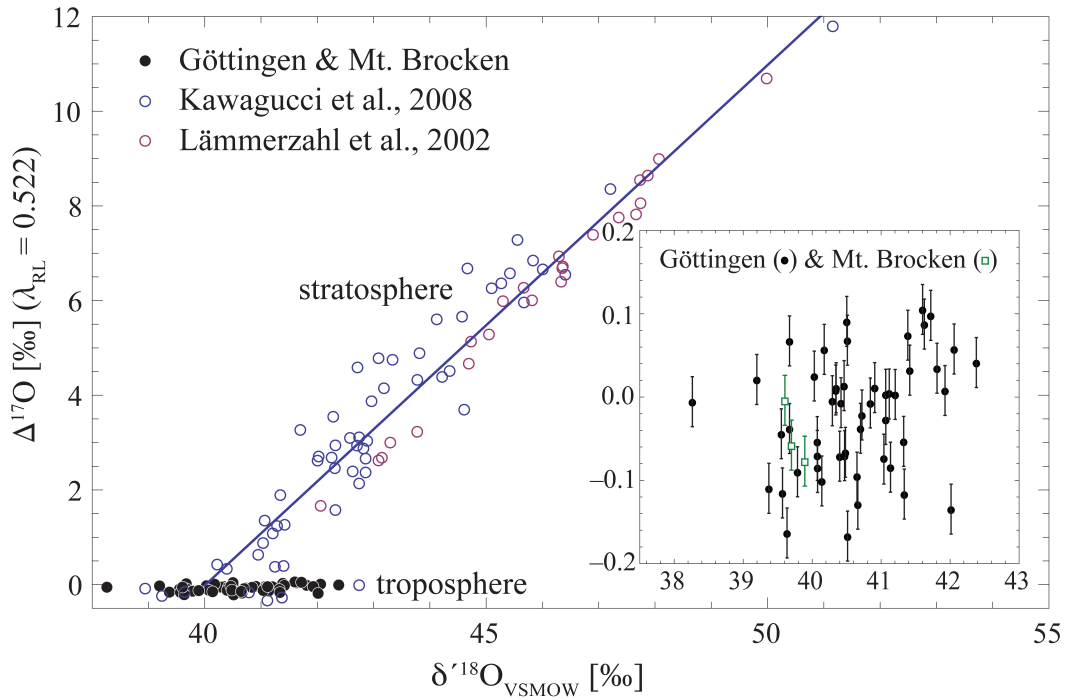


Fig. 5-4: Triple oxygen isotope composition of tropospheric and stratospheric CO₂. Tropospheric CO₂ from Göttingen and from Mt. Brocken plot on or close to the CO₂-water equilibration line, i.e. $\Delta^{17}\text{O} \approx 0\text{‰}$. These near-surface CO₂ data fall on the lower end of a stratosphere-troposphere mixing line (Kawagucci et al., 2008; Lämmerzahl et al., 2002), but do not show any correlation between $\delta^{18}\text{O}$ and $\Delta^{17}\text{O}$. The Mt. Brocken CO₂ was sampled on 2nd and 28th March and 17th July 2012, the Göttingen CO₂ was sampled between June 2010 and July 2012. Error bars show standard errors.

The $\delta^{18}\text{O}$ values of ambient air CO₂ sampled in Göttingen show a clear variation with time (Fig. 5-5). The variability in $\delta^{18}\text{O}$ is due to the seasonal variation in plant activity with an amplitude of about 1.5‰. The seasonality in $\delta^{18}\text{O}$ is about double the size than the seasonality observed at the continental background station Schauinsland (SW Germany) (see Cuntz et al., 2003a) due to local CO₂ sources from the biosphere.

The $\Delta^{17}\text{O}$ values of CO₂ sampled in Göttingen also show a temporal variation with a peak-to-peak range of about 0.25‰. From June 2010 to December 2011, the $\Delta^{17}\text{O}$ variation parallels the seasonal cycle of the measured $\delta^{18}\text{O}$ values (Fig. 5-5), e.g. maximum $\Delta^{17}\text{O}$ values ($\sim +0.08\text{‰}$) during spring/summer 2010 and 2011 and a local minimum ($\sim -0.05\text{‰}$) during winter 2010/2011. During the first half of 2012, however, the $\Delta^{17}\text{O}$ values scatter around -0.1‰ and do no longer parallel the seasonal cycle of $\delta^{18}\text{O}$.

Our $\Delta^{17}\text{O}$ model prediction for the global troposphere of $+0.06 \pm 0.05\text{‰}$ agrees well with the observational data for Göttingen CO₂ sampled during summer 2010 and 2011 (see Fig. 5-5). However, the global prediction deviates significantly from the mean $\Delta^{17}\text{O}$ value of $-0.08 \pm 0.05\text{‰}$ (SD) analyzed for Göttingen CO₂ sampled between July 2011 and July 2012.

It is beyond the scope of this study to investigate in detail the observed temporal variation in $\Delta^{17}\text{O}$ of ambient air CO₂ from Göttingen. However, it is apparent from the assimilation isofluxes (described in section 5.4.2 and shown in Fig. 5-2) that an increase in plant activity during spring and summer leads to an increase in the observed $\delta^{18}\text{O}$ values of tropospheric CO₂. At the same time, this should decrease the $\Delta^{17}\text{O}$ values of tropospheric CO₂ during spring and summer because of the predicted negative $\Delta^{17}\text{O}$ isoflux for assimilation. However, this is in contrast to the observational data, which show maximum $\Delta^{17}\text{O}$ values during early summer 2010 and 2011. Thus, it may be that the influx of stratospheric CO₂ significantly affects the temporal variation of $\Delta^{17}\text{O}$ values of Göttingen CO₂. A similar pattern was observed for atmospheric N₂O, where the seasonal cycle of N₂O mixing ratios in the troposphere is also significantly influenced by the influx of stratospheric air masses (Nevison et al., 2011).

To conclude, future investigations are required to clarify the cause for the temporal variation of $\Delta^{17}\text{O}$ of ambient air CO₂ from Göttingen. On the one hand, these studies should focus on the relevance of stratospheric influx, on the other hand, they should investigate experimentally the triple oxygen isotope composition of local CO₂ sources from the biosphere.

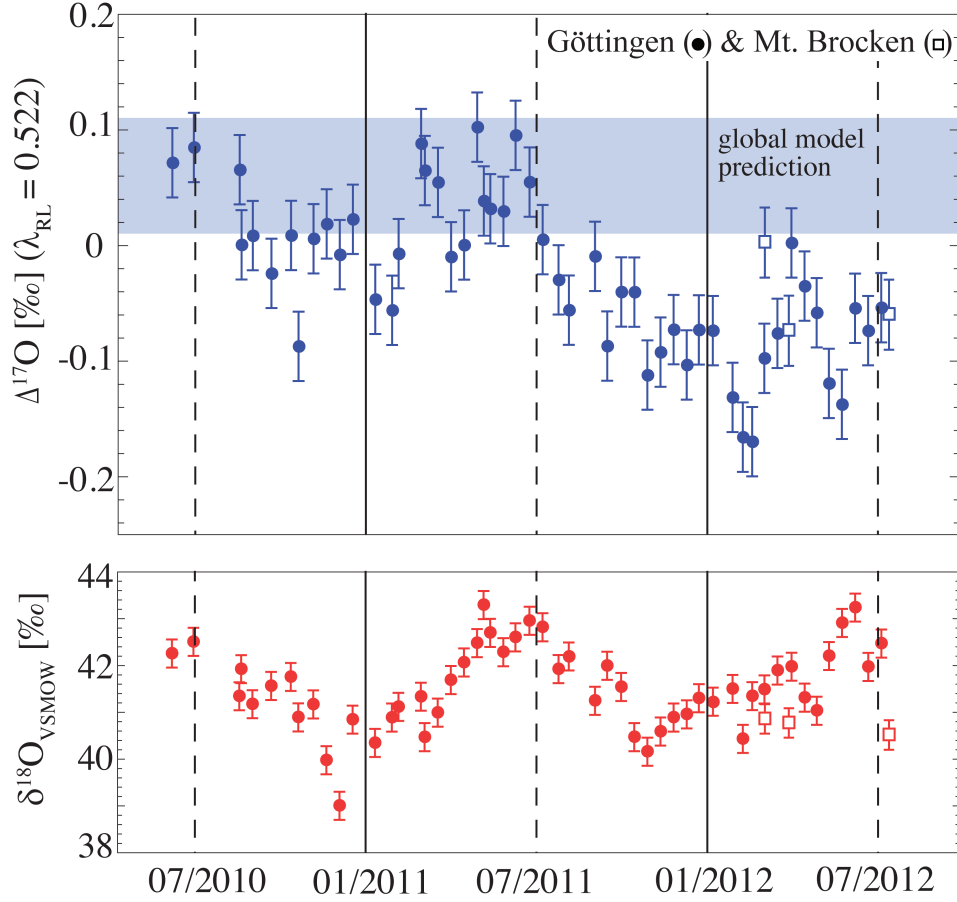


Fig. 5-5: Time series of the triple oxygen isotope composition of ambient air CO₂ from Göttingen. The $\Delta^{17}\text{O}$ composition of tropospheric CO₂ shows a temporal variation: From June 2010 to December 2011, the $\Delta^{17}\text{O}$ variation parallels the seasonal cycle of the measured $\delta^{18}\text{O}$ values. However, in 2012, the $\Delta^{17}\text{O}$ signal does no longer run parallel to the seasonal $\delta^{18}\text{O}$ cycle. The model prediction for the global troposphere ($\Delta^{17}\text{O} = +0.06 \pm 0.05\text{‰}$, see section 5.4.1) agrees well with the $\Delta^{17}\text{O}$ measurements in the first year, however, the model cannot explain the strong decrease in $\Delta^{17}\text{O}$ in 2012. It may be that the influx of stratospheric CO₂ has a significant impact on the observed temporal variation in $\Delta^{17}\text{O}$ of ambient air CO₂ from Göttingen.

5.5 Conclusions

Here, we present a refined model prediction for the global triple oxygen isotope composition of tropospheric CO₂. We predict a global mean $\Delta^{17}\text{O}$ composition of +0.06‰ and estimate an uncertainty of $\pm 0.05\text{‰}$ (SD) based on a Monte Carlo simulation. Despite the various refined assumptions on the biosphere-atmosphere interaction, we confirm the sensitivity of $\Delta^{17}\text{O}$ of tropospheric CO₂ to the terrestrial gross primary production. However, we suggest that the global mean of +0.06‰ is slightly lower than the previous estimate from Hoag et al. (2005) of +0.11‰.

Moreover, we present the first set of high-precision triple oxygen isotope data of tropospheric CO₂. Ambient air CO₂ sampled in Göttingen between June 2010 and July 2012 has a mean $\Delta^{17}\text{O}$ value of $-0.03 \pm 0.07\text{‰}$ (SD). The triple oxygen isotope data of background CO₂ sampled on top of the Brocken Mountain ($\Delta^{17}\text{O} = -0.04 \pm 0.04\text{‰}$ (SD)) fall within the range observed in Göttingen. Thus, the observational data only in part overlap with the model prediction for the global troposphere. The discrepancy between the observed and predicted mean $\Delta^{17}\text{O}$ value and the large interannual variation in $\Delta^{17}\text{O}$ needs further investigations. Future studies should focus on the relevance of stratospheric influx and the experimental determination of the triple oxygen isotope composition of local CO₂ sources from the biosphere in order to clarify the observed temporal variation in $\Delta^{17}\text{O}$ of ambient air CO₂.

5.6 Acknowledgments

We thank M. Cuntz and J. Kaiser for very helpful comments on the mass balance calculation. We also thank E. Barkan for calibration of our inhouse reference O₂ gas relative to VSMOW. This project was partly funded by the German Science Foundation (AP, project PA909/6-2).

5.7 References

- Appenzeller, C., Holton, J. R., Rosenlof, K. H., 1996. Seasonal variation of mass transport across the tropopause. *J. Geophys. Res.-Atmos.* 101, 15071-15078.
- Assonov, S. S., Brenninkmeijer, C. A. M., Koeppel, C., Röckmann, T., 2009. CO₂ isotope analyses using large air samples collected on intercontinental flights by the CARIBIC Boeing 767. *Rapid Commun. Mass Spec.* 23, 822-830.
- Barkan, A., Luz, B., 2011. The relationship among the three stable isotopes of oxygen in air, seawater and marine photosynthesis. *Rapid Commun. Mass Spec.* 25, 2367–2369.
- Beer, C., Reichstein, M., Tomelleri, E., Ciais, P., Jung, M., Carvalhais, N., Rödenbeck, C., Arain, M. A., Baldocchi, D., Bonan, G. B., Bondeau, A., Cescatti, A., Lasslop, G., Lindroth, A., Lomas, M., Luyssaert, S., Margolis, H., Oleson, K. W., Rouspard, O., Veenendaal, E., Viovy, N., Williams, C., Woodward, F. I., Papale, D., 2010. Terrestrial gross carbon dioxide uptake: global distribution and covariation with climate. *Science* 329, 834-838.
- Boden, T. A., Marland, G., Andreas, R. J., 2011. Global, regional, and national fossil-fuel CO₂ emissions. Carbon Dioxide Information Analysis Center, Oak Ridge National Laboratory, U.S. Department of Energy, Oak Ridge, Tenn., U.S.A.
- Boering, K. A., Jackson, T., Hoag, K. J., Cole, A. S., Perri, M. J., Thiemens, M., Atlas, E., 2004. Observations of the anomalous oxygen isotopic composition of carbon dioxide in the lower stratosphere and the flux of the anomaly to the troposphere. *Geophys. Res. Lett.* 31.
- Brenninkmeijer, C. A. M., 1991. Robust, high-efficiency, high-capacity cryogenic trap. *Anal. Chem.* 63, 1182-1184.
- Brenninkmeijer, C. A. M., Kraft, P., Mook, W. G., 1983. Oxygen isotope fractionation between CO₂ and H₂O. *Isot. Geosci.* 1, 181-190.
- Brenninkmeijer, C. A. M., Röckmann, T., 1996. Russian doll type cryogenic traps: improved design and isotope separation effects. *Anal. Chem.* 68, 3050-3053.
- Canadell, J. G., Le Quéré, C., Raupach, M. R., Field, C. B., Buitenhuis, E. T., Ciais, P., Conway, T. J., Gillett, N. P., Houghton, R. A., Marland, G., 2007. Contributions to accelerating atmospheric CO₂ growth from economic activity, carbon intensity, and efficiency of natural sinks. *Proc. Natl. Acad. Sci.* 104, 18866-18870.
- Ciais, P., Cuntz, M., Scholze, M., Mouillot, F., Peylin, P., Gitz, V., 2005. Remarks on the use of ¹³C and ¹⁸O isotopes in atmospheric CO₂ to quantify biospheric carbon fluxes. In: Flanagan, L. B., Ehleringer, J. R., and Pataki, D. E. Eds.), *Stable*

Isotopes and Biosphere - Atmosphere Interactions : Processes and Biological Controls. Elsevier.

- Ciais, P., Denning, A. S., Tans, P. P., Berry, J. A., Randall, D., Collatz, J. G., Sellers, P. J., White, J. W., Troler, M., Meijer, H. A. J., Francey, R. J., Monfray, P., Heimann, M., 1997. A three-dimensional synthesis study of $\delta^{18}\text{O}$ in atmospheric CO₂: Part 1 Surface fluxes. *J. Geophys. Res.* 102, 5857-5872.
- Cuntz, M., Ciais, P., Hoffmann, G., Allison, C. E., Francey, R. J., Knorr, W., Tans, P. P., White, J. W. C., Levin, I., 2003a. A comprehensive global three-dimensional model of $\delta^{18}\text{O}$ in atmospheric CO₂: 2. Mapping the atmospheric signal. *J. Geophys. Res.* 108, ACH2.1-ACH2.19.
- Cuntz, M., Ciais, P., Hoffmann, G., Knorr, W., 2003b. A comprehensive global three-dimensional model of $\delta^{18}\text{O}$ in atmospheric CO₂: 1. Validation of surface processes. *J. Geophys. Res.* 108, ACH1-ACH23.
- Farquhar, G. D., Lloyd, J., Taylor, J. A., Flanagan, L. B., Syvertsen, J. P., Hubick, K. T., Wong, S. C., Ehleringer, J. R., 1993. Vegetation effects on the isotope composition of oxygen in atmospheric CO₂. *Nature* 363, 439-443.
- Gamo, T., Tsutsumi, M., Sakai, H., Nakazawa, T., Tanaka, M., Honda, H., Kubo, H., Itoh, T., 1989. Carbon and oxygen isotopic ratios of carbon dioxide of a stratospheric profile over Japan. *Tellus B* 41B, 127-133.
- Gillon, J., Yakir, D., 2001. Influence of carbonic anhydrase activity in terrestrial vegetation on the ^{18}O content of atmospheric CO₂. *Science* 291, 2584-2587.
- Gillon, J. S., Yakir, D., 2000. Naturally low carbonic anhydrase activity in C₄ and C₃ plants limits discrimination against C¹⁸OO during photosynthesis. *Plant Cell Environ.* 23, 903-915.
- Heimann, M., Maier-Reimer, E., 1996. On the relations between the oceanic uptake of CO₂ and its carbon isotopes. *Global Biogeochem. Cy.* 10, 89-110.
- Hoag, K. J., Still, C. J., Fung, I. Y., Boering, K. A., 2005. Triple oxygen isotope composition of tropospheric carbon dioxide as a tracer of terrestrial gross carbon fluxes. *Geophys. Res. Lett.* 32, 1-5.
- Hofmann, M. E. G., Horváth, B., Pack, A., 2012b. Triple oxygen isotope equilibrium fractionation between carbon dioxide and water. *Earth Planet. Sci. Lett.* 319-320, 159-164.
- Hofmann, M. E. G., Pack, A., 2010. Technique for high-precision analysis of triple oxygen isotope ratios in carbon dioxide. *Anal. Chem.* 82, 4357-4361.

- Horváth, B., Hofmann, M. E. G., Pack, A., in press. On the triple oxygen isotope composition of carbon dioxide from some combustion processes. *Geochim. Cosmochim. Acta*.
- Hulston, J. R., Thode, H. G., 1965. Variations in the S³³, S³⁴, and S³⁶ contents of meteorites and their relation to chemical and nuclear effects. *J. Geophys. Res.* 70, 3475-3484.
- Kawagucci, S., Tsunogai, U., Kudo, S., Nakagawa, F., Honda, H., Aoki, S., Nakazawa, T., Tsutsumi, M., Gamo, T., 2008. Long-term observation of mass-independent oxygen isotope anomaly in stratospheric CO₂. *Atmos. Chem. Phys.* 8, 6189-6197.
- Kim, S.-T., Mucci, A., Taylor, B. E., 2007. Phosphoric acid fractionation factors for calcite and aragonite between 25 and 75 °C: Revisited. *Chem. Geol.* 246, 135-146.
- Lämmerzahl, P., Röckmann, T., Brenninkmeijer, C. A. M., Krankowsky, D., Mauersberger, K., 2002. Oxygen isotope composition of stratospheric carbon dioxide. *Geophys. Res. Lett.* 29, 1582.
- Landais, A., Barkan, E., Yakir, D., Luz, B., 2006. The triple isotopic composition of oxygen in leaf water. *Geochim. Cosmochim. Acta* 70, 4105-4115.
- Le Quéré, C., Raupach, M. R., Canadell, J. G., Marland, G., et al., 2009. Trends in the sources and sinks of carbon dioxide. *Nature Geosci.* 2, 831-836.
- Lloyd, J., Farquhar, G. D., 1994. C¹³ discrimination during CO₂ assimilation by the terrestrial biosphere. *Oecologia* 99, 201-215.
- Luz, B., Barkan, E., 2010. Variations of ¹⁷O/¹⁶O and ¹⁸O/¹⁶O in meteoric waters. *Geochim. Cosmochim. Acta* 74, 6276-6286.
- Miller, J. B., Yakir, D., White, J. W. C., Tans, P. P., 1999a. Measurement of ¹⁸O/¹⁶O in the soil-atmosphere CO₂ flux. *Global Biogeochem. Cy.* 13, 761-774.
- Miller, M. F., 2002. Isotopic fractionation and the quantification of ¹⁷O anomalies in the oxygen three-isotope system: an appraisal and geochemical significance. *Geochim. Cosmochim. Acta* 66, 1881-1889.
- Naegler, T., Ciais, P., Rodgers, K., Levin, I., 2006. Excess radiocarbon constraints on air-sea gas exchange and the uptake of CO₂ by the oceans. *Geophys. Res. Lett.* 33.
- Nevison, C. D., Dlugokencky, E., Dutton, G., Elkins, J. W., Fraser, P., Hall, B., Krummel, P. B., Langenfelds, R. L., O'Doherty, S., Prinn, R. G., Steele, L. P., Weiss, R. F., 2011. Exploring causes of interannual variability in the seasonal cycles of tropospheric nitrous oxide. *Atmos. Chem. Phys.* 11, 3713-3730.
- Pearcy, R. W., Ehleringer, J., 1984. Comparative ecophysiology of C₃ and C₄ plants. *Plant Cell Environ.* 7, 1-13.

- Peylin, P., Ciais, P., Tans, P. P., Six, K., Berry, J. A., Denning, A. S., 1996. ¹⁸O in atmospheric CO₂ simulated by a 3-D transport model: A sensitivity study to vegetation and soil fractionation factors. *Phys. Chem. Earth* 21, 463-469.
- Stern, L. A., Amundson, R., Baisden, W. T., 2001. Influence of soils on oxygen isotope ratio of atmospheric CO₂. *Global Biogeochem. Cy.* 15, 753-759.
- Still, C. J., Berry, J. A., Collatz, G. J., DeFries, R. S., 2003. Global distribution of C₃ and C₄ vegetation: Carbon cycle implications. *Global Biogeochem. Cy.* 17, -.
- Tans, P. P., 1998. Oxygen isotopic equilibrium between carbon dioxide and water in soils. *Tellus B* 50, 163-178.
- Thiemens, M. H., Jackson, T., Zipf, E. C., Erdman, P. W., van Egmond, C., 1995b. Carbon dioxide and oxygen isotope anomalies in the mesosphere and stratosphere. *Science* 270, 969-972.
- van der Werf, G. R., Randerson, J. T., Collatz, G. J., Giglio, L., Kasibhatla, P. S., Arellano, A. F., Olsen, S. C., Kasischke, E. S., 2004. Continental-scale partitioning of fire emissions during the 1997 to 2001 El Niño/La Niña period. *Science* 303, 73-76.
- Welp, L. R., Keeling, R. F., Meijer, H. A. J., Bollenbacher, A. F., Piper, S. C., Yoshimura, K., Francey, R. J., Allison, C. E., Wahlen, M., 2011. Interannual variability in the oxygen isotopes of atmospheric CO₂ driven by El Niño. *Nature* 477, 579-582.
- West, J. B., Sobek, A., Ehleringer, J. R., 2008. A simplified GIS approach to modeling global leaf water isoscapes. *Plos One* 3, e2447.
- Wingate, L., Ogée, J., Cuntz, M., Genty, B., Reiter, I., Seibt, U., Yakir, D., Maseyk, K., Pendall, E. G., Barbour, M. M., Mortazavi, B., Burlett, R. g., Peylin, P., Miller, J., Mencuccini, M., Shim, J. H., Hunt, J., Grace, J., 2009. The impact of soil microorganisms on the global budget of δ¹⁸O in atmospheric CO₂. *Proc. Natl. Acad. Sci.* 106, 22411-22415.
- Young, E. D., Galy, A., Nagahara, H., 2002. Kinetic and equilibrium mass-dependent isotope fractionation laws in nature and their geochemical and cosmochemical significance. *Geochim. Cosmochim. Acta* 66, 1095-1104.
- Yung, Y. L., Demore, W. B., Pinto, J. P., 1991. Isotopic exchange between carbon dioxide and ozone via O(¹D) in the stratosphere. *Geophys. Res. Lett.* 18, 13-16.

6 Conclusions and outlook

This thesis evaluates the potential of triple oxygen isotope analysis in CO₂ as a new tracer for the global carbon cycle. It was an integral part of this study to show that high-precision analysis of tropospheric CO₂ allows detecting small variations in $\Delta^{17}\text{O}$ in natural and anthropogenic carbon dioxide. This is a prerequisite for establishing $\Delta^{17}\text{O}$ in tropospheric CO₂ as a new tracer to complement conventional $\delta^{18}\text{O}$ and $\delta^{13}\text{C}$ analyses.

The new analytical technique described in chapter 2 has an analytical uncertainty in $\Delta^{17}\text{O}$ measurements of at least $\pm 0.05\text{‰}$ for a single measurement (standard deviation). Due to multiple analyses, the analytical uncertainty was generally reduced to $\pm 0.02\text{‰}$ to $\pm 0.03\text{‰}$. Thus, until today, this technique is probably the most precise method to analyze the triple oxygen isotope composition of carbon dioxide. However, the method requires a large amount of sample CO₂: At the beginning, about 3.5 mmol of CO₂ (~70 ml, STP) were used for one analysis (see chapter 2), but over the course of the project the sample size was reduced to about one-fifth (see chapter 3, 4 and 5).

The method described here for triple oxygen isotope analysis in atmospheric CO₂ can also be applied to carbonate samples. For this purpose, the carbonate sample has to be decomposed by reaction with phosphoric acid. The released CO₂ can then be analyzed according to the procedure described in Chapter 2. First high-precision analyses of terrestrial carbonates were carried out during the time of this PhD study (Hofmann et al., 2012c), but it was beyond the scope of this study to explore in detail the potential of ^{17}O analyses in biogenic and abiotic carbonates as a tracer for their formation process. Thus, in principle, the technique for ^{17}O analysis in CO₂ also opens up a new field for isotope analysis in carbonates, but the preliminary results showed that further enhancements in measurement precision are required so that this new tool may be used as a new tracer for paleoclimate reconstruction (Hofmann et al., 2012c).

In chapter 3, experimental results on the triple oxygen isotope equilibrium fractionation between CO₂ and water are presented. These laboratory studies showed that the triple oxygen isotope exponent $\theta_{\text{CO}_2\text{-water}}$ is equal to 0.522 ± 0.002 for $2\text{ °C} < T < 37\text{ °C}$. Subsequent to these laboratory studies, this exponent for CO₂-water equilibrium was also confirmed by theoretical studies (pers. comm. Yun Liu, also see footnote 1 in chapter 3). The knowledge of this exponent was essential for meaningful interpretation of the combustion data presented in chapter 4 and it was also of great importance for the global mass balance model presented in chapter 5.

In chapter 4, it was shown that combustion CO₂ can inherit a distinct triple oxygen isotope signature from ambient air O₂, and thus, anthropogenic CO₂ can clearly be distinguished from natural CO₂ sources to the troposphere. Combustion of natural gas and propane-butane produces carbon dioxide with a $\Delta^{17}\text{O}$ value of -0.32‰ to -0.30‰ (relative to $\lambda_{\text{RL}} = 0.522$ and $\gamma = 0\text{‰}$). Carbon dioxide from car exhaust also inherits the distinct triple oxygen isotope composition of ambient air O₂ with $\Delta^{17}\text{O} = -0.34\text{‰}$, but it might have exchanged with similarly anomalous combustion water in the car exhaust. For carbon dioxide from wood combustion, the ¹⁷O depletion is less pronounced with a mean $\Delta^{17}\text{O}$ value of -0.21‰ , due to CO₂-water equilibration and wood inherent oxygen. In contrast, the triple oxygen isotope composition of carbon dioxide in human breath is solely controlled by the isotopic composition of ambient water and does not carry a large oxygen isotope anomaly.

In chapter 5, the first high-precision triple oxygen isotope data of tropospheric CO₂ are presented. Tropospheric CO₂ sampled in Göttingen has a mean $\Delta^{17}\text{O}$ value of $-0.03 \pm 0.07\text{‰}$ (standard deviation) and shows a temporal variation with a peak-to-peak range of $\sim 0.25\text{‰}$. The tropospheric CO₂ data from the Brocken Mountain fall within the range observed in Göttingen. The observational data only in part overlap with the revised global model prediction of $+0.06 \pm 0.05\text{‰}$ (standard deviation). The modeling results suggest that the observed temporal variation in $\Delta^{17}\text{O}$ cannot be attributed to seasonal variations in plant activity, but it may be that the influx of stratospheric CO₂ significantly affects the temporal $\Delta^{17}\text{O}$ variations of tropospheric CO₂. Thus, future studies are required to explain the interannual variability of $\Delta^{17}\text{O}$ observed for Göttingen CO₂ and to explain the discrepancy between the predicted global mean and the observational $\Delta^{17}\text{O}$ data.

References

- Hofmann, M. E. G., Horváth, B., Pack, A., 2012c. Triple oxygen isotope exponent for phosphoric acid decomposition of carbonates. Sixth International Symposium on Isotopomers, Washington DC.

7 List of publications

The following summary gives a list of all publications that were released during the time of the PhD thesis.

Peer-review journals:

- **Hofmann, M. E. G.**, Horváth, B. and Pack, A., Triple oxygen isotope composition of tropospheric CO₂: Observational data and model simulation, in preparation
- Horváth, B., **Hofmann, M. E. G.**, and Pack, A., 2012, On the triple oxygen isotope composition of carbon dioxide from some combustion processes, *Geochim. Cosmochim. Acta*, in press
- **Hofmann, M. E. G.**, Horváth, B., and Pack, A., 2012. Triple oxygen isotope equilibrium fractionation between carbon dioxide and water. *Earth Planet. Sci. Lett.* 319-320, 159-164
- **Hofmann, M. E. G.** and Pack, A., 2010. Technique for high-precision analysis of triple oxygen isotope ratios in carbon dioxide. *Anal. Chem.* 82, 4357-4361

Conference abstracts:

- **Hofmann, M. E. G.**, Horváth, B., and Pack, A., 2012. *Global long-term mean triple oxygen isotope composition of tropospheric CO₂*, European Mineralogical Conference, Frankfurt
- Pack, A., Albrecht, N., **Hofmann, M. E. G.**, Bultmann, E. M., Horváth, B., and Gehler, A., 2012. *Variations in triple isotope fractionation exponents*, European Mineralogical Conference, Frankfurt
- Horváth, B., **Hofmann, M. E. G.**, and Pack, A., 2012. *Triple oxygen isotope variations in ambient air CO₂ from Göttingen*, JESIUM, Leipzig
- **Hofmann, M. E. G.**, Horváth, B., and Pack, A., 2012, *Global long-term mean triple oxygen isotope composition of tropospheric CO₂*, International Symposium on Isotopomers, Washington D.C.

-
- **Hofmann, M. E. G.**, Horváth, B., and Pack, A., 2012, Triple oxygen isotope exponent for phosphoric acid decomposition of carbonates, International Symposium on Isotopomers, Washington D.C.
 - Horváth, B., **Hofmann, M. E. G.**, and Pack, A., 2012. *Seasonal triple oxygen isotope variations in ambient air CO₂ from Göttingen*, International Symposium on Isotopomers, Washington D.C.
 - Pack, A., Albrecht, N., **Hofmann, M. E. G.**, Horváth, B., Gehler, A., 2012. *Experimental data on variations in triple oxygen isotope equilibrium fractionation exponents*, International Symposium on Isotopomers, Washington D.C.
 - **Hofmann, M. E. G.**, Horváth, B., and Pack, A., 2011. *Triple oxygen isotope composition of tropospheric carbon dioxide and terrestrial carbonates*, AGU, San Francisco.
 - Horváth, B., **Hofmann, M. E. G.**, and Pack, A., 2011. *Triple oxygen isotope composition of CO₂ as a tracer for global carbon fluxes and for regional CO₂ sources*, Annual Meeting of the German Association for Stable Isotope Research, Villigen-PSI.
 - Horváth, B., **Hofmann, M. E. G.**, and Pack, A., 2011. *Triple oxygen isotope composition as a potential tracer for mixing ratios of carbon dioxide sources in urban air*, XI. Isotope Workshop, Budapest.
 - **Hofmann, M. E. G.**, Horváth, B. and Pack, A., 2011. *Triple oxygen isotope equilibrium fractionation between CO₂ and water and its implication on tropospheric CO₂*, Tenth Informal Conference on Atmospheric and Molecular Science, Copenhagen.
 - Horváth, B., **Hofmann, M. E. G.** and Pack, A., 2011. *Triple oxygen isotope composition as a potential tracer for mixing ratios of carbon dioxide sources in urban air*, Tenth Informal Conference on Atmospheric and Molecular Science, Copenhagen.
 - **Hofmann, M. E. G.**, Horváth, B., Hinrichsen, S. and Pack, A., 2011. *Temperature dependence of the triple oxygen isotope equilibrium fractionation between carbon dioxide and water and its implication on the triple oxygen isotope signature of tropospheric carbon dioxide*, EGU, Vienna.

-
- Horváth, B., **Hofmann, M. E. G.**, Hinrichsen, S. and Pack, A., 2011. *Triple oxygen isotope composition of carbon dioxide from various anthropogenic sources and in urban air*, EGU, Vienna.
 - Pack, A., Horváth, B., **Hofmann, M. E. G.**, Goldmann, A., Albrecht, N., Gellissen, M., Zipfel, J., and Palme, H., 2011. *Defining the terrestrial oxygen isotope fractionation line and observed oxygen isotopic heterogeneity within the Allende meteorite*, Lunar and Planetary Science Conference, Houston.
 - **Hofmann, M. E. G.**, Horváth, B. and Pack, A., 2010. *Triple oxygen isotope composition of CO₂ from the biosphere, the troposphere and from combustion*. International Symposium on Isotopomers, Amsterdam.
 - Horváth, B., **Hofmann, M. E. G.**, Gehler, A. and Pack, A., 2010. *Triple oxygen composition of CO₂ from fossil fuel combustion and human respiration*, International Symposium on Isotopomers, Amsterdam.
 - **Hofmann, M. E. G.**, Horváth, B. and Pack, A., 2010. *Experimental determination of the exponent β for oxygen triple isotope fractionation between carbon dioxide and water*, EGU, Vienna.
 - Horváth, B., **Hofmann, M. E. G.** and Pack, A., 2010. *Triple oxygen composition of carbon dioxide from fossil fuel combustion*. EGU, Vienna.